

Asymmetric Decision Feedback Equalization

by

Kevin Scott Oler

A THESIS
SUBMITTED TO THE FACULTY OF GRADUATE STUDIES
IN PARTIAL FULFILLMENT OF THE REQUIREMENTS FOR THE
DEGREE OF MASTER OF SCIENCE

DEPARTMENT OF
ELECTRICAL AND COMPUTER ENGINEERING

CALGARY, ALBERTA
AUGUST, 1996

© KEVIN SCOTT OLER 1996

THE UNIVERSITY OF CALGARY
FACULTY OF GRADUATE STUDIES

The undersigned certify that they have read, and recommend to the Faculty of Graduate Studies for acceptance, a thesis entitled “Asymmetric Decision Feedback Equalization” submitted by Kevin Scott Oler in partial fulfillment of the requirements for the degree of Master of Science.

Dr. B. R. Petersen,
Chair and Co-supervisor
Department of Electrical and Computer
Engineering

Dr. A. B. Sesay, Supervisor
Department of Electrical and Computer
Engineering

Dr. S. A. Norman
Department of Electrical and Computer
Engineering

Dr. J. A. R. Blais
Department of Geomatics Engineering

Date

ABSTRACT

This thesis presents a new equalizer structure, the asymmetric decision feedback equalizer (ADFE). The mean square error (MSE) and bit error rate (BER) performance of the ADFE is analyzed and simulated. The ADFE is shown to have an identical MSE characterization, identical MSE performance, and similar BER performance, to the DFE. The BER of the ADFE is estimated by simulation, and by use of a finite discrete Markov process.

The ADFE is paired with a DFE to form the ADFE system, which equalizes communications between two transceivers with an asymmetric distribution of equalization complexity. The performance of this system is examined under various nonidealities including a mismatch in characterization signal-to-noise ratios (SNR's), timing error, adaptive training, finite precision arithmetic, and measured indoor wireless channels. Results stemming from the SNR mismatch indicate the potential for improved BER performance of the DFE and ADFE through a modification of MSE characterization.

ACKNOWLEDGMENTS

The author wishes to thank all who have contributed to this work, directly or otherwise. The supervisors, Dr. B. R. Petersen and Dr. A. B. Sesay, provided ample encouragement and guidance, as well as the freedom to explore.

The staff and students of Telecommunications Research Laboratories (*TRLabs*) provided willing assistance and advice on everything from accessing the indoor channel database to formatting figures. Especially useful was the precious time taken by senior students to share their valuable experience.

The Natural Sciences and Engineering Research Council of Canada (NSERC), *TRLabs*, and the University of Calgary provided financial support which made this work possible.

To Linda

TABLE OF CONTENTS

Approval Page	ii
Abstract	iii
Acknowledgments	iv
Dedication	v
Table of Contents	vi
List of Tables	x
List of Figures	xi
List of Symbols and Mathematical Notation	xiii
List of Abbreviations and Acronyms	xvii
1. Introduction	1
1.1 Subject Area	1
1.2 New Results	1
1.3 Thesis Overview	3
2. Background	5
2.1 Model for a Wireless Digital Communications System	6
2.1.1 Symbol Encoder	7
2.1.2 D/A Conversion and Pulse Shaping	7
Frequency Domain	8
Time Domain	9
Raised Cosine Pulse	9
2.1.3 Carrier Modulation	12
2.1.4 RF Amplifier	13
2.1.5 Antenna	13
2.1.6 Channel	14
Channel Impulse Response	14
Noise	15
2.1.7 Receiver Antenna	15
2.1.8 RF Amplifier and Bandlimiter	15
2.1.9 Automatic Gain Control	15
2.1.10 Carrier Demodulation	16
2.1.11 Synchronization and Sampling	16
2.1.12 Equalization	17
2.1.13 Detection	17

2.1.14	Criteria for Evaluation of a Digital Communications System	18
2.1.15	System Model for Analysis of Equalization.....	19
	Full Duplex Communications	20
2.2	Equalization	21
2.2.1	The Linear Transversal Equalizer	21
	Variations on the Transversal Equalizer	22
	Zero Forcing Criterion	23
	Wiener solution	25
	Minimum Probability of Error (MPE) Characterization	26
	Fractionally Spaced Equalization	26
2.2.2	The Decision Feedback Equalizer	27
	Structure of the DFE	27
	Heuristic Explanation.....	28
	Minimum Mean Square Error Characterization and Performance	29
	Bit Error Rate Performance	30
2.2.3	Other Nonlinear Equalizers	31
	TH Precoder	31
	Viterbi Decoding	32
2.2.4	Adaptive Equalization	32
	Implicit Method	33
	Explicit Method	35
	Training of Fractionally Spaced Equalizers	35
2.3	Conclusion	36
3.	Asymmetric Equalization	37
3.1	Asymmetric Complexity	37
3.2	Target System	38
3.3	Previous Results.....	39
	Gibbard System.....	40
3.4	Conclusion	41
4.	The ADFE.....	42
4.1	ADFE and ADFE System.....	42
4.2	MSE Characterization and Performance of ADFE	43
	ADFE Without Power Constraint	44
	ADFE with Power Constraint	45
4.3	ADFE System Training	50
	SNR Mismatch.....	52

4.4 Computational Complexity.....	54
Training.....	54
Execution.....	55
4.5 Fractionally Spaced Equalization.....	56
Reverse Link.....	56
Forward Link.....	57
MSE Analysis.....	57
4.6 Conclusions.....	59
5. Markov Model of Error Propagation.....	61
5.1 Decision Errors in the DFE.....	61
5.2 BER Estimation by Simulation.....	63
5.3 Error Propagation in the ADFE.....	63
5.4 Error Event Correlation.....	67
5.5 Conclusion.....	69
6. Non-Idealities.....	70
6.1 SNR mismatch.....	71
SNR Mismatch with Other Channels.....	73
First Pair of Channels (A, B).....	75
Second Pair of Channels (C, D).....	76
Third Pair of Channels (E, F).....	77
Fourth Pair of Channels (G, H).....	78
Channel A, Revisited.....	79
6.2 Sensitivity to Timing Error.....	81
Reverse Link (DFE).....	82
Forward Link (ADFE).....	83
Joint Timing Error.....	84
6.3 Adaptive Training.....	86
6.4 Finite Precision.....	88
6.5 Conclusions.....	95
SNR mismatch.....	96
Timing Error.....	97
Adaptive Training.....	97
Finite Precision.....	98
7. ADFE System Performance over Measured Channels.....	99
7.1 The Indoor Channel Database.....	99
7.2 Method of Simulation.....	100

Error Collection	100
Adaptive Training.....	101
Data Transmission and Retraining	101
Number of FF/FBF Equalizer Taps.....	102
Synchronization	102
7.3 Simulation Results	103
7.4 Conclusions	108
8. Conclusion	110
8.1 Summary of Thesis	110
8.2 Topics for Further Research	110
References	113
Appendix	118
Listing of markov.m	118
Listing of base2num.m	122
Listing of num2base.m	123

LIST OF TABLES

Table 2.1: Bit Representation of QPSK Symbols.....	7
Table 4.1: ADFE System Forward/Reverse Link Parameters.....	53
Table 4.2: Computational Complexity of Equalizers	55
Table 4.3: Computational Complexity of Equalization Systems.....	56
Table 5.1 Parameters for Figures 5.2 - 5.4	66
Table 6.1: Parameters for Figures 6.1, 6.2	73
Table 6.2: Parameters for Figures 6.3 - 6.11	74
Table 6.3: Parameters for Figures 6.12, 6.13	80
Table 6.4: Parameters for Figures 6.14 - 6.17	82
Table 6.5: Parameters for Figure 6.18	87
Table 6.6: Parameters for Figure 6.19	88
Table 6.7: Parameters for Figure 6.21	91
Table 6.8: Parameters for Figure 6.22	92
Table 6.9: Parameters for Figures 6.23, 6.24	93
Table 6.10: Parameters for Figure 6.25	95
Table 7.1: Summary of DFE Filter Lengths.....	102
Table 7.2: Parameters for Figure 7.1	103
Table 7.3: Parameters for Figures 7.2, 7.3	104
Table 7.4: BER of Selected Channels.....	106

LIST OF FIGURES

Figure 2.1:	Target System	5
Figure 2.2:	Wireless Digital Communications System	6
Figure 2.3:	Raised Cosine Pulse (time domain)	10
Figure 2.4:	Raised Cosine Pulse (frequency domain)	11
Figure 2.5:	I and Q Channels in Modulation	12
Figure 2.6:	Continuous and Sampled CIR	17
Figure 2.7:	Simplified Model of Communications System	19
Figure 2.8:	Full Duplex Wireless Communications System	20
Figure 2.9:	Linear Transversal Equalizer	21
Figure 2.10:	CIR of Channel to be Equalized	23
Figure 2.11:	Equalizer and Channel (frequency domain)	24
Figure 2.12:	Equalized Channel (time domain)	24
Figure 2.13:	Equalized Channel (frequency domain)	25
Figure 2.14:	Frequency Response of Wiener (MMSE) Equalizer	26
Figure 2.15:	Decision Feedback Equalizer	27
Figure 2.16:	Tomlinson-Harashima Precoder	31
Figure 3.1:	Asymmetric System	38
Figure 3.2:	Gibbard System	40
Figure 4.1:	ADFE	42
Figure 4.2:	ADFE system	43
Figure 4.3:	DFE Model	44
Figure 4.4:	Modified DFE Model	44
Figure 4.5:	ADFE Model with Constrained Transmit Power	46
Figure 4.6:	DFE / ADFE Model	46
Figure 5.1:	ADFE System	64
Figure 5.2:	Markov Model and Simulation Results	66
Figure 5.3:	BER with and without Error Propagation	67
Figure 5.4:	Autocorrelation of Error Event function	68
Figure 6.1:	MSE Performance of ADFE with SNR Mismatch	72
Figure 6.2:	BER of ADFE with SNR Mismatch	72
Figure 6.3:	BER of ADFE with SNR Mismatch (execution SNR 21 dB)	75

Figure 6.4:	Frequency spectra of CIR's	75
Figure 6.5:	Frequency spectra of ADFE FF (characterized at 20 dB SNR)	75
Figure 6.7:	Frequency Spectra of CIR's	76
Figure 6.8:	Frequency Spectra of ADFE FF (characterized at 20 dB SNR)	76
Figure 6.9:	BER of ADFE with SNR Mismatch	77
Figure 6.10:	Frequency Spectra of CIR's	77
Figure 6.11:	Frequency Spectra of ADFE FF (characterized at 20 dB SNR)	77
Figure 6.9:	BER of ADFE with SNR Mismatch	78
Figure 6.10:	Frequency Spectra of CIR's	78
Figure 6.12:	BER of ADFE and DFE with SNR Mismatch	79
Figure 6.13:	Signal Components within DFE/ADFE	81
Figure 6.14:	BER Timing Sensitivity of Reverse Link (DFE).....	82
Figure 6.15:	BER Timing Sensitivity of Forward Link (ADFE)	83
Figure 6.16:	BER Joint Timing Sensitivity of Forward Link (ADFE)	84
Figure 6.17:	Joint BER Timing Sensitivity of Forward Link, by Simulation.....	85
Figure 6.18:	DFE Adaptive RLS Training	86
Figure 6.19:	ADFE FBF Adaptive LS Training.....	87
Figure 6.20:	Quantizer Input/Output Characteristic	89
Figure 6.21:	Equalizer Performance with Finite Precision Arithmetic	90
Figure 6.22:	Equalizer Performance with Finite Precision Arithmetic	92
Figure 6.23:	Equalizer Performance with Finite Precision Arithmetic	93
Figure 6.24:	Residual Precursor ISI (convolution of FF and CIR)	94
Figure 6.25:	Equalizer Performance with Residual Precursor ISI.....	94
Figure 7.1:	Average BER for Measured Channels	103
Figure 7.2:	BER Distribution	104
Figure 7.3:	BER Distribution (relaxed error requirements)	105
Figure 7.4:	Indoor Channel Impulse Response	106
Figure 7.5:	Indoor Channel Impulse Response	107
Figure 7.6:	Indoor Channel Impulse Response	107
Figure 7.7:	Indoor Channel Impulse Response	107
Figure 7.8:	BER Performance versus Energy of CIR	108

LIST OF SYMBOLS AND MATHEMATICAL NOTATION

$\mathbf{0}_N$	a $N \times 1$ vector of zeros
$a(n)$	data symbols
$\hat{a}(n)$	estimated data symbols
A	amplifier gain
$d(n)$	desired or correct data symbols at receiver
$\tilde{d}(n)$	detected data symbols at receiver
D	normalized autocorrelation matrix of noise component of DFE/ADFE tap inputs; a diagonal matrix with ones along the diagonal elements corresponding to the FF and zeros for the FBF
e	base of the natural exponential function (2.71828182845905...)
$e(n)$	error signal; the difference between the desired and estimated signals
erfc(\cdot)	the error function, defined as $\text{erfc}(x) = \frac{2}{\sqrt{\pi}} \int_0^x e^{-t^2} dt$
E	the statistical expectation operator
f	frequency
f_c	carrier frequency
h	vector of finite impulse response filter coefficients representing the sampled channel impulse response
$h(n)$	discrete-time (sampled) channel impulse response
$h(t)$	continuous time channel impulse response
$H(f)$	Fourier transform of the continuous time or sampled channel impulse response
\mathbf{I}_N	$N \times N$ identity matrix
$\text{Im}[\cdot]$	imaginary part of a complex number
j	square root of -1, or an integer variable if otherwise defined
J	mean square error
J_{\min}	minimum mean square error

$J_{\min,ADFE}$	ADFE (forward link) minimum mean square error
$J_{\min,DFE}$	DFE (reverse link) minimum mean square error
J_{ADFE}	ADFE (forward link) mean square error
k	discrete time index, or a general integer
K_f	gain factor equal to magnitude of forward filter
L_2 norm	as used in this thesis, the square root of the sum of the squared magnitudes of a vector's elements
m	an integer variable
m_y	mean or expected value of the random variable $y(n)$
mod	modulo arithmetic, modulo operator (for TH precoding), or number of mod operations
M	threshold level for modulo arithmetic
n	discrete time index, or a general integer
N_0	the two-sided power spectral density of complex additive white Gaussian noise
N_b	number of feedback filter taps
N_f	number of forward filter taps
N_h	length of FIR representation of sampled channel impulse response
N_q	length of the vector \mathbf{q}
N_w	length of a finite impulse response filter
$O(\cdot)$	complexity; order of magnitude of number of operations
\mathbf{p}	crosscorrelation vector of equalizer inputs and desired signal
$\rho(t)$	pulse shape
$P(\cdot)$	probability function
$P(f)$	Fourier transform of pulse shape $\rho(t)$
P_i	the probability of being in state S_i
P_{ij}	probability of transition from state S_i to state S_j
\mathbf{q}	vector representation of $q(n)$
$q(n)$	convolution or combined impulse response of channel impulse response and transversal equalizer or forward filter

$Q(f)$	Fourier transform of $q(n)$
$Q[x]$	finite precision quantization operation
\mathbf{R}	autocorrelation matrix of equalizer inputs, without noise
$\text{Re}[\cdot]$	real part of a complex number
s	oversampling rate of fractionally spaced equalizer
$s(t)$	passband signal
$s'(t)$	amplified passband signal
$\text{sinc}(\cdot)$	the sinc function $\text{sinc}(t) = \begin{cases} \frac{\sin(\pi t)}{\pi t}, & t \neq 0 \\ 1, & t = 0. \end{cases}$
S_j	state j of finite discrete Markov process
t	continuous time
T_{eq}	sampling period of a fractionally spaced equalizer filter
T_{sym}	symbol period
$u(n)$	received signal; with or without additive noise depending on context
$v(t)$	additive noise
\mathbf{w}	vector of equalizer coefficients representing a finite impulse response filter
\mathbf{w}_b	feedback filter coefficients
\mathbf{w}_f	forward filter coefficients
$\mathbf{w}_{f,DFE}$	DFE (reverse link) forward filter coefficients
w_k	equalizer coefficient from a finite impulse response filter
\mathbf{w}_v	noise filter
\mathbf{w}_{ADFE}	ADFE (forward link) equalizer coefficients
\mathbf{w}_{DFE}	DFE (reverse link) equalizer coefficients
\mathbf{w}_{MMSE}	minimum mean square error equalizer coefficients
$W_f(f)$	Fourier transform of forward filter coefficients
$x(n)$	filter or equalizer input
$x(t)$	continuous time representation of transmitted data symbols

$X(f)$	Fourier transform of $x(t)$
$y(n)$	filter or equalizer output
$y_Q(n)$	output of a finite precision arithmetic FIR filter
z	complex discrete time z -transform variable
β	raised cosine pulse/filter rolloff parameter
χ	eigenvalue spread of autocorrelation matrix of the input signal
δ	initialization constant for RLS algorithm
$\delta(k)$	Kroneker delta function
Δ	delay between transmitted and received symbols
$\varepsilon(n)$	the error event function, defined as $\varepsilon(n) = \begin{cases} 0, & \tilde{d}(n) = d(n) \\ 1, & \tilde{d}(n) \neq d(n) \end{cases}$
$\phi_{\varepsilon\varepsilon}(k)$	the error event autocorrelation function, defined as $\phi_{\varepsilon\varepsilon}(k) = E[\varepsilon(n)\varepsilon(n-k)]$ $= P(\varepsilon(n) = 1, \varepsilon(n-k) = 1)$
$\Phi_{xx}(f)$	power density spectrum of $x(t)$
$\Phi_{aa}(f)$	power density spectrum of $a(n)$
μ	LMS step size parameter
π	pi; the ratio of the circumference of a circle to its diameter (3.14159265358979...)
σ_v^2	variance of noise
$\sigma_{v,ADFE}^2$	noise variance on forward link
$\sigma_{v,DFE}^2$	noise variance on reverse link
σ_y^2	variance of the random variable $y(n)$
Σ	summation

LIST OF ABBREVIATIONS AND ACRONYMS

A/D converter	analog to digital converter
add	number of addition operations
ADFE	asymmetric decision feedback equalizer
AGC	automatic gain control
amp	amplifier
AWGN	additive white Gaussian noise
b	bit
base	base station wireless transceiver
BER	bit error rate
BPSK	binary phase shift keying
CIR	channel impulse response
D/A converter	digital to analog converter
dB	decibel
DD	decision device
DFE	decision feedback equalizer
DSP	digital signal processing, digital signal processor
FBF	feedback filter
FF	forward filter
FS	fractionally spaced
FSE	fractionally spaced equalizer
Hz	Hertz; repetitions per second
I	in-phase channel
IF	intermediate frequency
ISI	intersymbol interference
LAN	local area network
LMS	least mean squares
LS	least squares
LSCE	least squares channel estimation
M	mega or 10^6 , as in MHz or Mb/s
MMSE	minimum mean square error

mod	modulo arithmetic, modulo operator (for TH precoding), or number of mod operations
MPE	minimum probability of (decision) error
MSE	mean square error
mult	number of multiplication operations
portable	portable wireless transceiver
Q	quadrature channel
QPSK	quadrature phase shift keying
RC	raised cosine pulse/filter
RF	radio frequency
RLS	recursive least squares
s	second
SNR	signal-to-noise ratio
SQRC	square root raised cosine pulse/filter
TDD	time division duplex
TH precoder	Tomlinson-Harashima precoder
TS	T_{sym} spaced
TSE	T_{sym} spaced equalizer
VA	Viterbi algorithm
ZF	zero forcing

1. Introduction

1.1 Subject Area

This thesis deals with the subject of equalization for indoor wireless digital communications. A new equalizer structure and system are presented. The system achieves a significant asymmetry in the distribution of computational complexity relating to equalization between two communicating transceivers. The system performance is described in terms of mean square error (MSE) and bit error rate (BER) performance. The number of arithmetic operations required for equalization, including adaptive training, are used to quantify the complexity of the system.

1.2 New Results

This thesis introduces a new equalization structure, dubbed the asymmetric decision feedback equalizer (ADFE). A mean square analysis is formulated in a manner which encompasses both the ADFE and the decision feedback equalizer (DFE). The minimum mean square error (MMSE) characterization of the ADFE with and without a constraint on transmitted power is obtained. The analysis of the power-constrained ADFE also applies to the (DFE), and the two equalizers are shown to have identical MSE performance and MMSE characterization, under equivalent conditions. The MMSE characterization of the ADFE with a fractionally spaced forward filter (FS FF) is also given.

The bit error rate (BER) of the ADFE is accurately predicted by the use of a finite discrete Markov process. This model takes into account the effects of noise, residual precursor intersymbol interference (ISI) and error propagation. Some results obtained by this model is verified by simulation. Previous modeling of the DFE feedback filter (FBF) by a Markov process does not accurately model residual precursor ISI and noise filtering in all cases [Monsen2].

The ADFE system is designed to equalize bidirectional time division duplex (TDD) wireless communications with an asymmetric distribution of complexity between the two communicating transceivers. The ADFE system includes a DFE, an ADFE, and efficient training algorithms.

The impact of timing error, adaptive training, and finite precision arithmetic on the performance of the ADFE system is examined.

Joint timing error and training signal-to-noise ratio (SNR) mismatch are two non-idealities which are particular to systems, such as the ADFE system, in which reciprocity is exploited to characterize a pre-equalizer. This thesis analyzes the effect of these nonidealities on BER performance. In addition, the effects of timing error, adaptive training, and finite precision arithmetic in the ADFE system are examined.

The SNR mismatch leads to some curious relationships between the training SNR and BER performance. In some cases, this result may be exploited to improve DFE or ADFE performance through a modified MMSE characterization.

The investigation into finite precision effects includes a comparison with the Gibbard precoder [Gibbard3], a modified Tomlinson-Harashima (TH) precoder [Tomlinson] [Harashima]. An unexpected divergence in performance levels of the ADFE and Gibbard precoder is discovered for a particularly harsh channel.

The performance of the ADFE system over an ensemble of indoor wireless channels is determined by simulation, using a database of channel measurements [Morrison1]. The mean BER and an approximate distribution of the BER over the ensemble of channels is presented.

1.3 Thesis Overview

Chapter 2 consists of background material which serves as a foundation for many of the concepts and issues presented in this thesis. It is divided into two sections which provide a brief description of the major components of a wireless digital communications system, and an overview of equalization. This chapter is directed towards those with a limited background in one or both of these areas. Those seeking rigorous and detailed treatment of these topics are directed towards the references, especially the texts [Haykin] [Proakis]. The reader who is already familiar with these basics may wish to skip this chapter entirely.

Chapter 3 presents a brief definition and overview of asymmetric equalization. Some previous work in this field is referenced.

Chapter 4 introduces a new equalizer structure: the asymmetric decision feedback equalizer (ADFE). An ADFE, paired with a decision feedback equalizer (DFE), forms the ADFE system which equalizes bidirectional data transmission. Training of the ADFE system is described. The computational complexity of the ADFE is tabulated and compared with similar equalizers. Finally, the merits of applying fractionally spaced equalization to the ADFE are discussed and the MMSE solution for the fractionally spaced ADFE is presented.

In Chapter 5, a finite discrete Markov process is used to model error propagation in the ADFE, to determine the bit error rate (BER) performance under specific conditions. Results by Markov model and by simulation are compared. The extent and effect of error propagation in the ADFE is examined.

Chapter 6 examines the impact on performance of a few non-idealities expected in the ADFE system: SNR training mismatch, timing error, adaptive training, and finite precision arithmetic. While performance of an equalizer is often optimized and measured in terms of mean square error (MSE), this chapter focuses on the BER as a metric of performance. In fact, the section on SNR mismatch reveals some significant discrepancies between MSE and BER performance, along with

the possibility of a modified MMSE characterization to improve BER performance.

Chapter 7 applies the ADFE system to the equalization of measured indoor wireless channels. This gives a better indication of the performance that may be expected in an implementation of the ADFE system. The average BER performance over an ensemble of channels is determined, as well as the distribution of BER performance across the ensemble. The performance is so highly dependent on the characteristics of each channel that further investigation quickly becomes more of a study in channel characteristics than in equalization.

Chapter 8, the conclusion, presents a summary of the results of this thesis and of areas for future research.

The Appendix contains an example of a Matlab program which predicts the BER of the ADFE over a particular channel by using a Markov model, as described in Chapter 5.

2. Background

The motivation for this thesis is the synthesis and investigation of equalization for the target system described below. Although many of the following concepts have general application in the fields of digital communications and signal processing, in this chapter they are considered only in relation to the target system.

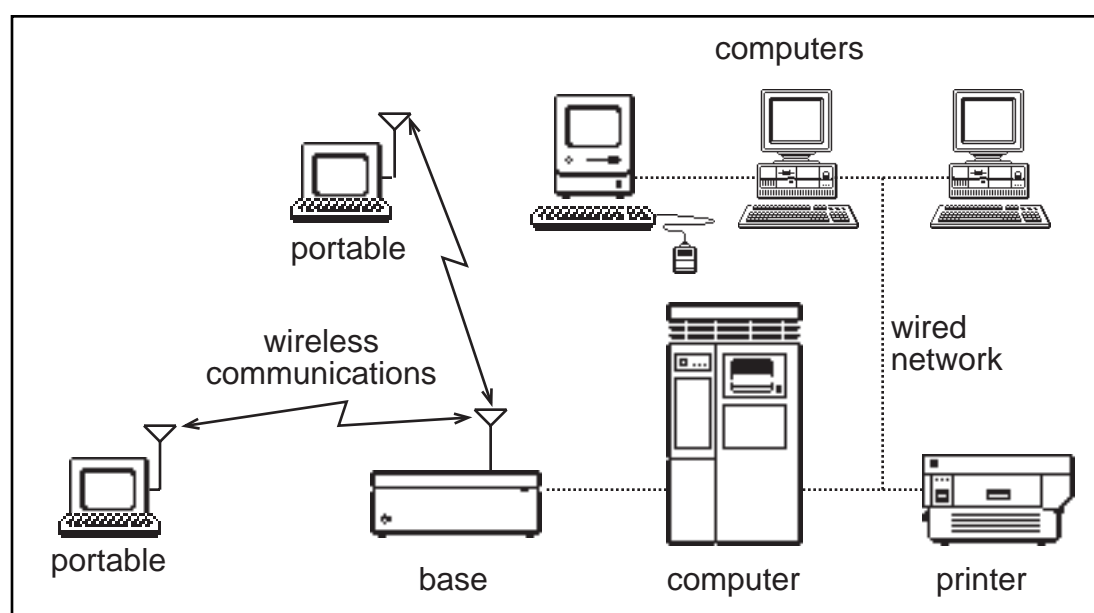


Figure 2.1: Target System

The target system is an indoor wireless communications link intended to supplement to coverage of an indoor wired computer network (LAN), as shown in Figure 2.1. The wired LAN may connect elements such as computers, printers, storage devices, and other networks. The wireless link allows access to the network from portable computers (notebook PC's). A base station, equipped with a wireless transmitter and receiver, serves as a gateway to the wired LAN. Once the base is installed, a portable requires no physical connection or setup to access the network, and may be used anywhere within the range of the base.

The subject area of this thesis encompasses digital communications, equalization, and signal processing. The background material presented is intended to allow one lacking familiarity with any of these fields to appreciate the main issues associated with the equalization of the target system.

Section 2.1 presents a simplified model of a wireless digital communications system as a means of reviewing the concepts thereof. Section 2.2 is an overview of methods of equalization.

2.1 Model for a Wireless Digital Communications System

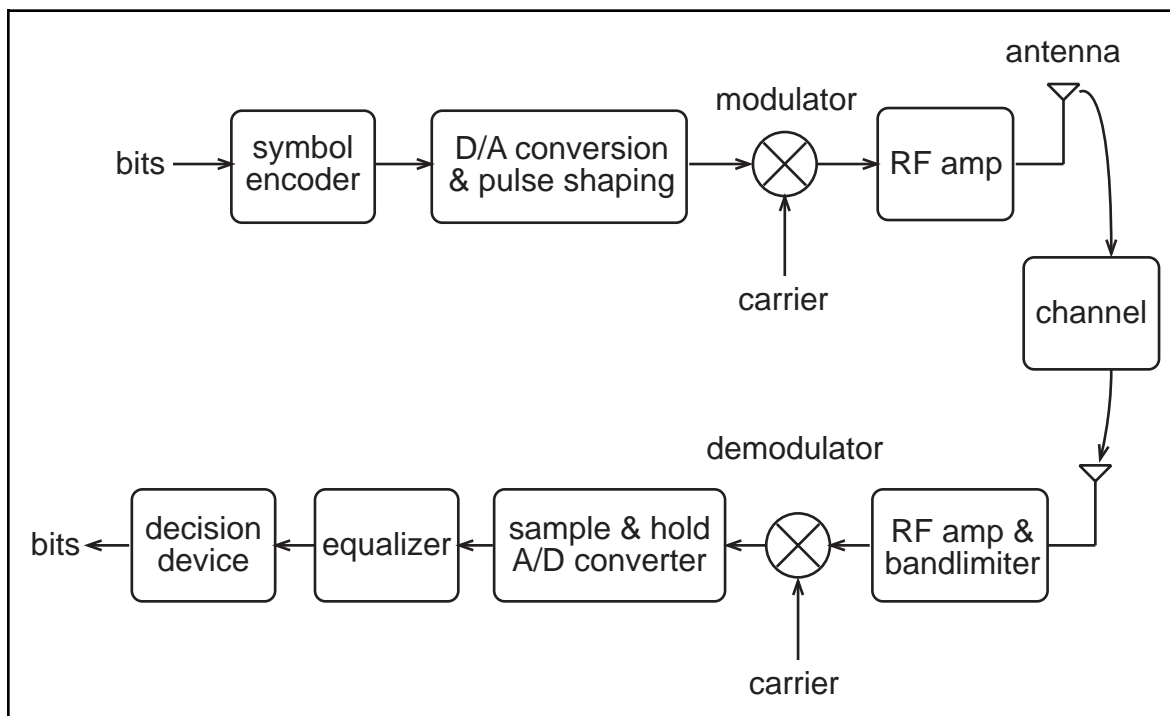


Figure 2.2: Wireless Digital Communications System

A model for a wireless digital communications system is shown in Figure 2.2. In its entirety, it is a discrete channel, in that its input and output are sequences of discrete data symbols. The symbols are henceforth assumed to be binary, or bits. The average probability that an output bit differs from the corresponding

input bit is called the bit error rate (BER). A system is usually required to achieve a BER below a limit, which may typically range from 10^{-3} to 10^{-8} [Freeburg] [Morris, page 2].

For analysis and simulation it is assumed that each element of the alphabet (0,1) appears with equal and independent probability. The resulting independence of data symbols simplifies the characterization of the signal at subsequent stages.

2.1.1 Symbol Encoder

The symbol encoder maps a pair of input bits into a quadrature phase shift keying (QPSK) symbol. One suitable rule for this mapping is given in Table 2.1.

Table 2.1: Bit Representation of QPSK Symbols

input bits	QPSK symbol $a(n)$
00	$-1-j$
01	$-1+j$
10	$+1-j$
11	$+1+j$

Alternative data modulations may include more or less bits per symbol, and may include complex dependencies on previous symbols [Proakis, pp. 172-185]. One QPSK symbol is generated every T_{sym} seconds, and the symbol generated at time $t = nT_{sym}$ symbol is denoted $a(n)$.

2.1.2 D/A Conversion and Pulse Shaping

This block, which follows the symbol encoder, performs digital to analog (D/A) conversion and pulse shaping. The QPSK symbols are converted from a discrete-time digital representation to a continuous time signal. If the pulse shape is $p(t)$, then the output of the D/A pulse shaping block $x(t)$ is given by

$$x(t) = \sum_{n=-\infty}^{\infty} a(n) p(t - nT_{sym}). \quad (2.1)$$

The pulse $p(t)$ is designed as a compromise between two criteria:

1. Frequency domain: to bandlimit the signal $x(t)$
2. Time domain: to avoid intersymbol interference in the received signal

Frequency Domain

Let $P(f)$ and $X(f)$ be the Fourier transforms of $p(t)$ and $x(t)$, respectively.

$$P(f) = \int_{-\infty}^{\infty} p(t) e^{-j2\pi ft} dt, \quad (2.2)$$

$$X(f) = \int_{-\infty}^{\infty} x(t) e^{-j2\pi ft} dt. \quad (2.3)$$

The average power density spectrum of $x(t)$ is given by [Proakis, 193]

$$\Phi_{xx}(f) = \frac{1}{T_{sym}} |P(f)|^2 \Phi_{aa}(f) \quad (2.4)$$

where

$$\Phi_{aa}(f) = \frac{1}{2} \sum_{m=-\infty}^{\infty} E[a^*(k) a(k+m)] e^{-j2\pi f m T_{sym}}.$$

Given the definition of $a(n)$ as independent QPSK symbols, we have

$$\Phi_{xx}(f) = \frac{1}{T_{sym}} |P(f)|^2. \quad (2.5)$$

Thus the frequency content and hence bandwidth of the transmitted signal is determined by the pulse shape $p(t)$. The bandwidth of $p(t)$ cannot be arbitrarily limited, as $P(f)$ must have nonzero frequency components within the range

$|f| \leq \frac{1}{2T_{sym}}$ in order to avoid time domain intersymbol interference (if $p(t)$ is a

baseband signal).

Time Domain

Suppose we wish to form an estimate, $\hat{a}(n)$, of the original data sequence $a(n)$ by sampling the information signal ($x(t)$ in this case). This is expressed mathematically as

$$\begin{aligned}\hat{a}(n) &= x(t - nT_{sym}) \\ &= \sum_{k=-\infty}^{\infty} a(k)p((n-k)T_{sym}) \\ &= a(n)p(0) + \sum_{\substack{k=-\infty \\ k \neq 0}}^{\infty} a(n-k)p(kT_{sym}).\end{aligned}\tag{2.6}$$

The desired symbol is given by $a(n)p(0)$, while $\sum_{\substack{k=-\infty \\ k \neq 0}}^{\infty} a(k)p((n-k)T_{sym})$ is

intersymbol interference (ISI), which degrades the accuracy of estimates and may contribute to decision errors. Additional processing may be used to reduce the ISI, at the expense of undesirable complexity. The pulse $p(t)$ is usually designed so that $p(kT_{sym}) = 0$ for $k \neq 0$, to eliminate the ISI term from Equation 2.6.

In partial-response signaling, $p(kT_{sym})$ is allowed to be nonzero for more than one value of k , and this controlled ISI is accounted for in data reception. Partial-response signaling, in conjunction with nonlinear receivers, may be used to obtain desirable frequency-domain characteristics of the information signal $x(t)$ [Kabal].

Raised Cosine Pulse

As stated previously, $p(t)$ and $x(t)$ must be allowed to occupy the bandwidth of at least $1/(2T_{sym})$ to avoid introducing ISI. This minimal bandwidth is not achievable in practice as it would require ideal (unrealizable) filters and perfect synchronization in detection. The filter and synchronization requirements can be

relaxed by selecting a pulse with increased, or excess, bandwidth. The raised cosine (RC) pulse is chosen for use in this thesis [Proakis, pp. 535-536]. The amount of excess bandwidth is controlled by a parameter β which ranges from 0 to 1. The time and frequency domain representations of the RC pulse are described in Equations 2.7 and 2.8.

$$p_{RC}(t) = \frac{T_{sym}}{\pi t} \sin\left(\frac{\pi t}{T_{sym}}\right) \frac{\cos\left(\frac{\beta \pi t}{T_{sym}}\right)}{1 - \frac{4\beta^2 t^2}{T_{sym}^2}}, \quad (2.7)$$

$$P_{RC}(f) = \begin{cases} T_{sym}, & 0 \leq |f| \leq \frac{(1-\beta)}{2T_{sym}} \\ \frac{T_{sym}}{2} \left[1 - \sin\left(\frac{\pi T_{sym}}{\beta} \left(f - \frac{1}{2T_{sym}}\right)\right) \right], & \frac{(1-\beta)}{2T_{sym}} \leq |f| \leq \frac{(1+\beta)}{2T_{sym}} \\ 0, & |f| > \frac{(1+\beta)}{2T_{sym}}. \end{cases} \quad (2.8)$$

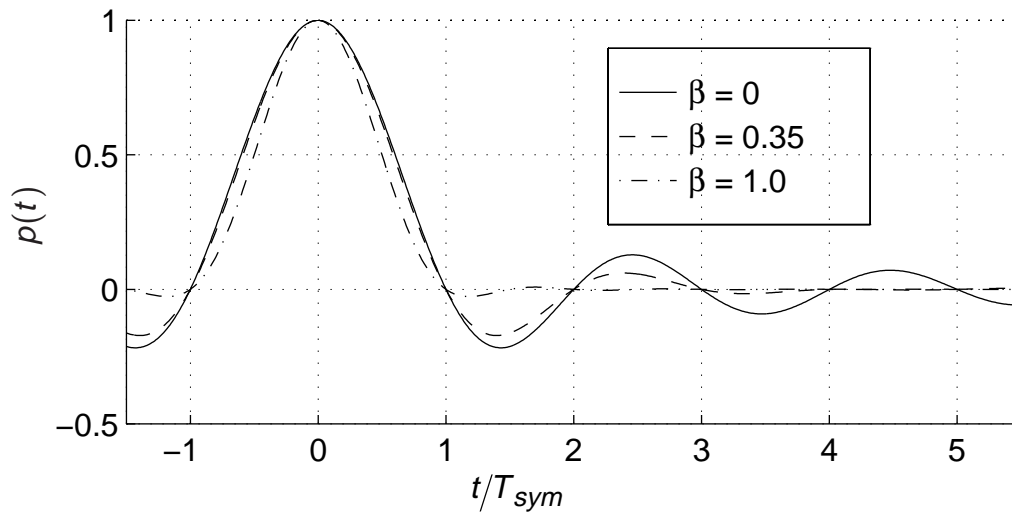


Figure 2.3: Raised Cosine Pulse (time domain)

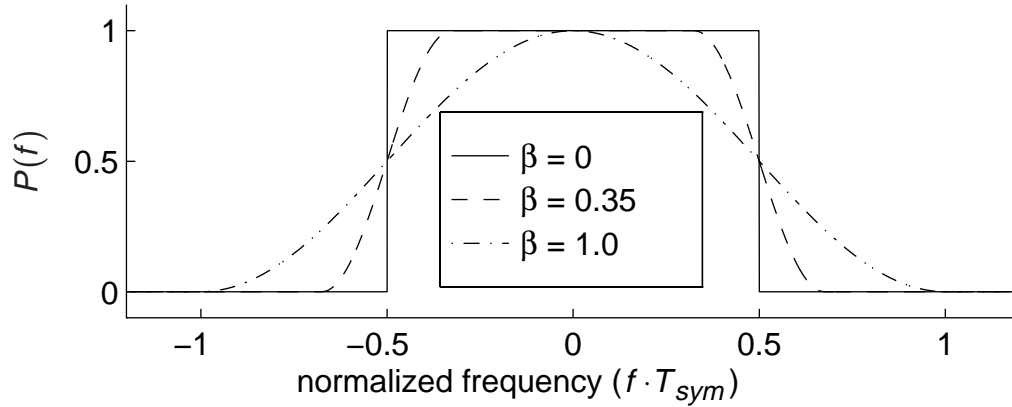


Figure 2.4: Raised Cosine Pulse (frequency domain)

Figures 2.3 and 2.4 illustrate the time and frequency domain characteristics of the RC pulse for $T_{sym} = 1$ and $\beta = 0, 0.35$, and 1 . A larger value of β results in a pulse which has greater bandwidth, but decays more rapidly in the time domain.

It is common practice to use a square root raised cosine (SQRC) pulse shape for $p(t)$, and incorporate a matched filter at the receiver, to improve the SNR of the received signal [Chennakeshu] [Hagmanns]. The matched filter has time and frequency characterization identical to that of the SQRC pulse.

$$P_{SQRC}(f) = \sqrt{T_{sym} P_{RC}(f)}, \quad (2.9)$$

$$\begin{aligned} p_{SQRC}(t) = & \frac{(1-\beta)}{\sqrt{T_{sym}}} \operatorname{sinc}\left(\frac{(1-\beta)t}{T_{sym}}\right) \\ & + \frac{\beta}{\sqrt{T_{sym}}} \cos\left(\frac{\pi t}{T_{sym}} - \frac{\pi}{4}\right) \operatorname{sinc}\left(\frac{\beta t}{T_{sym}} - \frac{1}{4}\right) \\ & + \frac{\beta}{\sqrt{T_{sym}}} \cos\left(\frac{\pi t}{T_{sym}} + \frac{\pi}{4}\right) \operatorname{sinc}\left(\frac{\beta t}{T_{sym}} - \frac{1}{4}\right), \end{aligned} \quad (2.10)$$

where the sinc function is defined as

$$\operatorname{sinc}(x) = \frac{\sin(\pi x)}{\pi x}. \quad (2.11)$$

A SQRC pulse with rolloff $\beta = 0.35$ is used in the IS-54 cellular radio standard [TIA] and within this thesis. The noncausal pulse can be approximated by truncating and delaying the ideal RC or SQRC pulse.

2.1.3 Carrier Modulation

The carrier modulation of the information-bearing signal $x(t)$ is mathematically expressed as multiplication by a complex sinusoid of the carrier frequency.

$$s(t) = \text{Re}\left[x(t)e^{j2\pi f_c t}\right]. \quad (2.12)$$

In the frequency domain, this has the effect of shifting the spectrum $X(f)$ from being centered around zero frequency (baseband) to the carrier frequency (passband). A complex baseband signal will have a real passband representation. In practice, a complex baseband signal is represented in Cartesian form by two signal channels: the in-phase (I) and quadrature (Q) channels. This doubles the information rate achievable with a real (as opposed to complex) baseband signal, with no increase in the bandwidth of the transmitted signal.

Equation (2.10) may be rewritten for implementation with real operations.

$$s(t) = x_I(t) \cos(2\pi f_c t) - x_Q(t) \sin(2\pi f_c t), \quad (2.13)$$

where $x_I(t) = \text{Re}[x(t)]$ and $x_Q(t) = \text{Im}[x(t)]$.

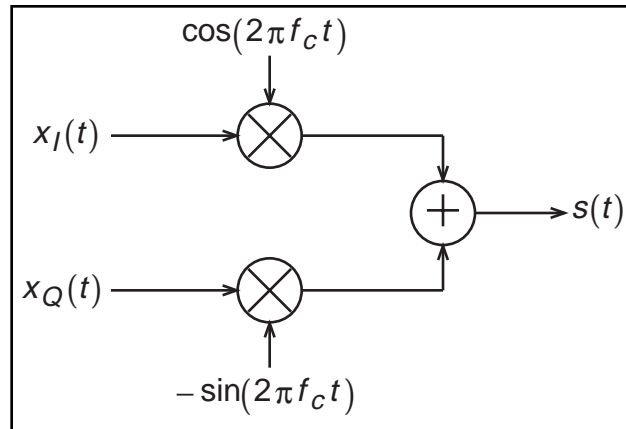


Figure 2.5: I and Q Channels in Modulation

The carrier frequency is chosen so as to allow for effective propagation of the signal as an electromagnetic wave, and to avoid interference with transmission from other devices. Regulatory bodies control the use of the radio spectrum for various devices and users.

2.1.4 RF Amplifier

Up to this point, the information has been represented digitally or as a low-power voltage signal. Before transmission, it is necessary to amplify the radio frequency (RF, or passband) signal to achieve sufficient signal power at the receiver. A measure of the quality of a signal is the signal-to-noise ratio (SNR),

$$SNR = \frac{\text{signal power}}{\text{noise power}}. \quad (2.14)$$

Different SNR's may be obtained by taking signal and noise power measurements at different points in the system. One of the most common is the SNR at the input to the receiver. In general, if the SNR is high, then the effect of noise on the signal is small and will cause few or no errors in the detection of the transmitted data.

The ideal RF amplifier accepts a passband voltage signal $s(t)$ as its input, and produces an output $s'(t)$ which is a scaled version of the input.

$$s'(t) = A s(t). \quad (2.15)$$

Real amplifiers approximate this linear behavior to varying degrees, but introduce nonlinearities such as saturation. Linearity and power efficiency are usually conflicting goals in amplifier design. This work assumes ideal linear amplification.

2.1.5 Antenna

The antenna is a passive circuit construction of conductors which converts its input electrical signal into electromagnetic waves which propagate through surrounding media. Antennas may be designed to accommodate a selected

signal bandwidth and direction of transmission. The principle of reciprocity as applied to antennas states that antenna characteristics such as selectivity of bandwidth and direction will be identical whether an antenna is used for transmission or reception. Antenna diversity, or the use of multiple transmit and/or receive antennas to improve transmission, is not investigated in this work, although the concepts in this thesis can be generalized to multiple antenna transceivers.

2.1.6 Channel

The wireless channel may refer to the media traversed by the signal between transmission and reception. It also refers to the their effect on the signal. This effect is commonly modeled by a channel impulse response (CIR) and additive white Gaussian noise.

Channel Impulse Response

The received signal is the convolution of the transmitted signal with the CIR $h(t)$. The CIR generally introduces time dispersion into the signal, which may result in ISI. A CIR with ISI has a frequency response $H(f)$ (the Fourier transform of $h(t)$) which is nonconstant (excepting a phase shift due to constant delay) over the bandwidth of interest. Thus, ISI is the time domain manifestation of frequency selective fading.

The nature of a wireless channel may change significantly with movement of the transmitter, receiver, or any other surrounding objects. This causes the CIR to vary with time. Such variation may be neglected over a sufficiently short interval of time, known as the coherence time of the channel. The coherence time depends on the rate of movement and the carrier frequency.

The channel attenuates the transmitted signal. A uniform attenuation across the entire signal bandwidth is known as flat fading. While this does not distort the signal, it is impossible to recover the loss in SNR, unless a method such as antenna diversity is used to obtain an alternate channel.

Noise

Noise generally refers to distortion which is independent of the signal of interest. It arises from sources such as other RF transmitters, electrical devices, and background electromagnetic emissions. Noise is also introduced by analog circuitry at the transmitter and receiver. Analog and digital circuitry also introduce distortions, such as quantization and amplifier nonlinearities, that have are difficult to analyze. These effects are often modeled as independent noise.

The noise statistics will vary with time and place. It is a common practice to model the combined effect of all noise sources as additive white Gaussian noise injected into the received signal.

2.1.7 Receiver Antenna

The receiver antenna converts the electromagnetic waves in its vicinity into electrical signals. The principle of reciprocity may be applied to the concatenation of transmit antenna, CIR, and receive antenna, to conclude that their net impulse response will be identical for signal transmission in either direction. This is useful for different signals utilizing the same carrier frequency, and over periods of time in which the CIR does not change appreciably.

2.1.8 RF Amplifier and Bandlimiter

The received signal is filtered to remove components outside of the bandwidth of the desired signal, and amplified.

2.1.9 Automatic Gain Control

Automatic gain control (AGC) scales the received signal so as to ensure a relatively constant average power. This allows analog and digital elements to minimize distortion due to effects such as thermal noise, quantization noise, and saturation. AGC error can result in an arbitrary scaling of the received signal

which may contribute to data errors if the data symbols are distinguished by magnitude.

2.1.10 Carrier Demodulation

Carrier demodulation recovers the baseband signal from the passband signal by multiplication with a sinusoid of the carrier frequency. The baseband signal has both I and Q components. Bandpass filtering is required as part of demodulation to remove undesired harmonics. Many systems incorporate heterodyning, in which the received signal is first demodulated to an intermediate frequency (IF), then to baseband.

2.1.11 Synchronization and Sampling

The signal experiences some delay in traversing the channel, and the receiver is required to implicitly estimate this delay in synchronizing itself to the received signal. Synchronization is complicated by the time dispersion introduced by the CIR, which causes the signal that is transmitted at any instant to arrive at the receiver over a range of delays. The sampling instant, or timing phase, may be chosen to coincide with the peak of a received symbol pulse, or to maximize the received signal power, or by some other criterion. Little or no information is lost in discarding the signal content between samples, as the signal has previously been bandlimited. Qureshi presents a more analytical discussion of the implications of timing phase [Qureshi, pp. 1372-1373].

Although the CIR $h(t)$ is physically a continuous function of time, it may be represented by a sampled equivalent $h(n)$ if we are only interested in the received signal after sampling. For a given $h(t)$, different $h(n)$ are available, depending on the timing phase. A hypothetical example of a CIR and one available sampled equivalent are shown in Figure 2.6.

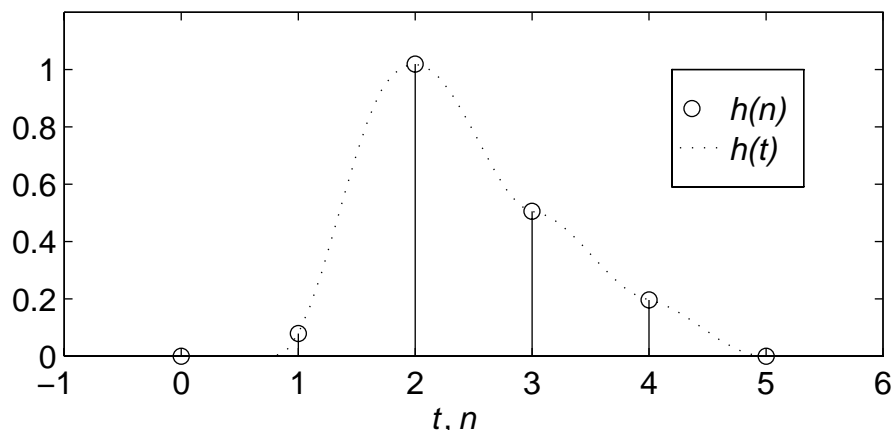


Figure 2.6: Continuous and Sampled CIR

Unless otherwise specified, the sampling period is equal to the symbol period T_{sym} . In some instances, it is desirable to sample at a higher rate.

If the sampled CIR has more than one nonzero sample, then it is usually necessary to choose which one corresponds to the main arrival or ray. All other nonzero elements represent ISI. ISI previous to the main ray is precursor ISI, while that following the main ray is postcursor ISI. In Figure 2.6, if $h(2)$ is chosen as the main ray, then $h(1)$ is a precursor, and $h(3)$, $h(4)$, and $h(5)$ are postcursors.

2.1.12 Equalization

Equalization has been defined in a general sense as “any device or signal processing algorithm that is designed to deal with intersymbol interference.” [Proakis, 554]. An equalizer may be located at the receiver (a post-equalizer) or at the transmitter (a pre-equalizer or precoder). A brief overview of equalization is found in Section 2.2. Equalization may be omitted if the amount of ISI is small enough that system performance is satisfactory without an equalizer.

2.1.13 Detection

The detector applies a decision rule to its input to estimate the original data sequence. The simplest rule is to choose the data symbol closest to each input

sample. Detection may be an integral part of the equalizer itself. The detected symbols are converted to their bit representation.

2.1.14 Criteria for Evaluation of a Digital Communications System

A wireless digital communications system may be characterized and evaluated by its performance and the required resources.

Performance:

Data rate is the (equivalent) number of bits which are transmitted and received per second.

Error performance is usually indicated by the bit error rate (BER), which is the average probability of a received bit being in error. The distribution of bit errors may also be of interest, as some error-correcting schemes are more effective against independent rather than correlated errors. The BER is often given as a function of the SNR at the input to the receiver.

Other performance criteria include outage, range of operation, and resistance to intentional interference (antijamming). Not all criteria are relevant for all systems.

Resources:

Bandwidth is the range of frequencies occupied by the transmitted signal. To avoid mutual interference, wireless transmissions must be sufficiently separated by some means, such as time, space, or frequency, or code, in the case of spread spectrum signals.

Power is required to generate the transmitted signal and to operate components at the transmitter and receiver. Power consumption is especially of concern for battery powered portable units.

Complexity may be roughly described as the number and sophistication of basic elements required to implement the system. Since this thesis focuses on digital equalization, complexity is usually expressed in the number of arithmetic operations required by equalization.

Size and Weight - The size and weight affect the mobility and convenience of use of portable transceivers.

Cost - The financial of designing, producing, and utilizing a communications system can serve as a general indicator of the resources required.

2.1.15 System Model for Analysis of Equalization

In order to focus on the equalization of a wireless communications system, some parts of the system are simplified. Figure 2.7 illustrates the simplified model of a one-way (or half-duplex) system which will be used for the most of this thesis.

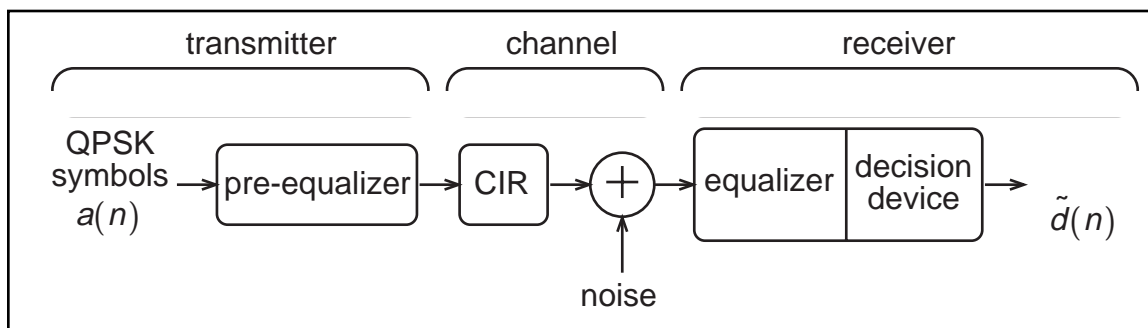


Figure 2.7: Simplified Model of Communications System

The pre-equalizer or (post) equalizer may be optional. The equalizers and CIR introduce a delay Δ between transmitted and received symbols. The correct or desired received symbol at time n is $a(n - \Delta)$, or $d(n)$.

Modeling of the transmitted signal and channel is simplified through use of the baseband equivalent [Proakis, pp. 148-153]. This may be roughly described as

removing the steps of carrier modulation and demodulation, and shifting the CIR from the passband to the baseband. $H(f)$ is effectively replaced by $H(f-f_c)$. Although the (passband) CIR will be real, its baseband equivalent may be complex. Thus, the signal and channel are represented by their complex baseband equivalents throughout the system. The benefit of doing so is to eliminate many redundant computations from time-domain analysis and simulation.

The CIR and all signals are discrete-time, usually at a sampling rate of $1/T_{sym}$. Samples of the Gaussian noise are independent, with the following probability distribution for both the real and imaginary parts [Proakis, page 23].

$$p(x) = \frac{1}{\sqrt{2\pi}\sigma_v} \exp\left(\frac{-x^2}{2\sigma_v^2}\right) \quad (2.16)$$

where σ_v^2 is the variance of the noise.

Full Duplex Communications

The model of a communications system shown in Figure 2.2 illustrates one-way, or half-duplex, communications. To achieve bidirectional or full duplex communications, each of the two communicating transceivers must have a transmitter and a receiver. Transmission from the base to the portable is called the forward link, and transmission from the portable to the base is called the reverse link.

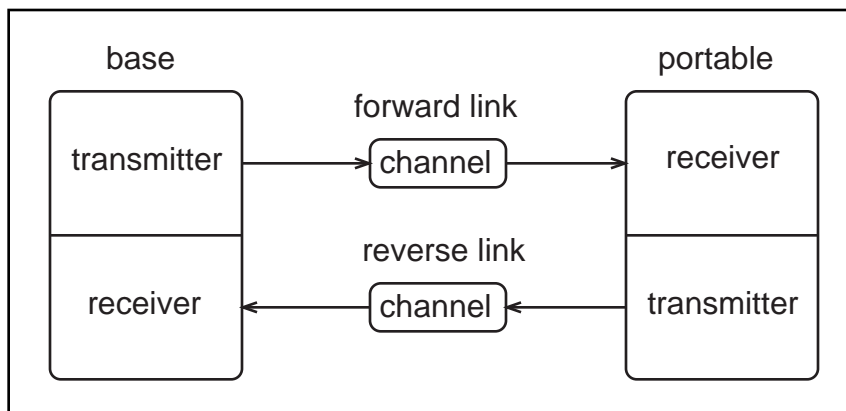


Figure 2.8: Full Duplex Wireless Communications System

Full duplex communications in a wireless system requires separation of forward and reverse link transmission. This separation may be accomplished in time, frequency, code (spread spectrum), or even signal polarization. Separation in time, by alternating between forward and reverse link transmission, is known as time division duplex (TDD).

2.2 Equalization

Equalization originated with the use of linear circuits (loading coils) to compensate for, or equalize, the non-ideal frequency response of twisted-pair telephone lines [Qureshi, page 1349]. This is a form of equalization by channel inversion, in which the frequency response of the equalizer is inversely proportional to that of the channel.

Equalization has since come to include signal processing applied to compensate for ISI. ISI is the time-domain manifestation of a nonconstant frequency response. Digital processing for equalization is often performed in the discrete time domain. All equalization in this thesis will be performed in this domain.

2.2.1 The Linear Transversal Equalizer

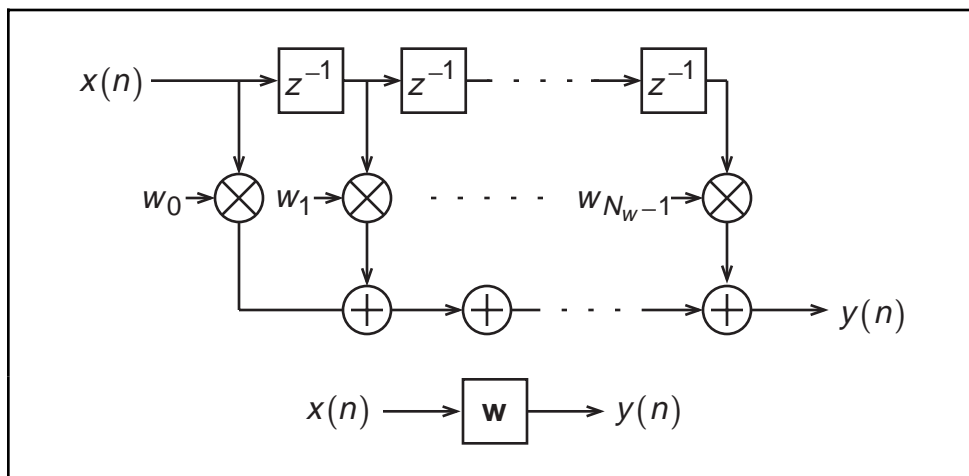


Figure 2.9: Linear Transversal Equalizer

The simplest digital equalizer is the linear transversal equalizer, shown in Figure 2.9. It implements the following convolution:

$$y(n) = \sum_{k=0}^{N_w-1} w_k x(n-k). \quad (2.17)$$

The w_k are the filter coefficients or tap-weights. The transversal filter may be represented by the vector \mathbf{w} ,

$$\mathbf{w} = [w_0 \ w_1 \ \cdots \ w_{N_w-1}]. \quad (2.18)$$

Variations on the Transversal Equalizer

Other structures, such as the lattice [Haykin, pp. 357-358] may be used to implement the same arithmetic operation with more desirable numerical properties, such as reduced sensitivity to finite precision arithmetic.

The transversal equalizer is usually placed at the receiver, but may also be used as a pre-equalizer, located at the transmitter [Lucky]. This may introduce undesirable time and frequency domain variations in the power of the transmitted signal.

A linear feedback equalizer [Proakis, pp. 572-576], implementing Equation 2.19, is possible, but is generally only useful when the filter coefficients are not adaptive. The output $y(n)$ is given by

$$y(n) = \sum_{j=0}^{N_w-1} w_j x(n-j) + \sum_{k=1}^{N_b} b_k y(n-k). \quad (2.19)$$

The performance of a linear feedback equalizer is nearly equivalent to that of a transversal equalizer. A feedback equalizer with predetermined and fixed coefficients may allow for equalization with fewer overall coefficients. If the equalizer is to be adaptive, the feedback equalizer must be carefully monitored for stability.

Zero Forcing Criterion

Some means must be established for determining the equalizer coefficients w_k . The zero forcing (ZF) criterion [Qureshi, pp. 1352-1353] [Proakis, pp. 555-561] provides a solution for the filter coefficients which minimizes the peak intersymbol interference in the equalized signal. For example, suppose a ZF transversal equalizer with 8 taps is applied to the following CIR (Figure 2.10).

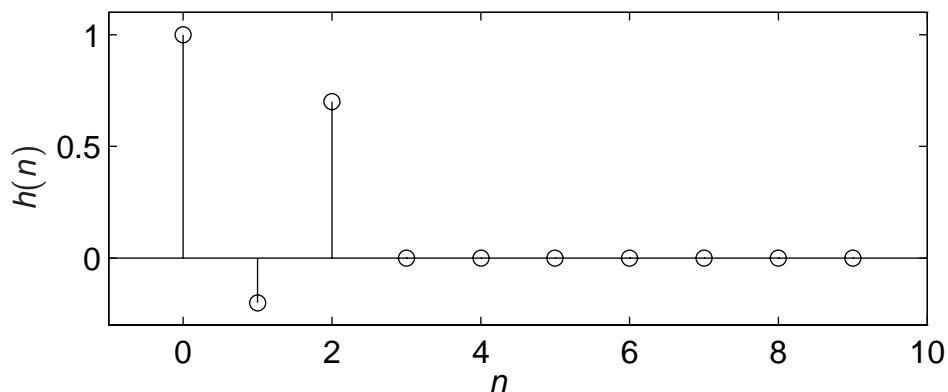


Figure 2.10: CIR of Channel to be Equalized

Figure 2.11 shows the CIR and equalizer frequency responses. The equalizer approximates the inverse of the channel frequency response, which reduces the ISI in the equalized signal. In doing so, the equalizer introduces a high gain around a normalized frequency of 0.2, which will amplify the additive noise. The net result is a reduction in ISI at the expense of a reduction in SNR. In cases such as this example where the channel frequency response is close to or equals zero at one or more frequencies (a spectral null), the ZF equalizer is not effective.

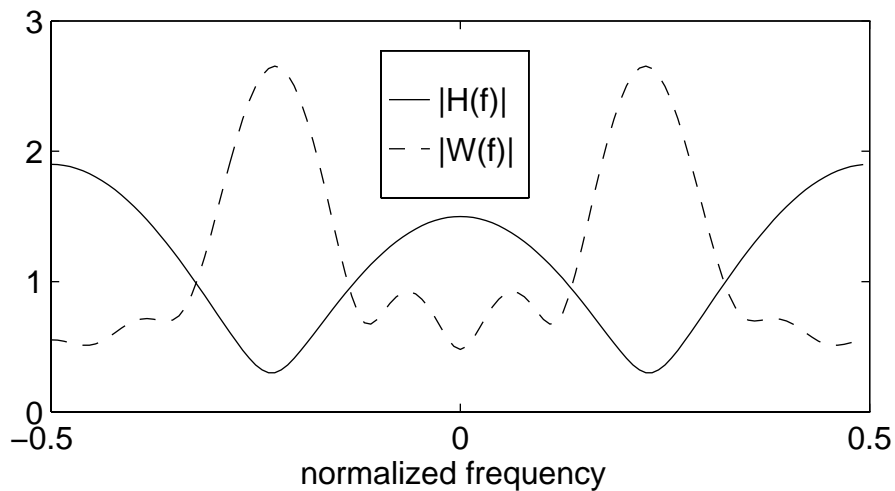


Figure 2.11: Equalizer and Channel (frequency domain)

The effective channel after equalization, $q(n)$, (Figure 2.12), is the convolution of the CIR and the equalizer taps. The frequency response, $Q(f)$, is shown in Figure 2.13.

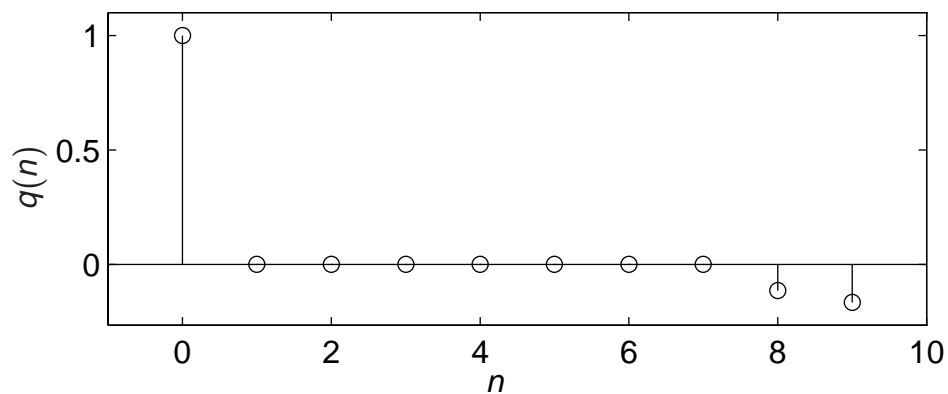


Figure 2.12: Equalized Channel (time domain)

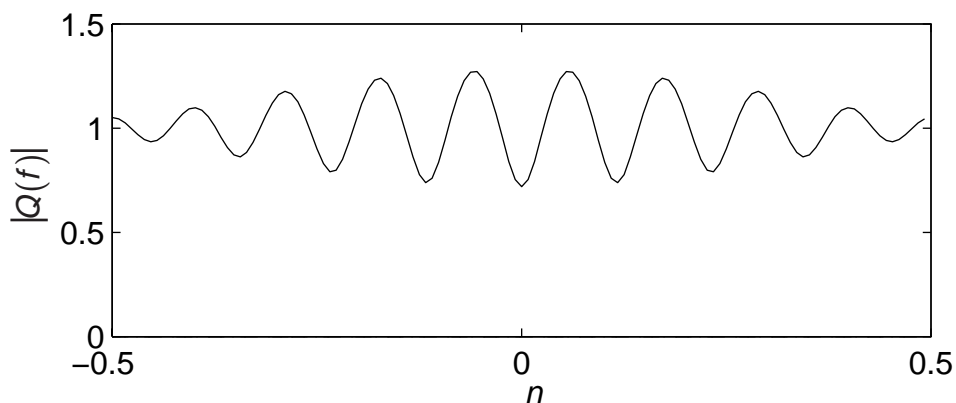


Figure 2.13: Equalized Channel (frequency domain)

Wiener solution

The Wiener solution [Haykin, pp. 158-185] [Qureshi, pp. 1352-1365] is closely related to ZF, but is slightly more robust. It is also known as the minimum mean square error (MMSE) criterion, as it seeks the equalizer which minimizes J , the mean-square value of the error signal.

$$J = E\left[|e(n)|^2\right] \quad (2.20)$$

The error signal $e(n)$ is the difference between the equalizer output $y(n)$ and the actual data symbol $d(n)$.

$$e(n) = d(n) - y(n). \quad (2.21)$$

This solution minimizes the combined error due to ISI and additive noise. When the SNR is high, the noise is of little effect and the Wiener equalizer approaches the ZF equalizer. Figure 2.14 illustrates the frequency responses of an 8-tap Wiener equalizer at varying SNR's, for the CIR shown in Figure 2.10.

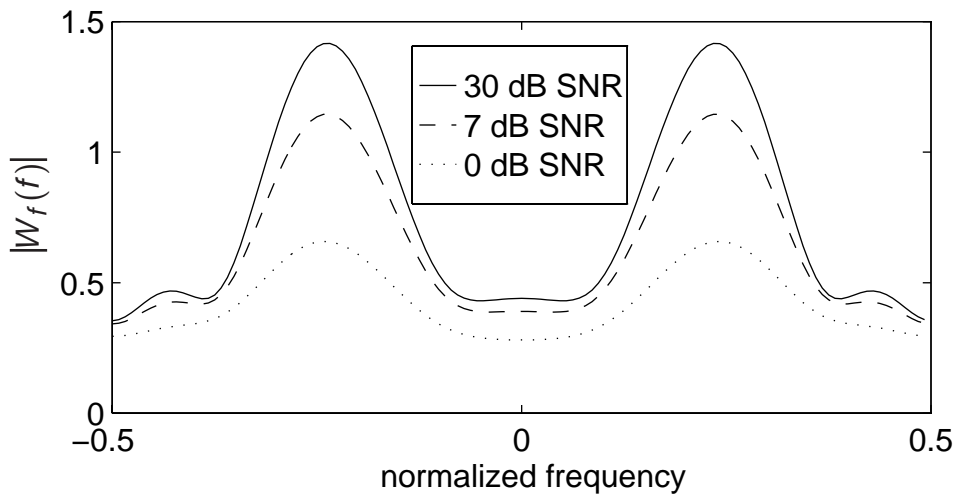


Figure 2.14: Frequency Response of Wiener (MMSE) Equalizer

Although this Wiener solution will have lower mean-square error (MSE) than the ZF solution, both are unable to effectively equalize the given channel due to the severity of the ISI, or alternatively, the near null in the channel frequency response.

Minimum Probability of Error (MPE) Characterization

The MPE criterion yields the equalizer characterization which minimizes the probability of a decision error [Shamash]. Although viewed as superior to the ZF or MMSE criteria, MPE is considerably more complex.

Fractionally Spaced Equalization

An equalizer with a tap spacing T_{eq} of less than T_{sym} is known as a fractionally spaced equalizer (FSE) [Gitlin1]. The optimal linear equalizer is equivalent to a T_{sym} spaced equalizer (TSE) with an infinite number of taps and a (continuous time) receiver filter matched to the received signal characteristics (including channel distortion) [Qureshi, page 1358]. In practice, a FSE is generally superior to a TSE as the former can adaptively synthesize an excess bandwidth matched filter. As well, a finite-length FSE is better able to synthesize an arbitrary delay characteristic to compensate for non-ideal timing phase than a finite TSE [Ungerboeck].

It might seem that a FSE would require more taps than a TSE, by a factor of T_{sym}/T_{eq} , so that the time spans of both equalizers are equal. However, the FSE can often equalize more effectively than the TSE, with little or no increase in the number of taps. A system employing a FSE may enjoy a compensatory reduction in complexity due to relaxed synchronization requirements. FSE/TSE comparisons often use the same number of taps for both equalizers.

2.2.2 The Decision Feedback Equalizer

Structure of the DFE

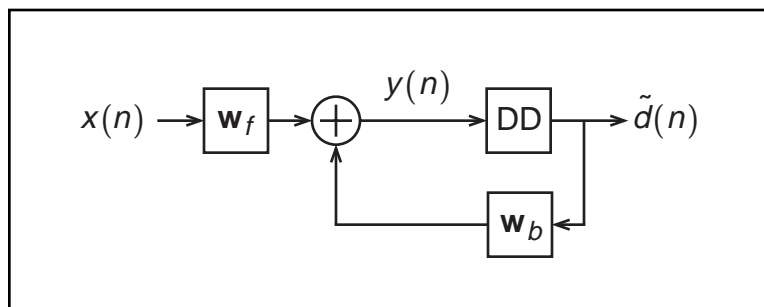


Figure 2.15: Decision Feedback Equalizer

Although decision feedback equalizer (DFE) is classified as a nonlinear equalizer, its structure is closely related to the linear transversal equalizer. It is characterized by N_f forward coefficients, and N_b feedback coefficients. The DFE implements the following input/output relation:

$$y(n) = \sum_{j=0}^{N_f-1} w_f(j)x(n-j) + \sum_{k=1}^{N_b} w_b(k)\tilde{d}(n-k). \quad (2.22)$$

While the quantized data symbol $\tilde{d}(n)$ is the most useful output in practice, the estimated symbol prior to quantization is used for analysis of the MSE performance. The decision device (DD) selects as its output the data symbol closest to its input. Equation (2.23) gives the quantization rule for QPSK.

$$\begin{aligned} \operatorname{Re}[\tilde{d}(n)] &= \begin{cases} -1, & \operatorname{Re}[y(n)] < 0 \\ +1, & \text{otherwise} \end{cases} \\ \operatorname{Im}[\tilde{d}(n)] &= \begin{cases} -1, & \operatorname{Im}[y(n)] < 0 \\ +1, & \text{otherwise.} \end{cases} \end{aligned} \quad (2.23)$$

When a decision error is made, so that $\tilde{d}(n) \neq d(n)$, this erroneous input to the FBF will result in generate an output which exacerbates, rather than cancels, subsequent ISI. This generally increases the probability of subsequent decision errors. This effect, known as error propagation, also complicates the analysis of the DFE. Error propagation is considered to have little impact on BER performance at high SNR's as the BER performance degradation due to error propagation may be overcome with a small increase in SNR.

Some forms of the DFE include a pre-equalizer (a transversal filter) at the transmitter [Salz] [Salazar] [Yang]. Salazar [Salazar] obtained a formulation for the DFE in which the FF contributes to the reduction of the postcursor ISI. The DFE may incorporate a fractionally spaced FF. Belfiore and Park [Belfiore] present a useful review of the DFE along with a modified DFE structure.

Heuristic Explanation

The following heuristic explanation may assist in understanding the rationale for decision feedback equalization. Consider that the ISI component of the equalizer input is deterministic, as it is completely determined by the CIR and the data sequence $d(n)$. With a perfect knowledge of both, an equalizer could perfectly reconstruct the precursor and postcursor ISI component of the received signal. The ISI may be subtracted from the received signal to yield the desired data sequence corrupted only by additive noise. The noise is not enhanced, as it would be in the case of a linear equalizer. Such a method of removing ISI without enhancing the additive noise would form a highly effective equalizer. However, this requires knowledge of the data sequence prior to equalization and detection. Mueller and Salz [Mueller] investigate the consequences of such ISI cancellation with prior knowledge of some of the data symbols.

The DFE exploits the equalizer's knowledge (with presumably high probability of correctness) of previously detected symbols to cancel the effect of their ISI on the current symbol. Thus, the feedback filter (FBF) removes postcursor ISI. The forward filter (FF) is itself a linear filter, which reduces only precursor ISI. It is worth mentioning that the FF is dependent on, and will alter, the postcursor ISI in the CIR. Thus, the FBF coefficients are usually not the negative of the CIR postcursors.

Minimum Mean Square Error Characterization and Performance

As with the linear equalizer, the mean square error (MSE) of the DFE is defined as the mean square value of the difference between the desired and estimated symbols (Equations 2.20, 2.21).

The MMSE is the minimum achievable MSE, given a CIR, noise power, and DFE with N_f forward taps and N_b feedback taps. The MMSE coefficients are the FF and FBF coefficients which yield the minimum mean square output error. MSE analysis of the DFE usually neglects the effect of error propagation by assuming that all past decisions (the input to the FBF) are correct.

An infinite DFE has a FF and FBF with infinite taps. Although not realizable, the infinite DFE is sometimes simpler to analyze, and may be approximated by a DFE with a sufficient number of taps. From Salz [Salz] the MMSE of an infinite-length DFE may be shown to be

$$J_{\min} = \exp \left\{ T_{\text{sym}} \int_{-\frac{1}{2T_{\text{sym}}}}^{\frac{1}{2T_{\text{sym}}}} \ln \left[\frac{N_0}{|H(f)|^2 + N_0} \right] df \right\}. \quad (2.24)$$

N_0 is the power spectral density of the complex additive white Gaussian noise.

$H(f)$ is the Fourier transform of the sampled CIR;

$$H(f) = \sum_{n=-\infty}^{\infty} h(n) e^{-j2\pi f n}.$$

Salz also showed that given a CIR and SNR, an infinite DFE will always achieve a MMSE equal to or less than an infinite linear equalizer.

The solution for the MMSE and MMSE coefficients for a non-infinite DFE is given in Chapter 4. The ZF solution is also applicable to the DFE, but with suboptimal MSE performance.

Bit Error Rate Performance

Error propagation complicates the BER analysis of the DFE. The BER may be determined analytically through the use of relatively benign assumptions, such as complete precursor cancellation by the FF [Austin]. If one wishes to avoid these assumptions, simulation is a recourse for estimating the BER performance of the DFE over a given channel.

The MMSE or ZF coefficients are usually applied to the DFE. The minimum probability of decision error (MPE) characterization of the DFE has been discovered [Shamash] [Belfiore]. This solution has found little application due to the computational complexity involved, and the satisfactory BER performance of the simpler MMSE DFE.

Based on the preceding heuristic explanation of the DFE, and its MSE performance, one might expect that the DFE achieves BER performance superior to that of the transversal equalizer. Although analytical results or proof of this are not generally attainable, simulations indicate that this is true. The DFE is significantly superior to the transversal equalizer for channels with spectral nulls.

2.2.3 Other Nonlinear Equalizers

TH Precoder

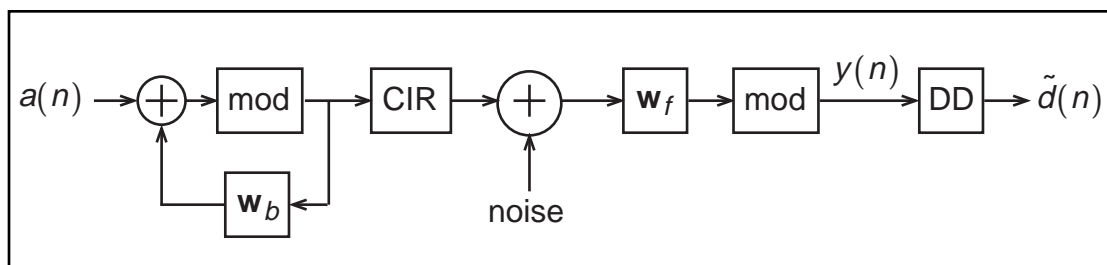


Figure 2.16: Tomlinson-Harashima Precoder

The Tomlinson-Harashima (TH) precoder [Tomlinson] [Harashima] is closely related to the DFE. In this context, the mod operator is a function which differs from the usual mathematical definition of modulo arithmetic, as follows:

If $y = \text{mod } x$ then

$$\begin{aligned} y &= x + 2kM, \\ \text{such that } -M &\leq y < M \\ \text{and } k &\text{ is an integer.} \end{aligned} \tag{2.25}$$

M is usually set to twice the largest data symbol coordinate. Other values of M are possible [Gibbard1, pp. 74-75]. For complex arithmetic, M is determined and this mod operator is applied independently to each coordinate. For example, if $M = 2$ then $\text{mod } 2.5 - j3 = (2.5 - 4) + j(-3 + 4) = -1.5 + j$.

The ZF characterization of the TH precoder is identical to that of a DFE under equivalent conditions [Pottie]. It has been demonstrated that the MMSE DFE coefficients, approximated by adaptive training, may be applied to the TH precoder with similar BER performance [Ebel] [Gibbard3].

An advantage of TH precoding is that a communications link with a TH precoder at the transmitter does not suffer from error propagation as would a DFE. This property is useful when the data has been coded for error correction [Proakis, page 440].

Viterbi Decoding

The Viterbi algorithm (VA) is “a maximum likelihood sequence estimator of the state sequence of a finite-state Markov process observed in memoryless noise” [Qureshi, page 1366] [Forney]. Although originally developed for use in decoding convolutional codes, it can also be applied to equalization.

The VA estimates the most likely sequence of transmitted data, rather than estimating the data symbol-by-symbol. It offers performance superior to that of the DFE or TH precoder, at the expense of increased complexity. The complexity is proportional to m^{L-1} , where m is the size of the symbol alphabet and L is the length of the sampled CIR (including the transmit and receive filters).

2.2.4 Adaptive Equalization

In a wireless communications system, the channel characteristics (CIR, noise power) are generally unknown. As well, the channel may be time-varying. Hence, an equalizer must be adapted to the channel, and possibly updated at regular intervals. This equalizer training is generally accomplished by transmitting a known data sequence (the training sequence). At the receiver, a training algorithm is applied to the desired and received signals to characterize the equalizer. An estimate of the CIR may or may not be formed as an intermediate step.

When the equalizer has been characterized, useful data may be transmitted, equalized, and detected. In most situations, the detected data has a high probability of equality to the transmitted data, and can be used to continue adaptive training. This is referred to as decision-directed training. Blind equalization trains the equalizer without the benefit of an initial training sequence [Proakis, pp. 587-593]. Decision-directed training and blind equalization are not investigated in this thesis.

Implicit Method

The implicit method of training computes equalizer coefficients without forming an explicit estimate of the CIR as an intermediate step. The LMS and RLS algorithms may be used to estimate the MMSE characterization of the linear equalizer or the DFE.

Least Mean Squares (LMS)

The LMS algorithm [Haykin, pp. 299-304] is one of the least complex training methods, in terms of operations per training symbol. It utilizes a stochastic estimate of the gradient of the MSE as a function of the equalizer tap weights. The weights are iteratively updated to reduce the MSE, according to the estimated gradient and a step-size parameter, μ . The length of training sequence required for convergence is generally longer than other methods, and varies according to μ and χ , the eigenvalue spread of the autocorrelation matrix of the received signal. If the spectrum of the channel has one or more nulls, χ will be large, and convergence difficult to achieve. If μ is too large, the algorithm may become unstable. LMS training may be applied to the linear equalizer or DFE. The LMS algorithm is generally not suitable for a mobile wireless channel because it cannot converge quickly enough to track changes in the channel.

Least Squares Methods

Least-squares (LS) methods yield a direct solution for the equalizer coefficients that minimize the sum of squared estimation errors for each training symbol. Over a reasonable training interval and conditions, this solution converges to the MMSE solution. LS methods are available in varying degrees of computational complexity. The explicit LS solution requires $O(N^3)$ arithmetic operations to obtain the LS solution for an N -tap equalizer. The Recursive Least Squares (RLS) algorithm uses the matrix inversion lemma to recursively update the LS solution for each training symbol, with $O(N^2)$ operations per training symbol [Haykin, pp. 480-485]. The 'fast' LS methods yield a recursive solution with $O(N)$ operations per training symbol [Haykin, pp. 570-678].

LS methods converge rapidly, requiring a number of training symbols on the order of the number of taps, and are relatively insensitive to the eigenvalue spread of the channel (χ). The main concerns with LS methods are computational complexity and stability.

The RLS algorithm [Haykin, page 485] is used to investigate adaptive training of the equalizers in this thesis, except where least squares channel estimation (LSCE) is specified.

An approximate initialization of the RLS algorithm is obtained by

$$\mathbf{P}(0) = \delta^{-1} \mathbf{I}_{N_f + N_b}$$

where δ is a small positive constant. A typical value, assuming that AGC scales the received signal $u(n)$ to approximately unity magnitude, is $\delta = 0.01$.

$\mathbf{I}_{N_f + N_b}$ is the identity matrix of dimensions $N_f + N_b$.

$$\mathbf{w}(0) = \mathbf{0}$$

For each symbol of the training sequence $n = 1, 2, \dots$ compute

$$\pi(n) = \mathbf{U}^H(n) \mathbf{P}(n-1)$$

$$\kappa(n) = \lambda + \pi(n) \mathbf{U}(n)$$

$$\mathbf{k}(n) = \frac{\mathbf{P}(n-1) \mathbf{U}(n)}{\kappa(n)}$$

$$\alpha(n) = d(n) - \mathbf{w}^H(n-1) \mathbf{U}(n)$$

$$\mathbf{w}(n) = \mathbf{w}(n-1) + \mathbf{k}(n) \alpha^*(n)$$

$$\mathbf{P}(n) = \frac{1}{\lambda} (\mathbf{P}(n-1) - \mathbf{k}(n) \pi(n))$$

$u(n)$ is the received signal,

$$\mathbf{u}(n) = [u(n) \ u(n-1) \ \dots \ u(n-N_f+1)]^T$$

$d(n)$ is the training symbol received at time n ,

$$\mathbf{d}(n-1) = [d(n-1) \ d(n-2) \ \dots \ d(n-N_b)]^T$$

$$\mathbf{U}(n) = \begin{bmatrix} \mathbf{u}(n) \\ \mathbf{d}(n-1) \end{bmatrix}$$

$\mathbf{w}_f = [w_f(0) \ w_f(1) \ \dots \ w_f(N_f-1)]^T$ is the FF tap-weight vector.

$\mathbf{w}_b = [w_b(1) \ w_b(2) \ \dots \ w_b(N_b)]^T$ is the FBF tap-weight vector.

$\mathbf{w}(n) = \begin{bmatrix} \mathbf{w}_f \\ \mathbf{w}_b \end{bmatrix}$ is the combined tap-weight vector at time n .

A superscripted H indicates Hermitian transposition, and the asterisk indicates complex conjugation.

Explicit Method

The explicit method of training first estimates the CIR (and possibly noise power or statistics), then computes an appropriate set of equalizer coefficients from this estimate [Shuckla] [Crozier1]. LMS [Shukla] or LS methods [Crozier2] may be used for the channel estimation. Explicit training has received both positive [Shuckla] and mixed [Gibbard1] reviews in the literature. Implicit training is more prevalent in practice. Explicit training is more useful where the sampled CIR is rapidly varying, with a small number of significant precursors and postcursors.

Training of Fractionally Spaced Equalizers

The LMS algorithm [Gitlin2] and LS algorithms [Falconer] [Cioffi] are applicable to fractionally spaced equalizers (transversal and DFE).

This thesis uses a straightforward modification of the RLS algorithm for training of the fractionally spaced DFE. $u(n)$ is the received signal with a sampling period of T_{eq} (rather than T_{sym}), and the training computations are performed once per

training symbol. Otherwise, this fractionally spaced RLS algorithm is identical to the T_{sym} spaced version described previously.

2.3 Conclusion

While this overview of communications and equalization is by no means complete, it is hoped that it will assist the reader in understanding the relevance and implications of the remainder of this thesis. Many crucial parts of the communications system have been omitted, so as to emphasize those parts that have more relevance to equalization. The references given in this chapter, especially the texts ([Proakis], [Haykin]), provide greater depth of coverage of these topics to the interested reader.

3. Asymmetric Equalization

This chapter defines and reviews the concept of asymmetric equalization, and some previous research in this area.

3.1 Asymmetric Complexity

The complexity of equalization may be roughly defined as the number and sophistication of components or arithmetic operations required for its implementation. This complexity may have a significant effect on the size, weight, cost, and power requirements of a transceiver. For example, Gibbard estimates that equalization of an indoor wireless link is commercially feasible at data rates of up to about 20 Mb/s, using 2 high-performance programmable DSP chips (LSI Logic L64260 high speed versatile FIR filter) which would consume 3 watts power [Gibbard1, pp. 100-101].

Symmetric and asymmetric equalization refer to the distribution of complexity between transceivers. Symmetric equalization implies an equal distribution of complexity. Asymmetric equalization implies an unequal distribution, and more specifically refers to an intentional shift of complexity from one transceiver to the other, while maintaining effective equalization of both links. Full asymmetry is achieved if all complexity relating to equalization is transferred to one transceiver.

Asymmetric equalization utilizes pre and post-equalization. In general, asymmetry is achieved by using pre-equalization and post-equalization at the base to equalize the forward and reverse links with little or no equalization performed at the portable. Figure 3.1 illustrates a hypothetical fully asymmetric system.

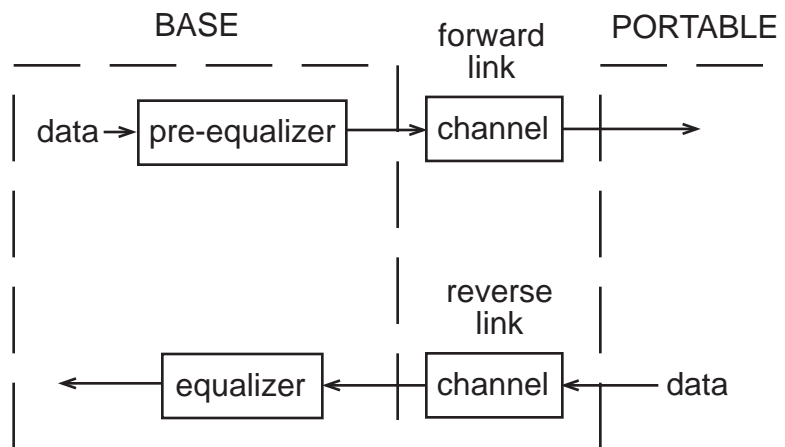


Figure 3.1: Asymmetric System

The complexity of equalization may be divided into two main parts: (1) characterization of the adaptive equalizer, and (2) processing or equalization of the data signal. Reciprocity may be useful in reducing the complexity of characterization, by using the same or similar parameters for pre and post-equalization.

3.2 Target System

This thesis investigates equalization of an indoor wireless communications system, which will be referred to as the target system. It is intended to permit wireless access to wired computer network via a portable computer equipped with a wireless transceiver. This transceiver is referred to as the portable. The portable communicates with the wired network through a fixed base station, referred to as the base.

It is assumed that equalization is required to mitigate the effects of ISI, as is generally the case for indoor wireless communication at symbol rates above 1 MHz [Despins]. As the portable or its surroundings may move during transmission, the channel is time variant and adaptive equalization is required.

This thesis will only consider the case of a single base and portable. The extension to multiple portables and/or base stations is likely in a real system, but

not considered here. Another potentially useful extension is to equip the base with multiple antennas.

Data transmission is in time-division duplex (TDD) format, alternating between forward and reverse link frames. Both links utilize the same carrier frequency so that the passband CIR's are identical, according to the principle of reciprocity. The frames are of sufficiently short duration so that the channel changes little over a pair of subsequent frames. Thus, adaptive equalization parameters determined at the beginning of a reverse link frame will be applicable up to the end of the next forward link frame.

In the target system, the base is stationary and its size and weight are of little concern. The size and weight of the portable must be minimized so that it is convenient to transport and use. The base has electrical power available from fixed connections, while the portable must rely on batteries. The batteries contribute to the size and weight of the portable, and require charging. One base may serve a number of portable units, so the cost of the portables will have a greater effect than that of the base on the overall cost of the system.

Thus, it is desirable to apply asymmetric equalization to the target system to reduce the complexity of the portable.

3.3 Previous Results

There are some proposals and results for asymmetric equalization extant in the literature, although it is often not termed as such. The term asymmetry, or asymmetric signal processing, was first applied to the shifting of equalization complexity by Gibbard et al. [Gibbard3]. The reader is cautioned that the terms asymmetry or asymmetric are used otherwise in the literature. For example, it has been used to refer to an imbalance between the I and Q channels [Sari], or differing forward/reverse link data rates [Stephens].

Zhuang et al. [Zhuang1] propose an asymmetric system employing a linear pre-equalizer and a DFE. Reciprocity is exploited in the characterization of the pre-equalizer. Another system by Zhuang et al. [Zhuang2] uses nonlinear phase precoding.

Other asymmetric systems have been proposed, which also exploit reciprocity to characterize the pre-equalizer [Karr] [Korevaar].

Gibbard System

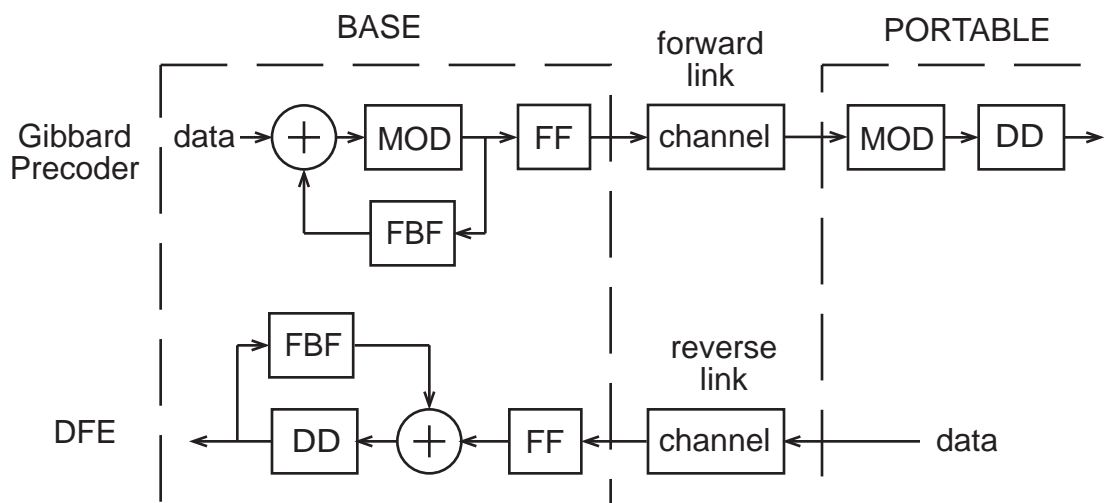


Figure 3.2: Gibbard System

Gibbard et al. [Gibbard3] propose an asymmetric system with a DFE and a modified TH precoder, or Gibbard precoder, located at the base (Figure 3.2). A TH precoder normally incorporates a FF at the receiver, but the Gibbard precoder locates the FF at the transmitter, with similar effect.

The performance of the modified TH precoder is close to that of a normal TH precoder, which is also close to that of the DFE. The Gibbard system has been shown to effectively equalize the indoor wireless multipath channel.

A high degree of asymmetry is achieved as the only equalization function implemented at the portable is the modulo operation. Reciprocity is exploited by

using the DFE parameters to directly characterize the precoder FF and FBF. Thus, additional training is not required for the forward link equalization.

The precoder is shown to advantageously shape the power spectrum of the transmitted signal. Transmit power is reduced at frequencies corresponding to deep spectral nulls in the CIR. This is a property of the MMSE (or LS) FF.

Two drawbacks of the Gibbard system are the computational requirements at the base, and the AGC sensitivity at the portable. The pre-equalizer requires more full-precision multiplications per symbol than does the DFE, since the input to the precoder FBF is not quantized data symbols.

As the FF associated with the forward link is located at the transmitter, it is unable to adaptively correct for amplitude variations in the received signal. Thus the portable must have very precise AGC because any scaling of its received signal will change the effective modulo operator levels. An AGC error of 1 dB may cause a tenfold increase in the BER [Gibbard3].

3.4 Conclusion

Asymmetric equalization is desirable when the complexity of one transceiver (typically the portable) is to be minimized at the expense of the other (the base). It can be achieved by combining conventional equalizers, such as the DFE and TH precoder. Reciprocity may be useful in the characterization of asymmetric equalization systems.

4. The ADFE

This chapter introduces a new equalizer structure, dubbed the asymmetric decision feedback equalizer (ADFE). The ADFE system, which employs a DFE and an ADFE to equalize bidirectional communications, is also introduced. The MSE characterization and performance of the ADFE is analyzed and compared with that of the DFE in Section 4.2. Section 4.3 presents the training of the ADFE system. Section 4.4 outlines the adaptive training of the ADFE system, and Section 4.5 analyzes the inclusion of a fractionally spaced forward filter in the ADFE and the ADFE system.

4.1 ADFE and ADFE System

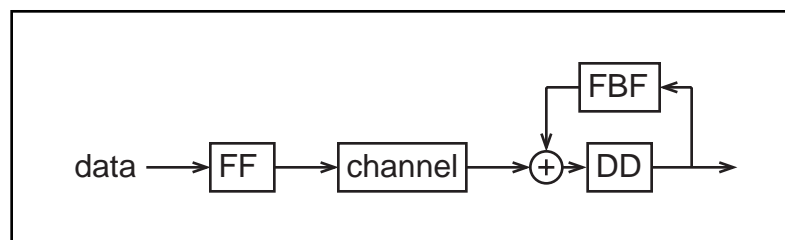


Figure 4.1: ADFE

The asymmetric decision feedback equalizer (ADFE) is an equalizer which consists of a FF at the transmitter, and a FBF at the receiver. It is similar to the DFE, described in Chapter 2, which consists of a FF and FBF at the receiver. In both equalizers, the FF reduces precursor ISI and the FBF cancels postcursor ISI.

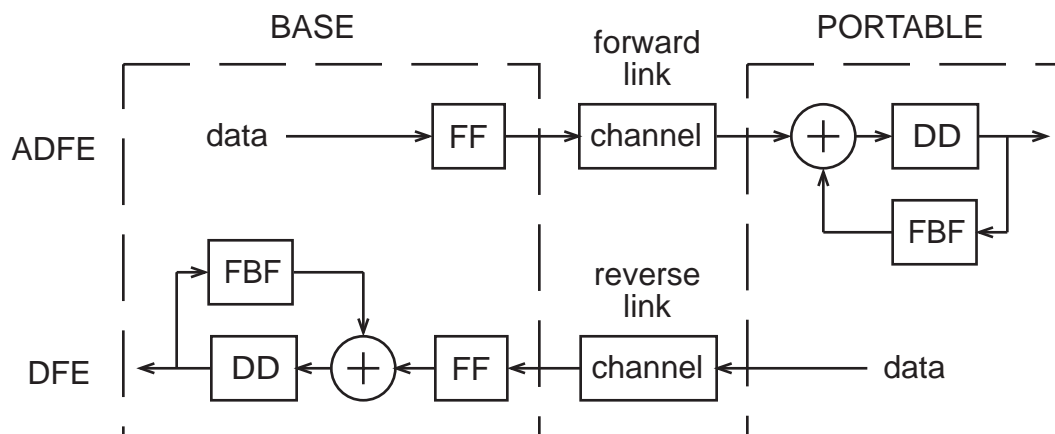


Figure 4.2: ADFE system

The ADFE system is a means of equalizing TDD communications between a base and portable. It includes a DFE to equalize the reverse link, and an ADFE to equalize the forward link. As will be shown, the adaptive characterization and the execution of the FBF at the portable may be simplified considerably. This simplification of the portable unit results in a highly asymmetric equalization system.

4.2 MSE Characterization and Performance of ADFE

The MSE often serves as a useful metric of performance of an equalizer, as it usually leads to a much more tractable analysis than does the BER. This section deals with the MSE optimization and performance of the ADFE. The effect of error propagation is neglected.

ADFE Without Power Constraint

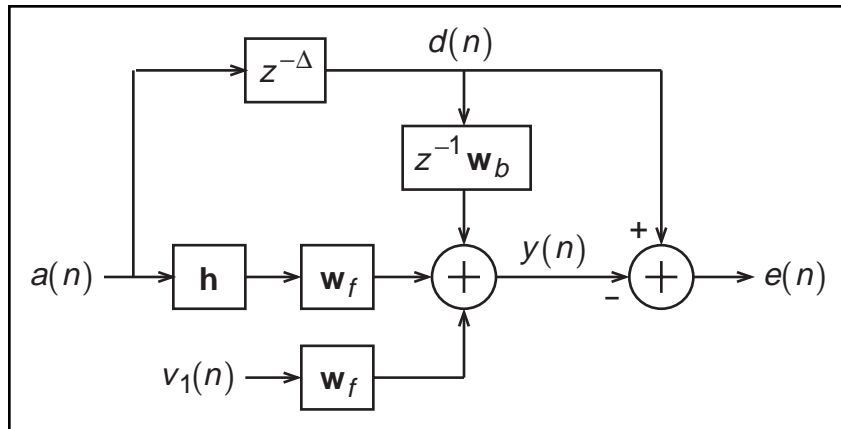


Figure 4.3: DFE Model

An initial investigation into the MSE performance of the ADFE with an optimum and infinite-length FF, and no constraint on transmitted power, may be made using Equation 2.24.

$$J_{\min} = \exp \left\{ T_{\text{sym}} \int_{-\frac{1}{2T_{\text{sym}}}}^{\frac{1}{2T_{\text{sym}}}} \ln \left[\frac{N_0}{|H(f)|^2 + N_0} \right] df \right\}. \quad (2.24)$$

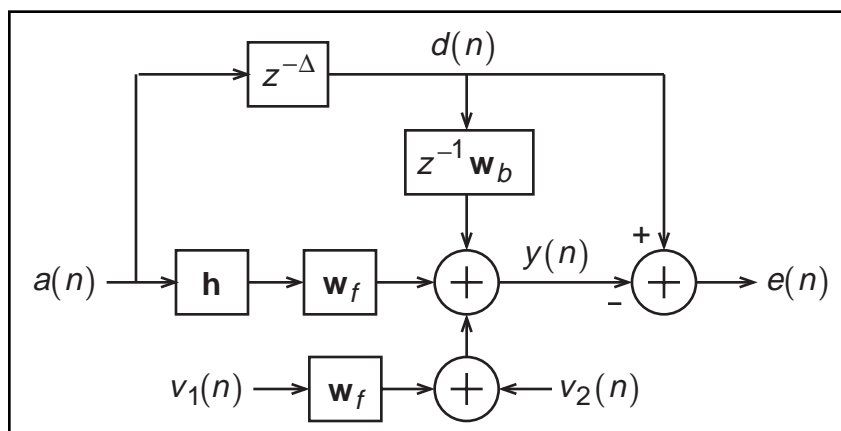


Figure 4.4: Modified DFE Model

The DFE of Figure 4.3 may be modified by adding another noise source, $v_2(n)$, which is not filtered by \mathbf{w}_f . The reason for this modification is to obtain a MSE model that applies to the ADFE. As the CIR (\mathbf{h}) and the FF (\mathbf{w}_f) represent linear convolutions, they may be commuted without otherwise affecting the system. Figure 4.3, which incorporates these modifications, approaches an ADFE with noise $v_2(n)$, as the power in the noise $v_1(n)$ approaches zero. The MMSE of the ADFE is indicated by the following limit, based on Equation 2.24:

$$J_{\min,ADFE} = E[v_2^2(n)] + \lim_{N_0 \rightarrow 0} \exp \left\{ T_{sym} \int_{-\frac{1}{2T_{sym}}}^{\frac{1}{2T_{sym}}} \ln \left[\frac{N_0}{|H(f)|^2 + N_0} \right] df \right\}. \quad (4.1)$$

The limit approaches zero as long as $|H(f)|^2 \neq 0$. This MMSE ADFE equalizer is apparently related to the ZF-DFE [Ebel, page 29], as both endeavor to eliminate ISI without regard for noise. This result would not be desirable in an implementation of the ADFE, as the transmit power spectrum may become very large for frequencies over which $|H(f)|^2$ is small. As this analysis places no constraint on the transmitted power, the optimum FF may introduce an arbitrary power gain in the transmitted signal and alter the SNR.

ADFE with Power Constraint

For the remainder of this thesis, a modification will be incorporated into the ADFE to allow for a more realistic analysis. A gain factor, equal to the inverse of the norm of the FF, is introduced following the FF. This gain constrains the transmitted power so that the received SNR is independent of the FF. An inverse gain is inserted at the receiver, as shown in Figure 4.5.

This modification reflects the practical limitation of transmitted power. A real system has many gains which are usually not explicitly represented in the analysis of post-equalizers (such as the DFE) because the FF may introduce an arbitrary gain without affecting the SNR.

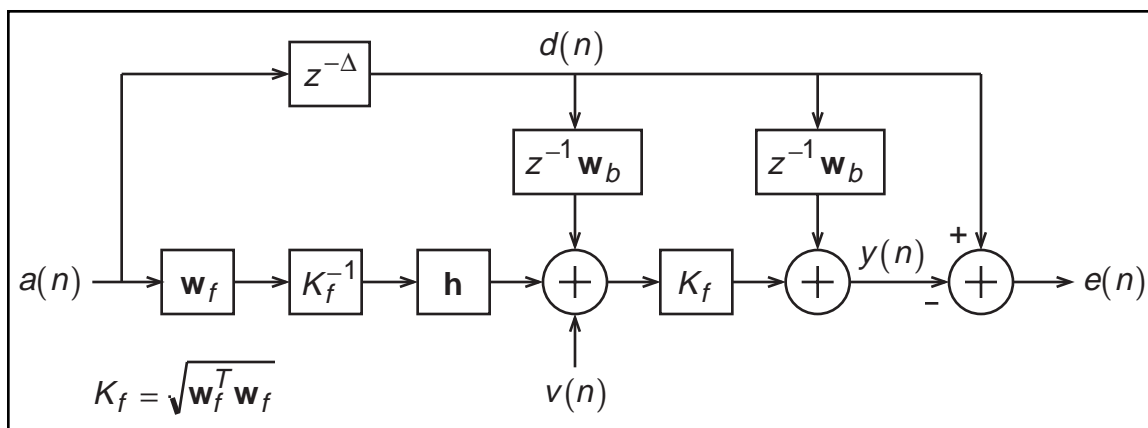


Figure 4.5: ADFE Model with Constrained Transmit Power

With these two complementary gains, the magnitude of the equalized signal is approximately equal to that of the desired signal. If phase modulation (such as BPSK or QPSK) is used, it is not necessary in practice to estimate and implement the gain at the receiver, as the output of the decision device is a function of the phase (not magnitude) of its input. However, this gain is necessary for the MSE analysis.

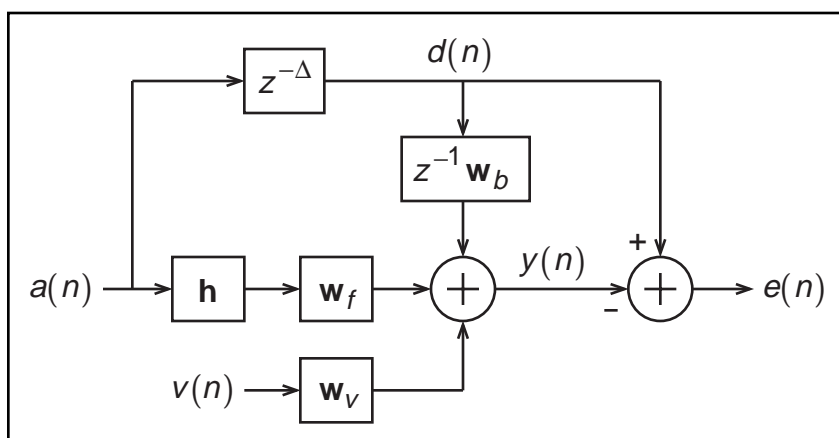


Figure 4.6: DFE / ADFE Model

Figure 4.6 is equivalent to the modified ADFE of DFE, depending on the definition of the noise filter \mathbf{w}_v . Thus, the following MSE analysis of Figure 4.6 is applicable to either equalizer. This analysis assumes BPSK data with real signals and filters, but may be extended to encompass complex signals and filters.

Representations of Filters

$\mathbf{w}_f = [w_f(0) \ w_f(1) \ \dots \ w_f(N_f - 1)]^T$ is the FF of the equalizer.

$\mathbf{w}_b = [w_b(1) \ w_b(2) \ \dots \ w_b(N_b)]^T$ is the FBF of the equalizer.

$\mathbf{h} = [h(0) \ h(1) \ \dots \ h(N_h - 1)]^T$ is the sampled channel impulse response.
 $h(k) = 0$ for $k < 0$ and $k \geq N_h$.

\mathbf{w}_v shapes the noise input to the decision device.

$$\mathbf{w}_v = \begin{cases} \mathbf{w}_f & \text{DFE} \\ \left[\sqrt{\mathbf{w}_f^T \mathbf{w}_f} \ \mathbf{0}_{N_f-1}^T \right]^T & \text{ADFE} \end{cases}$$

z^{-k} is a delay of k samples.

As all filters are causal, Δ is the synchronization delay between transmitted and detected symbols.

Representations of Signals

$a(n)$ is the sequence of transmitted data symbols.

$$\begin{aligned} P(a(n) = -1) &= 0.5, \\ P(a(n) = 1) &= 0.5, \\ E[a(n)a(n-k)] &= \delta(k), \end{aligned}$$

$$\mathbf{A}(n) = \begin{bmatrix} a(n) & a(n-1) & \dots & a(n-N_f+1) \\ a(n-1) & a(n-2) & \dots & a(n-N_f) \\ \vdots & \vdots & \ddots & \vdots \\ a(n-N_h+1) & a(n-N_h) & \dots & a(n-N_f-N_h+2) \end{bmatrix},$$

$d(n)$ is the desired symbol, or the symbol to be detected at time n .

$$d(n) = a(n - \Delta),$$

$$\mathbf{d}(n-1) = [d(n-1) \ d(n-2) \ \dots \ d(n-N_b)]^T.$$

$v(n)$ is additive white Gaussian noise.

$$\begin{aligned}
E[v(n)] &= 0, \\
E[v(n)v(n-k)] &= \delta(k)\sigma_v^2, \\
E[v(n)a(n-k)] &= 0, \\
\mathbf{v}(n) &= [v(n) \ v(n-1) \ \dots \ v(n-N_f+1)]^T.
\end{aligned}$$

$u(n)$ is the received signal without the noise component, in the ADFE. It is the received signal filtered by the FF and without the noise component, in the DFE.

$$u(n) = \mathbf{h}^T \mathbf{A}(n) \mathbf{w}_f.$$

$y(n)$ is the equalized signal, and the input to the decision device,

$$y(n) = u(n) + \mathbf{w}_v^T \mathbf{v}(n) + \mathbf{w}_b^T \mathbf{d}(n-1).$$

$e(n)$ is the error signal,

$$e(n) = d(n) - y(n).$$

The MMSE coefficients \mathbf{w}_f and \mathbf{w}_b , which minimize the mean-square error, J , are sought.

$$J = E[e^2(n)], \tag{4.2}$$

$$J = E\left[\left(d(n) - u(n) - \mathbf{w}_v^T \mathbf{v}(n) - \mathbf{w}_b^T \mathbf{d}_{Nb}(n-1)\right)^2\right], \tag{4.3}$$

$$\begin{aligned}
J &= E[d^2(n)] + \mathbf{w}_f^T E[\mathbf{A}^T(n) \mathbf{h} \mathbf{h}^T \mathbf{A}(n)] \mathbf{w}_f + \\
&\quad \mathbf{w}_b^T E[\mathbf{d}_{Nb}(n-1) \mathbf{d}_{Nb}^T(n-1)] \mathbf{w}_b - 2 \mathbf{w}_f^T E[d(n) \mathbf{A}^T(n)] \mathbf{h} \\
&\quad - 2 \mathbf{w}_f^T E[\mathbf{A}^T(n) \mathbf{h} \mathbf{d}_{Nb}^T(n-1)] \mathbf{w}_b \\
&\quad + \mathbf{w}_v^T E[\mathbf{v}(n) \mathbf{v}^T(n)] \mathbf{w}_v.
\end{aligned}$$

The following correlation matrices may be used to simplify the above expression.

$$\mathbf{R}_1 = E[\mathbf{A}^T(n) \mathbf{h} \mathbf{h}^T \mathbf{A}(n)] = \begin{bmatrix} r_{hh}(0) & r_{hh}(1) & \dots & r_{hh}(N_f-1) \\ r_{hh}(1) & r_{hh}(0) & \dots & r_{hh}(N_f-2) \\ \vdots & \vdots & \ddots & \vdots \\ r_{hh}(N_f-1) & r_{hh}(N_f-2) & \dots & r_{hh}(0) \end{bmatrix},$$

$$r_{hh}(k) = \sum_{j=0}^{Nh-k-1} h(j)h(j+k),$$

$$\mathbf{r}_2 = \mathbb{E} \left[d(n) \mathbf{A}^T(n) \right] \mathbf{h} = \begin{bmatrix} h(\Delta) \\ h(\Delta-1) \\ \vdots \\ h(\Delta - N_f + 1) \end{bmatrix},$$

$$\mathbf{R}_3 = \mathbb{E} \left[\mathbf{A}^T \mathbf{h} d^T(n-1) \right],$$

$$\mathbf{R}_3 = \begin{bmatrix} h(\Delta+1) & h(\Delta+2) & \cdots & h(\Delta+N_b) \\ h(\Delta) & h(\Delta+1) & \cdots & h(\Delta+N_b-1) \\ \vdots & \vdots & \ddots & \vdots \\ h(\Delta-N_f+2) & h(\Delta-N_f+3) & \cdots & h(\Delta-N_f+N_b+1) \end{bmatrix},$$

$$J = 1 + \mathbf{w}_f^T \mathbf{R}_1 \mathbf{w}_f + \sigma_v^2 \mathbf{w}_v^T \mathbf{w}_v + \mathbf{w}_b^T \mathbf{I}_{N_b} \mathbf{w}_b - 2 \mathbf{w}_f^T \mathbf{r}_2 - 2 \mathbf{w}_f^T \mathbf{R}_3 \mathbf{w}_b. \quad (4.4)$$

For both the DFE and ADFE, $\mathbf{w}_v^T \mathbf{w}_v = \mathbf{w}_f^T \mathbf{w}_f$.

$$J = 1 + \mathbf{w}_f^T \left(\mathbf{R}_1 + \sigma_v^2 \mathbf{I}_{N_f} \right) \mathbf{w}_f + \mathbf{w}_b^T \mathbf{I}_{N_b} \mathbf{w}_b - 2 \mathbf{w}_f^T \mathbf{r}_2 - 2 \mathbf{w}_f^T \mathbf{R}_3 \mathbf{w}_b. \quad (4.5)$$

The expression for J may be rendered more compact by combining some matrices as follows:

$$\mathbf{w} = \begin{bmatrix} \mathbf{w}_f \\ \mathbf{w}_b \end{bmatrix} \quad \mathbf{R} = \begin{bmatrix} \mathbf{R}_1 & \mathbf{R}_3 \\ \mathbf{R}_3^T & \mathbf{I}_{N_b} \end{bmatrix} \quad \mathbf{p} = \begin{bmatrix} \mathbf{r}_2 \\ \mathbf{0}_{N_b} \end{bmatrix}$$

\mathbf{D} is a diagonal matrix with $D_{ii} = \begin{cases} 1, & i = 1, 2, \dots, N_f \\ 0, & i = N_f + 1, N_f + 2, \dots, N_f + N_b. \end{cases}$

$$J = 1 + \mathbf{w}^T \left(\mathbf{R} + \sigma_v^2 \mathbf{D} \right) \mathbf{w} - 2 \mathbf{w}^T \mathbf{p}. \quad (4.6)$$

J_{\min} , the minimum mean-squared error, is obtained when [Haykin, pp. 165-171]

$$\mathbf{w} = \mathbf{w}_{MMSE} = \left(\mathbf{R} + \sigma_v^2 \mathbf{D} \right)^{-1} \mathbf{p}. \quad (4.7)$$

The MMSE coefficients \mathbf{w}_{MMSE} identical whether the equalizer is a DFE or an ADFE.

$$J_{\min} = 1 - \mathbf{w}_{MMSE}^T \mathbf{p}. \quad (4.8)$$

The MMSE, J_{\min} , is also the same for the DFE and ADFE. In fact, the MSE in the case of nonoptimal coefficients is also the same for both equalizers (Equation 4.6). The ISI component of the error signal $e(n)$ is identical for both equalizers, while the noise component is white for the ADFE, and coloured by \mathbf{w}_f for the DFE.

The equivalence of \mathbf{w}_{MMSE} and J_{\min} for the DFE and ADFE applies when the sampled CIR, synchronization delay, SNR, and number FF and FBF taps are identical for both equalizers. The equivalence of J also requires that the equalizer coefficients \mathbf{w} be identical for both equalizers.

In the ADFE system it is desirable to exploit this equivalence result for the characterization of the ADFE FF. Reciprocity can guarantee the same continuous time CIR on the forward and reverse links, over a sufficiently short time interval. However, it is not always possible to guarantee identical an SNR and timing synchronization. The effect of a forward/reverse link SNR mismatch is examined in this chapter and in Chapter 6; the issue of timing in the ADFE system is addressed in Chapter 6.

4.3 ADFE System Training

In the ADFE system, the channel conditions are initially unknown and time-varying. Adaptive training is alternated with data transmission to allow the equalizers to adapt to changing channel conditions. Training and data transmission is composed of four steps:

1. Reverse Link Training: The portable transmits a synchronization and training sequence. Any predetermined data sequence of sufficient length will serve as a training sequence, provided that it is nearly white (its

magnitude frequency domain representation is nearly constant). The base receives this signal, and adapts its synchronization, AGC, and DFE coefficients. RLS training is used to achieve equalizer convergence with a relatively short training sequence.

2. Reverse Link Data Transmission: The portable transmits a frame of data, which is received, equalized, and detected by the base.
3. Forward Link Training: The base uses the FF coefficients from the DFE to directly characterize the ADFE FF. A gain factor may be incorporated to achieve a desired level of output power. The base transmits a synchronization and training signal, which is pre-equalized by the FF. The training sequence is designed for reduced-complexity LSCE at the portable [Crozier2]. The portable estimates the combined impulse response of the channel and FF, and the negative of the postcursor ISI is transferred to the FBF coefficients.
4. Forward Link Data Transmission: The base transmits a frame of data. Pre-equalization by the FF reduces precursor ISI in the received signal, and the FBF at the portable cancels postcursor ISI.

The equalization complexity at the portable is reduced to channel identification, simple synchronization, and implementation of a FBF. As is shown in Section 4.4, the complexity involved is minimal.

In practice, a “fast” RLS algorithm might be used for reverse link training, in order to reduce the computational complexity. A plethora of algorithms and variants, including lattice structures [Ling] are available. They generally achieve convergence similar to RLS, but introduce the problem of instability arising from finite precision arithmetic. The RLS algorithm is used for adaptive training in this thesis, and the selection or design of a more suitable replacement is left to future research.

The lengths of the training sequences will depend on the number of equalizer taps and the nature of the channels. A rule of thumb for LS based training algorithms is to use at least twice as many training symbols as equalizer taps. Chapter 6 presents simulation results on the required lengths of training sequences for the ADFE system.

SNR Mismatch

The FF coefficients obtained by reverse link training are an estimate of MMSE coefficients based on the reverse link CIR and SNR. The forward link CIR is identical to the reverse link CIR, due to reciprocity and the assumption of identical timing phase. The forward link SNR may differ from that of the reverse link due to differing transmit powers and interferers. Thus, the ADFE FF is characterized for a different SNR than it will be applied to. The following scenario demonstrates the effect of this SNR mismatch on MSE performance.

Forward Link: The MMSE equalizer coefficients, \mathbf{w}_{DFE} , are determined for the reverse link. In practice, they would be approximated by the portable transmitting a known training sequence and the base applying an adaptive training algorithm.

Reverse Link: The base uses \mathbf{w}_{DFE} to directly characterize the ADFE FF. The remote determines the MMSE FBF by adaptive training. The forward link SNR is different from the reverse link SNR. As both transmit powers are normalized to unity, this difference is reflected entirely in the noise power.

Table 4.1: ADFE System Forward/Reverse Link Parameters

	reverse link (DFE)	forward link (ADFE)
noise power	$\sigma_{V,DFE}^2$	$\sigma_{V,ADFE}^2$
optimal coefficient vector	\mathbf{w}_{DFE}	\mathbf{w}_{ADFE}
coefficient vector used	\mathbf{w}_{DFE}	\mathbf{w}_{DFE}
MMSE	$J_{\min,DFE}$	$J_{\min,ADFE}$
actual MSE	$J_{\min,DFE}$	J_{ADFE}
correlation matrices	\mathbf{R}, \mathbf{p}	\mathbf{R}, \mathbf{p}

The non-optimum (due to the SNR mismatch) forward link MSE, J_{ADFE} , may be expressed in terms of the forward link MMSE, $J_{\min,ADFE}$, and the coefficient error, $\mathbf{w}_{ADFE} - \mathbf{w}_{DFE}$ [Haykin, page 171].

$$J_{ADFE} = J_{\min,ADFE} + (\mathbf{w}_{ADFE} - \mathbf{w}_{DFE})^T (\mathbf{R} + \sigma_{V,ADFE}^2 \mathbf{D}) (\mathbf{w}_{ADFE} - \mathbf{w}_{DFE}). \quad (4.9)$$

If \mathbf{w}_{ADFE} is close to \mathbf{w}_{DFE} , as may be expected if $\sigma_{V,ADFE}^2$ and $\sigma_{V,DFE}^2$ are both small, then the MSE penalty will also be small.

The values of the forward and reverse link MSE may also be compared.

$$\begin{aligned} J_{ADFE} - J_{\min,DFE} &= (\sigma_{V,ADFE}^2 - \sigma_{V,DFE}^2) \mathbf{w}_{DFE}^T \mathbf{D} \mathbf{w}_{DFE} \\ &= (\sigma_{V,ADFE}^2 - \sigma_{V,DFE}^2) |\mathbf{w}_{f,DFE}|^2, \end{aligned} \quad (4.10)$$

where $\mathbf{w}_{f,DFE}$ is the vector of (MMSE) DFE FF coefficients, such that

$$\mathbf{w}_{DFE} = \begin{bmatrix} \mathbf{w}_{f,DFE} \\ \mathbf{w}_{b,DFE} \end{bmatrix}.$$

If the forward link SNR exceeds the reverse link SNR ($\sigma_{V,ADFE}^2 < \sigma_{V,DFE}^2$), then

$$J_{\min,ADFE} < J_{ADFE} < J_{\min,DFE} \quad (4.11)$$

and the forward link MSE performance, although suboptimal, exceeds that of the reverse link.

The effect of SNR mismatch on BER performance is examined in Chapter 6.

4.4 Computational Complexity

In this and subsequent chapters, the ADFE is shown to have performance very close to that of the DFE. The principal difference between the two is the amount and distribution of computational complexity. In this section, the complexity of training and of execution (equalization subsequent to training) in the ADFE system is addressed.

All figures for computational complexity are approximate, as they are based on simplifying assumptions such as 4 real multiplications per complex multiplication (a complex multiplication can be done with 3 real multiplications), and N additions to sum N numbers (N numbers can be summed using $N - 1$ additions).

Training

Characterization of the ADFE system equalizers requires the rapid convergence available from LS based algorithms. The base uses RLS, or a “fast” RLS algorithm. The operations (multiplications and additions) required for training an N -tap equalizer range from $O(N)$ to $O(N^2)$ per training symbol [Haykin].

The portable uses LSCE channel estimation for training. If a training sequence with ideal correlation properties is used, the portable requires only one signed complex addition per training symbol per tap. As these ‘ideal’ sequences have a length which increases logarithmically with the number of taps, it may be

necessary to use a non-ideal sequence, and suffer a slight decrease in accuracy and/or increase in complexity [Crozier2].

Execution

The FF and FBF filters which compose the ADFE are both transversal FIR filters. Such filters would normally require a complex multiplication and addition per tap, but the nature of signals within the ADFE allows for some simplification. Table 4.2 compares the execution complexity of the DFE, Gibbard precoder, and ADFE for unidirectional transmission. The figures given are the number of real multiplications, additions, and modulo operations required per QPSK symbol. The ADFE FF and FBF, and the DFE FBF are implemented with signed additions replacing multiplications, as their inputs are QPSK symbols. The multiplications are the most expensive of these operations in terms of execution time and/or hardware complexity; the modulo and addition operations are roughly equivalent in complexity. Each equalizer has N_f FF taps and N_b FBF taps.

Table 4.2: Computational Complexity of Equalizers

	transmitter			receiver		
	mult	add	mod	mult	add	mod
DFE	-	-	-	$4N_f$	$4N_f + 4N_b$	-
Gibbard	$4N_f + 4N_b$	$4N_f + 4N_b$	2	-		2
ADFE	-	$4N_f$	-	-	$4N_b$	-

The filters which have QPSK symbols as inputs may also be implemented by using an index, formed from the bit representation of input symbols, to look up the filter output in a table. If separate tables are used for the real and imaginary parts, the ADFE FF and FBF can be implemented with 4 table lookups and 2 real additions per QPSK symbol. The table initialization requirements are $N \cdot 2^{N+1}$ real additions for a filter with N complex taps. It is possible to implement subsections of a filter with table lookup and sum the outputs of each section.

Table 4.3 compares the operations required at the base and portable for 3 equalization systems (bidirectional transmission). They use a DFE, Gibbard precoder, and ADFE, respectively, to equalize the forward link. All use a DFE to equalize the reverse link. The number of real operations required to equalize one QPSK symbol on each of the forward and reverse links are tabulated.

Table 4.3: Computational Complexity of Equalization Systems

	base			portable		
	mult	add	mod	mult	add	mod
DFE/DFE	$4N_f$	$4N_f + 4N_b$	-	$4N_f$	$4N_f + 4N_b$	-
Gibbard	$8N_f + 4N_b$	$8N_f + 8N_b$	2	-		2
ADFE	$4N_f$	$8N_f + 4N_b$	-	-	$4N_b$	-

The complexity of the DFE/DFE system is divided evenly between base and portable. The other two systems are asymmetric, with a concentration of complexity at the base. While the Gibbard system achieves a higher degree of asymmetry than the ADFE system, the ADFE system has much looser AGC requirements, which may further simplify the portable. The ADFE also requires fewer overall multiplications than the other two systems. In some situations, it might be feasible to equalize both the forward and reverse links with an ADFE, so that no multiplications are required for execution of the equalizers. In this case, however, both transceivers would be required to train a FF, which does require multiplications and is fairly complex.

4.5 Fractionally Spaced Equalization

Reverse Link

The DFE may incorporate a fractionally spaced (FS) FF. It is expected that this would improve performance, or reduce synchronization complexity, by rendering the DFE essentially insensitive to small (less than T_{sym}) variations in timing phase. It would also allow the FF to independently manipulate the frequency

response of the excess bandwidth [Qureshi, page 1365]. Training and equalization are implemented in much the same manner as for a T_{sym} spaced (TS) FF. The FS FF may require more taps than a TS FF.

The DFE FBF usually operates with T_{sym} spaced sampling, as its input is the detected data sequence.

Forward Link

The ADFE FF may also be implemented with fractional spacing, being directly characterized by the DFE FS FF. The synchronization advantages of the FSE would be lost in the forward link, since the portable must establish synchronization independent of the base. However, the benefit of advantageous shaping of the excess bandwidth of the transmitted signal would be retained. In any case, once the FS FF is obtained for the DFE, it is simpler to re-use it for the ADFE than to determine a TS FF therefrom.

As in the reverse link, the forward link FBF operates with T_{sym} spaced sampling. However, a fractionally spaced CIR estimate may be useful, as it would allow synchronization and training to be combined. A choice of the synchronization would be made based on the CIR, and then T_{sym} spaced postcursor ISI would be extracted to characterize the FBF. The ensuing relaxation in synchronization requirements might offset the increased complexity of FS channel estimation.

MSE Analysis

The MSE analysis of a DFE or ADFE may be generalized from a TS FF to fractional spacing, with some minor changes to the notation and results. As in Section 4.2, the ADFE is constrained to unity transmit power, and the FF is of finite length. The MMSE and MMSE coefficients are identical for the DFE and ADFE, and $e(n)$ is coloured for the DFE and white for the ADFE.

Analysis of a FSE is complicated by the need to account for at least two different sampling periods: T_{sym} , the symbol period, and T_{eq} , the sample period of the

fractionally spaced FF, and the sampling of other fractionally spaced signals. In this analysis, all signals and filters (except the FBF) are represented in discrete time with a sample period of T_{eq} . Signals that are normally defined at intervals of T_{sym} (such as $a(n)$ and $d(n)$) are upsampled and zero-interpolated. Some of the vectors and matrices are redefined to accommodate the combination of T_{eq} and T_{sym} spacing.

In this case, the expression $a \equiv b \pmod{s}$ implies that $a = b + Ks$ where K is an arbitrary integer. This differs from the mod operator of the TH precoder.

$s = T_{sym}/T_f$ is a positive integer (other formulations of the FSE with rational s are also possible).

$$\begin{aligned}
 a(n) &= \begin{cases} \pm 1, & n \equiv 0 \pmod{s} \\ 0, & \text{otherwise.} \end{cases} \\
 \mathbf{d}(n-s) &= [d(n-s) \quad d(n-2s) \quad \dots \quad d(n-N_b s)]^T \\
 y(n) &= u(n) + \mathbf{w}_v^T \mathbf{v}(n) + \mathbf{w}_b^T \mathbf{d}(n-s) \\
 J &= E[e^2(n)], \quad n \equiv \Delta \pmod{s}
 \end{aligned} \tag{4.12}$$

\mathbf{R}_1 is a matrix with elements

$$\mathbf{R}_1(i, j) = \sum_{\substack{k=0 \\ k+i-\Delta \equiv 1 \pmod{s}}}^{N_h-1} h(k)h(k-i+j), \quad i, j = 1, 2, \dots, N_f. \tag{4.13}$$

$$\mathbf{r}_2 = \begin{bmatrix} h(\Delta) \\ h(\Delta-1) \\ \vdots \\ h(\Delta-N_f+1) \end{bmatrix}$$

\mathbf{R}_3 is a matrix with elements

$$\mathbf{R}_3(i, j) = h(js - i + \Delta + 1), \quad \begin{matrix} i = 1, 2, \dots, N_f \\ j = 1, 2, \dots, N_b. \end{matrix} \tag{4.14}$$

$$\mathbf{w} = \begin{bmatrix} \mathbf{w}_f \\ \mathbf{w}_b \end{bmatrix} \quad \mathbf{R} = \begin{bmatrix} \mathbf{R}_1 & \mathbf{R}_3 \\ \mathbf{R}_3^T & \mathbf{I}_{N_b} \end{bmatrix} \quad \mathbf{p} = \begin{bmatrix} \mathbf{r}_2 \\ \mathbf{0}_{N_b} \end{bmatrix}$$

\mathbf{D} is a diagonal matrix with $D_{ii} = \begin{cases} 1, & i = 1, 2, \dots, N_f \\ 0, & i = N_f + 1, N_f + 2, \dots, N_f + N_b. \end{cases}$

$$J = 1 + \mathbf{w}^T (\mathbf{R} + \sigma_v^2 \mathbf{D}) \mathbf{w} - 2 \mathbf{w}^T \mathbf{p} \quad (4.15)$$

$$\mathbf{w}_{MMSE} = (\mathbf{R} + \sigma_v^2 \mathbf{D})^{-1} \mathbf{p} \quad (4.16)$$

4.6 Conclusions

In this chapter, the ADFE and the ADFE system were introduced. The MSE performance and MMSE characterization of the ADFE with and without a constraint on transmitted power was given. The analysis of the power-constrained ADFE was formulated to also encompass the DFE, and it was shown that both equalizers share the same MSE performance and MMSE coefficients, under equivalent conditions.

An efficient method of adaptively training the DFE and ADFE in the ADFE system was presented. Efficient LSCE [Crozier2] is directly applicable to training the portable, while a fast RLS algorithm may be selected for training the base.

A potential SNR mismatch in the ADFE system is discussed and the ensuing MSE degradation is quantified.

The computational complexity, measured in the number of arithmetic operations, is tabulated for the DFE, Gibbard precoder, ADFE. As well, the complexity of three different systems, employing each of these three equalizers on the forward link, is compared. Although the ADFE system does not achieve as high a degree of asymmetry as the Gibbard system, it has looser AGC requirements at the portable and reduced overall complexity.

The MMSE characterization and performance of the fractionally spaced ADFE was also presented.

5. Markov Model of Error Propagation

While the BER may be close to the ultimate measure of performance of a digital communications system [Belfiore] it is very difficult to determine for a DFE system, due to error propagation (Section 5.1). Section 5.2 describes how simulation is used to estimate BER performance of equalizers in this thesis. Section 5.3 presents an exact method of modeling error propagation in the ADFE. This method leads to interesting results for the correlation of decision errors, which are presented in Section 5.4.

5.1 Decision Errors in the DFE

A decision error occurs when the output of the decision device differs from the desired symbol, which happens when distortion drives the input to the decision device closer to another symbol value than to the desired symbol. The signal input to the decision device experiences distortion due to noise, precursor ISI, attenuation of the desired signal, and postcursor ISI. With the assumption of a linear AWGN channel, the noise distortion will be Gaussian, but not white, as it is filtered by the forward filter w_f .

The precursor ISI is non-Gaussian, and arises from imperfect precursor cancellation by the forward filter. Although an infinite ZF FF will eliminate precursor ISI, its overall performance is inferior to that of the MMSE FF, due to noise amplification.

The MMSE FF may reduce the magnitude of the equalized main ray. Although this may appear to be counterproductive, it does reduce the mean-squared error by suppressing noise. In most cases, the effect of this attenuation is small, especially when the SNR is high. For example, this attenuation is equivalent to a

multiplicative factor of 0.9629 for a [1 2 1] sampled CIR with many (50) forward taps, and a SNR of 20 dB. Although the attenuation affects the MSE, it will not affect the probability of bit error if the quantizer output depends only on the sign of its input, as in BPSK or QPSK signaling.

Non-ideal values of the feedback coefficients \mathbf{w}_b , or an insufficient number of feedback taps, will give rise to non-Gaussian postcursor ISI at the decision device.

Analysis of DFE decision errors may be simplified by assuming that at the input to the decision device the noise is Gaussian and white, that there is no precursor ISI, and that the feedback taps are of sufficient number and exact values to eliminate postcursor ISI [Altekar] [Monsen2] [Austin].

If a decision error is made (i.e. $\tilde{d}(n) \neq d(n)$) then the feedback filter will contribute to, rather than remove, postcursor ISI. The net effect is to double the postcursor distortion. This effect is known as error propagation. It has a significant effect on the error performance of the DFE, and complicates the analysis considerably.

Austin [Austin] used a finite discrete Markov process to model the effect of error propagation and predict the BER of a DFE system. As the number of states required grows exponentially with the number of significant postcursors, this method is impractical if the number of precursors, postcursors, and equalizer taps is moderately large.

Subsequent authors [Altekar] [Duttweiler] have used a reduced state representation of error propagation to derive upper bounds on the probability of error.

5.2 BER Estimation by Simulation

For many equalizers, including the DFE, simulation is used to estimate BER performance under specific conditions. Digital and analog signals within the system are represented digitally within a simulation program which runs on a computer. Simplifications such as additive white Gaussian noise and the baseband equivalent CIR are used to reduce the number of computations and to supplement the imperfect knowledge of the system being modeled.

The detected data symbols are compared to the desired (transmitted) ones and bit errors are counted. The BER is simply the ratio of bit errors to the total number of transmitted bits. Due to the random nature of error events, it is desirable to collect a significant number of errors to improve the accuracy of this estimate of the BER. At low bit error rates, the number of transmitted bits (and the computational load) can become quite large. For example, to collect 100 bit errors for a BER of 10^{-5} requires transmission of 10^7 bits. In this thesis, at least 100 errors are collected per BER estimate, unless otherwise stated. If a maximum number of bits (typically 10^7) is transmitted before 100 errors are collected, the simulation is halted and no BER result is presented for that particular trial.

Data is transmitted in frames of at least 2000 symbols (BPSK or QPSK). While using finite-length data frames will interrupt error propagation, the effect should be negligible at low error rates. In any case, an implementation of the ADFE system would also regularly interrupt data transmission in either direction to accommodate TDD transmission.

5.3 Error Propagation in the ADFE

The Markov state model may be applied to the ADFE without any need for assumptions regarding the statistics of filtered noise, nor precursor elimination. Although not applied in this thesis, the assumptions of precursor elimination and

ideal feedback coefficients could be used to reduce the number of states. The following model is assumed for analysis of the ADFE in this thesis.

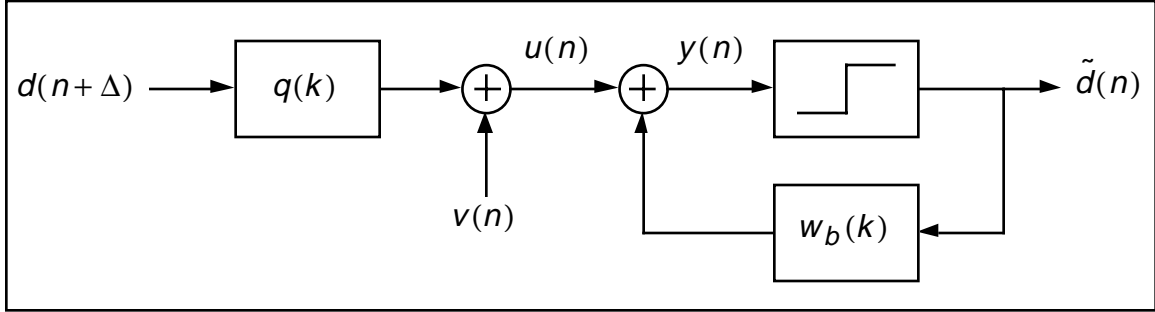


Figure 5.1: ADFE System

$w_f(k)$, $k = 0, 1, \dots, N_f - 1$ are the pre-equalizer coefficients.

$h(k)$, $k = 0, 1, \dots, N_h - 1$ is the channel impulse response.

$d(n + \Delta)$ are data symbols to be transmitted.

$v(n)$ is the additive white Gaussian noise.

The pre-equalizer and channel impulse response are combined by convolution to form $q(k)$.

$$q(k) = \sum_{j=0}^{N_h-1} h(j) w_f(k-j), \quad (5.1)$$

$$N_q = N_h + N_f - 1, \quad (5.2)$$

$$u(n) = \sum_{k=0}^{N_q-1} q(k) d(n + \Delta - k) + v(n), \quad (5.3)$$

$$\begin{aligned} y(n) &= u(n) + \sum_{k=1}^{N_b} w_b(k) \tilde{d}(n-k) \\ &= \sum_{k=0}^{N_q-1} q(k) d(n + \Delta - k) + v(n) + \sum_{k=1}^{N_b} w_b(k) \tilde{d}(n-k), \end{aligned} \quad (5.4)$$

$$\tilde{d}(n) = \begin{cases} -1, & y(n) \leq 0 \\ +1, & y(n) > 0. \end{cases} \quad (5.5)$$

The state of the system may be defined by

$$\begin{aligned} S_j &= \left\{ \begin{array}{l} d(n-\Delta-k), k=0,1,\dots,N_q-1 \\ \tilde{d}(n-k), k=1,2,\dots,N_b \end{array} \right\} \\ &= \left[\begin{array}{l} d(n+\Delta) \ d(n+\Delta-1) \ \dots \ d(n+\Delta-N_q+1) \\ \tilde{d}(n-1) \ \tilde{d}(n-2) \ \dots \ \tilde{d}(n-N_b) \end{array} \right]. \end{aligned} \quad (5.6)$$

For simplicity, BPSK is assumed for this analysis, and all signals are assumed to have no imaginary component. Other modulations such as QPSK may be represented with complex arithmetic, with an increased number of system states.

As each data symbol may take on the values ± 1 , and the number of states is $2^{N_q+N_b}$. Each state has four nonzero transition probabilities as $d(n+\Delta+1) = \pm 1$ and $\tilde{d}(n) = \pm 1$. The nonzero transition probabilities are

$$\begin{aligned} P_{ij} &= P(\tilde{d}(n) = -1, d(n+\Delta+1) = -1 | S_j) \\ &= \frac{1}{2} P(y(n) \leq 0 | S_j). \end{aligned} \quad (5.7)$$

$y(n)$ is a Gaussian random variable with mean

$$m_y = \sum_{k=0}^{N_q-1} q(k) d(n+\Delta-k) + \sum_{k=1}^{N_b} w_b(k) \tilde{d}(n-k) \quad (5.8)$$

and variance

$$\sigma_y^2 = E[v^2(n)] \quad (5.9)$$

Thus the four transition probabilities are given by

$$P(\tilde{d}(n) = -1, d(n+\Delta+1) = \pm 1 | S_j) = \frac{1}{4} \operatorname{erfc}\left(\frac{m_y}{\sqrt{2}\sigma_y}\right) \quad (5.10)$$

and

$$P(\tilde{d}(n) = +1, d(n+\Delta+1) = \pm 1 | S_j) = \frac{1}{4} \operatorname{erfc}\left(\frac{-m_y}{\sqrt{2}\sigma_y}\right). \quad (5.11)$$

The state transition matrix may be filled in by computing the probabilities of all possible transitions. The state probabilities P_i and BER can be computed from the transition matrix. This BER includes the effects of ISI, noise, and error propagation. Figure 5.2 compares ADFE BER results obtained by Markov model and by simulation.

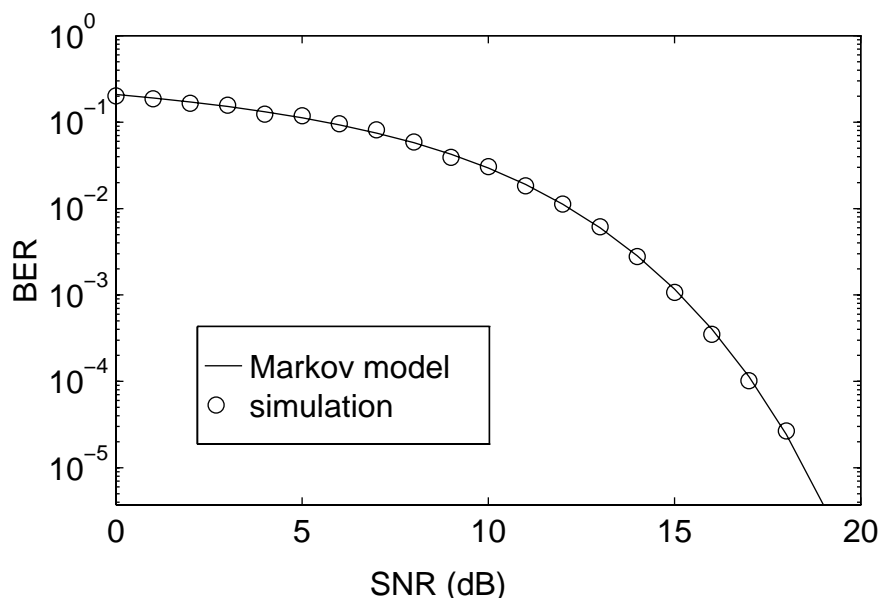


Figure 5.2: Markov Model and Simulation Results

Table 5.1 Parameters for Figures 5.2 - 5.4

CIR	[1 2 1]
equalizer	ADFE
N_f	3
N_b	1
characterization	MMSE

The BER in the absence of error propagation may be determined from the state probabilities as the probability of a bit error given no prior errors. Figure 5.3 shows the BER of the ADFE with and without error propagation.

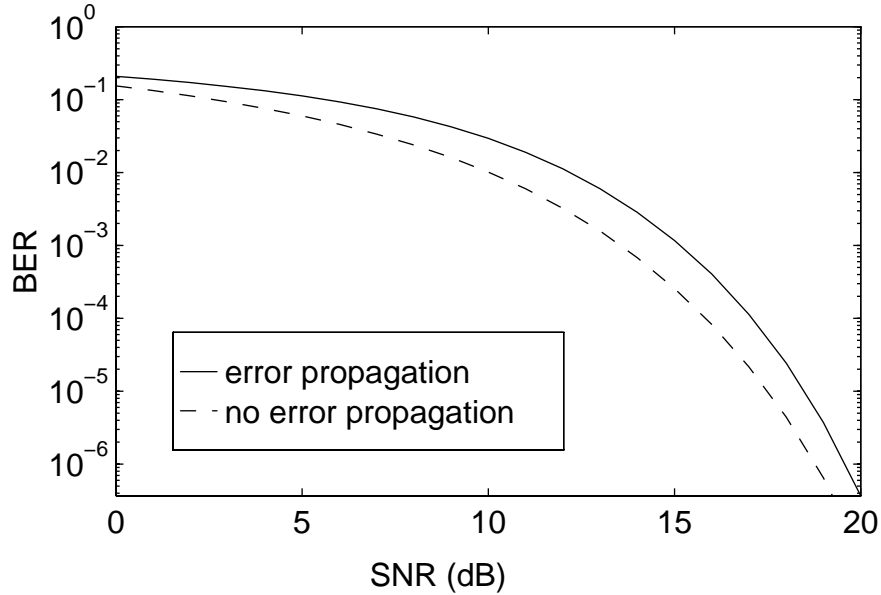


Figure 5.3: BER with and without Error Propagation

In the range from 15 to 20 dB SNR, the BER increases by approximately a factor of 5 due to error propagation. However, the SNR penalty (the increase in SNR required to compensate for error propagation) is small (about 1 dB) because the BER curve becomes steep for higher values of the SNR.

This method of modeling error propagation may be applied to the ADFE with a FS FF. In this case, the number of states is $2^{N_q+N_b}$ where N_q is the number of contiguous nonzero elements in the T_{sym} spaced convolution of the FF and CIR.

5.4 Error Event Correlation

The error event function $\varepsilon(n)$ is defined to assist in the examination of error propagation and correlation.

$$\varepsilon(n) = \begin{cases} 0, & \tilde{d}(n) = d(n) \\ 1, & \tilde{d}(n) \neq d(n). \end{cases} \quad (5.12)$$

The error event autocorrelation function, $\phi_{\varepsilon\varepsilon}(k)$, is defined as follows.

$$\begin{aligned}\phi_{\varepsilon\varepsilon}(k) &= E[\varepsilon(n)\varepsilon(n-k)] \\ &= P(\varepsilon(n) = 1, \varepsilon(n-k) = 1).\end{aligned}\tag{5.13}$$

Two properties worthy of mention are:

1. The zeroth lag autocorrelation is the average probability of bit error, or the BER.
2. If errors are independent, then the autocorrelation at all nonzero lags is the probability of error squared.

The second property may be used to examine the degree of correlation between errors. If the autocorrelation is close to the error probability squared, then errors are nearly independent. For this reason, the squared error probability is shown for comparison in the following graph.

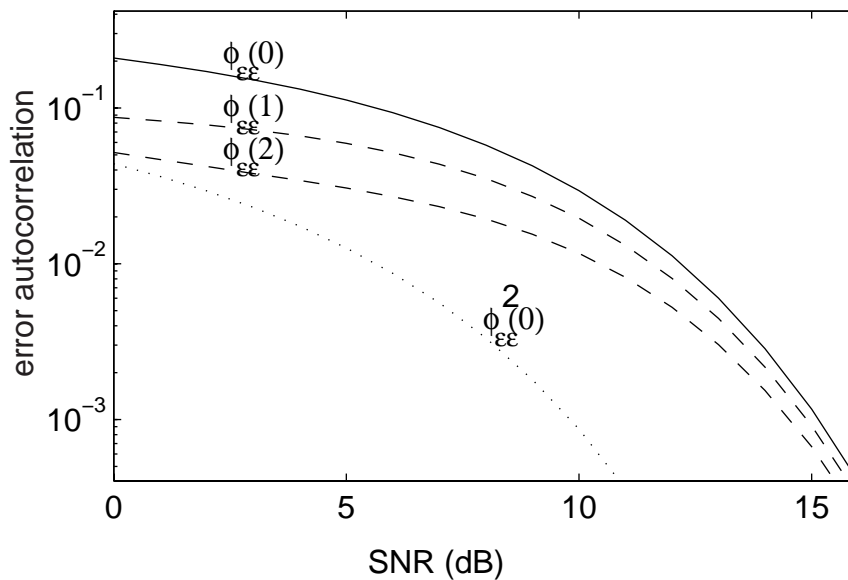


Figure 5.4: Autocorrelation of Error Event function

Figure 5.4 sheds further light on the nature of error propagation in the ADFE. At higher SNR's, the probability of a single error is only slightly greater than that of two or three consecutive errors. This would indicate that error propagation has a

significant impact on performance. However, these probabilities decrease sharply with increasing SNR, hence the small SNR penalty.

This high probability of errors following an initial error may significantly affect the performance of error-correcting codes applied to the data stream. Such codes generally perform best against uncorrelated errors [Proakis, page 440]. Interleaving of the data stream may be required to decorrelate error events.

5.5 Conclusion

In this chapter, a Markov model was shown to effectively model the effects of additive noise, residual precursor ISI, and error propagation to determine the BER performance of an ADFE link with a small number of CIR samples and equalizer taps. In addition, information on error propagation was extracted from the state transition matrix and an error event correlation function was defined and plotted. The program used to implement these computations is listed in the Appendix.

The speed of computation and accuracy of results are two principal advantages of this method over simulation. One caveat for the Markov model is that it may yield unreasonable results, such as a negative BER, when the expected BER is small (lower than 10^{-9}). This is probably due to the limited (albeit high) numerical precision used to initialize and solve the state transition matrix.

6. Non-Idealities

As implementation of the ADFE system to establish its performance is beyond the scope of this thesis, modeling and simulation are used to predict performance. The accuracy of these results is limited by the accuracy and completeness of the models.

The simplified model of a communications system, shown in Figure 2.7 and applied in Chapter 5, may serve as an initial indication of the performance of the ADFE. However, this model omits a number of non-idealities which are expected in a real system. It is of interest to examine the effect of these non-idealities on system performance, as measured by BER, to achieve a better indication of how a full implementation would behave.

Each section of this chapter considers only one, or a few, non-idealities. This piecemeal approach has the advantage of limiting the complexity and quantity of results. The disadvantage is that the results are less conclusive, as the combined effect of multiple nonidealities is not given. The intent of this chapter is not to provide an exhaustive tabulation system performance under real conditions, but rather to indicate the probable extent of degradation due to expected non-idealities.

Section 6.1 examines the effect of SNR mismatch on BER and MSE. Although this effect stems from reverse link training in the ADFE system, it is manifested only on the forward link. Hence, this investigation is confined to the ADFE. Certain conditions are shown to precipitate an improvement, rather than degradation, in BER performance due to an SNR mismatch. The concept of a SNR mismatch was introduced in Section 4.3.

Section 6.2 examines the effect of timing error on BER performance of the ADFE system forward and reverse links. The performance of synchronous and

fractionally spaced equalizers is compared. As well, a joint timing sensitivity peculiar to some asymmetric systems is introduced and examined.

Section 6.3 presents results based on adaptive training for characterization of the equalizers of the ADFE system.

Section 6.4 examines the effect of finite precision arithmetic on the performance of the ADFE, along with comparison to the Gibbard precoder.

6.1 SNR mismatch

In the ADFE system, the forward link is pre-equalized by a FF which is adaptively characterized by the reverse link CIR and SNR. While the principle of reciprocity implies that the forward link CIR will be identical to the reverse link CIR, the SNR will probably differ. This SNR mismatch is investigated by determining the performance of an ADFE at an execution SNR (the forward link SNR), which differs from the MMSE characterization (reverse link) SNR.

As the role of the forward link (ADFE) FBF is to cancel postcursor ISI, it is determined entirely by the FF and CIR, and is independent of the forward link SNR. For this reason, the FF is of greater interest in investigating the effect of SNR mismatch and is given greater emphasis in the following results.

Figures 6.1 and 6.2 illustrate the effect of the SNR mismatch on MSE and BER performance. As one would expect, Figure 6.1 indicates that the minimum MSE is obtained when the characterization SNR and execution SNR are equal. A SNR mismatch appears to introduce a moderate degradation.

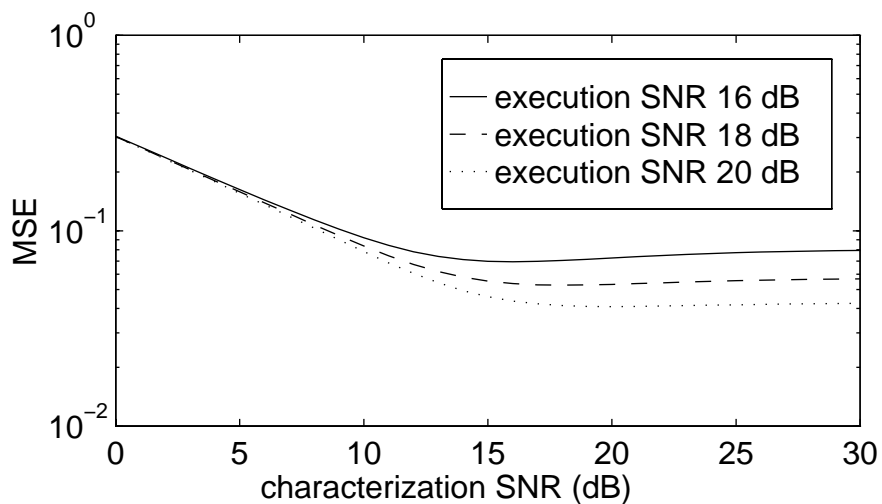


Figure 6.1: MSE Performance of ADFE with SNR Mismatch

The BER results are not so straightforward. For the given CIR, it appears to be advantageous to characterize or train at a fixed SNR of about 10 dB, regardless of the execution SNR. This illustrates the discrepancy between the MMSE and MPE criteria.

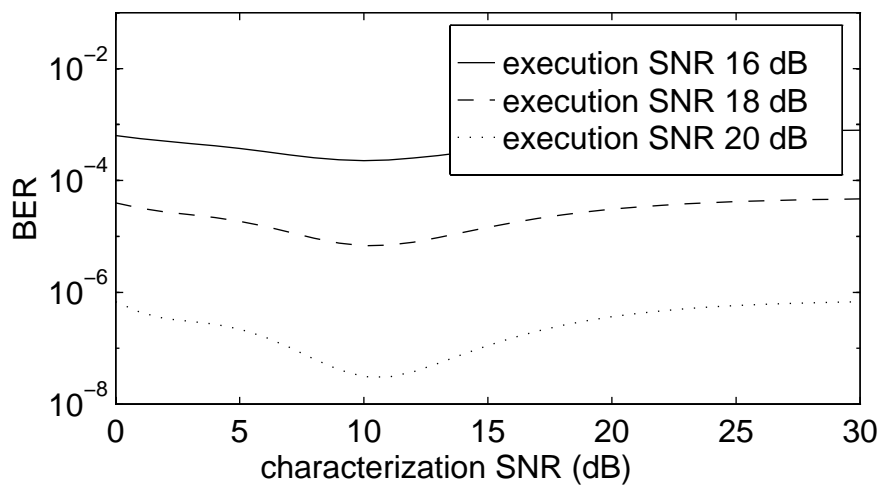


Figure 6.2: BER of ADFE with SNR Mismatch

Table 6.1: Parameters for Figures 6.1, 6.2

equalizer	ADFE
CIR	[1 2 1]
delay	1
N_f	4
N_b	1
data format	BPSK
BER	Markov model
equalizer characterization	MMSE

Further experiments reveal that the effect of SNR mismatch varies considerably with CIR and equalizer. A thorough analysis might be able to extract the underlying principles and derive algorithms for enhancing performance of real systems, but that is beyond the scope of this work. Instead, the remainder of this section illustrates some of the implications of the SNR mismatch under different conditions, with some hypotheses regarding the causes.

SNR Mismatch with Other Channels

Consider the sixteen different sampled CIR's represented by $[\pm 1 \pm 2 \pm 2 \pm 1]$. As it is expected that a CIR and its negative will exhibit identical performance, eight are chosen (leaving behind their negatives) to form a subset of CIR's for further investigation of SNR mismatch.

These eight CIR's are grouped into pairs, for ease of viewing and comparison, according to the following criteria in descending order of priority:

1. BER performance under SNR mismatch
2. similarity of magnitude frequency spectrum (symmetry about the normalized frequency $f = 0.25$)

For each pair of channels, three figures are shown:

1. BER versus characterization SNR

2. magnitude of the frequency spectra of the CIR's
3. magnitude of the frequency spectra of the FF's (characterized at 20 dB SNR)

As BER performance over these channels varies considerably, the execution SNR's are adjusted to bring the BER's into ranges which meet reasonable performance objectives yet do not exhibit numerical problems (see Section 5.4).

Table 6.2: Parameters for Figures 6.3 - 6.11

equalizer	ADFE
CIR A	[1 2 2 1]
B	[-1 2 -2 1]
C	[-1 -2 2 1]
D	[-1 2 2 -1]
E	[-1 2 2 1]
F	[1 -2 2 1]
G	[1 2 2 -1]
H	[1 2 -2 1]
delay	1
N_f	4
N_b	2
data format	BPSK
BER	Markov model
equalizer characterization	MMSE

First Pair of Channels (A, B)

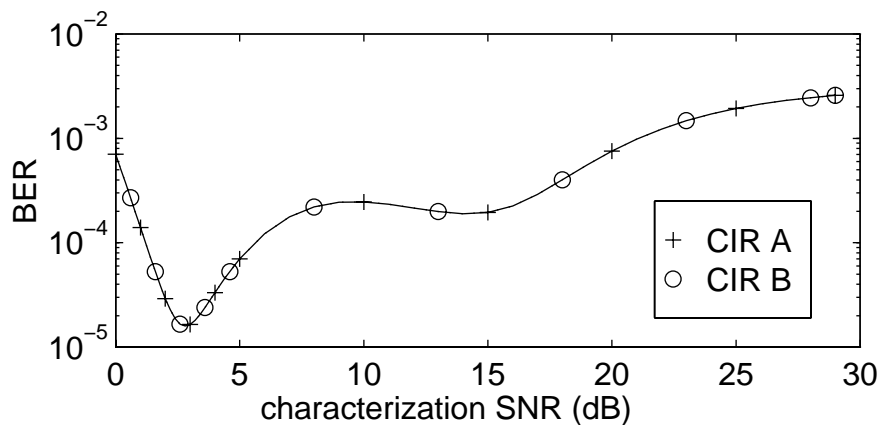


Figure 6.3: BER of ADFE with SNR Mismatch (execution SNR 21 dB)

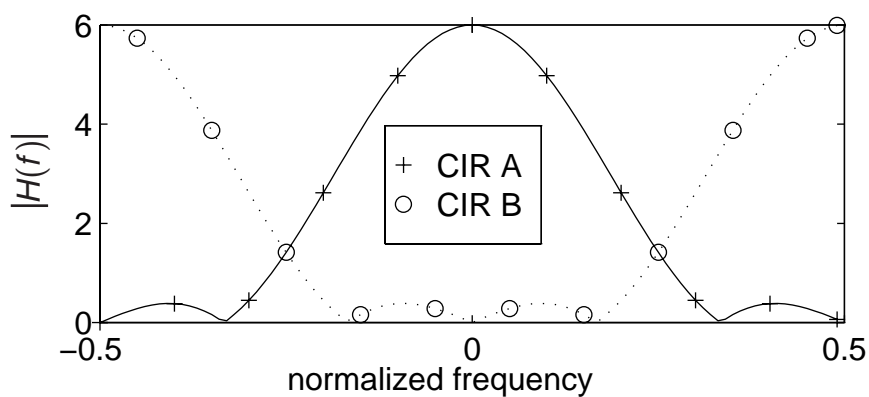


Figure 6.4: Frequency spectra of CIR's

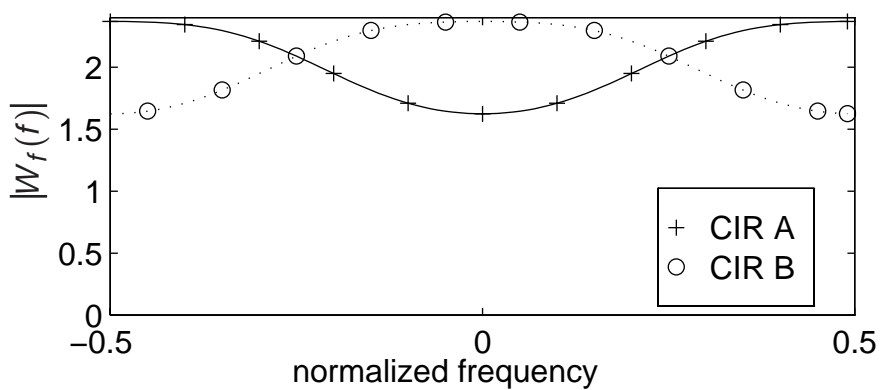


Figure 6.5: Frequency spectra of ADFE FF (characterized at 20 dB SNR)

Second Pair of Channels (C, D)

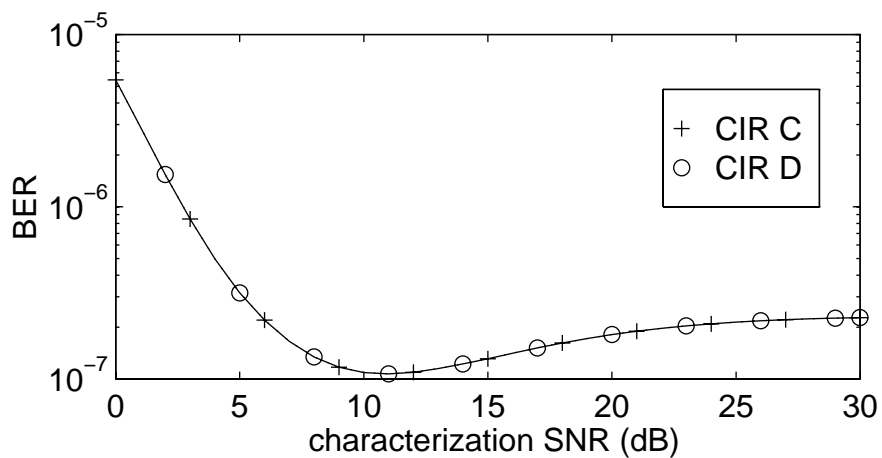


Figure 6.6: BER of ADFE with SNR mismatch (execution SNR 15 dB)

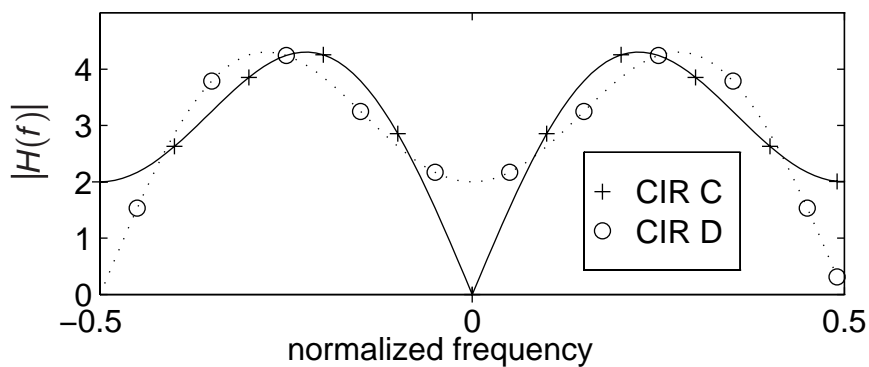


Figure 6.7: Frequency Spectra of CIR's

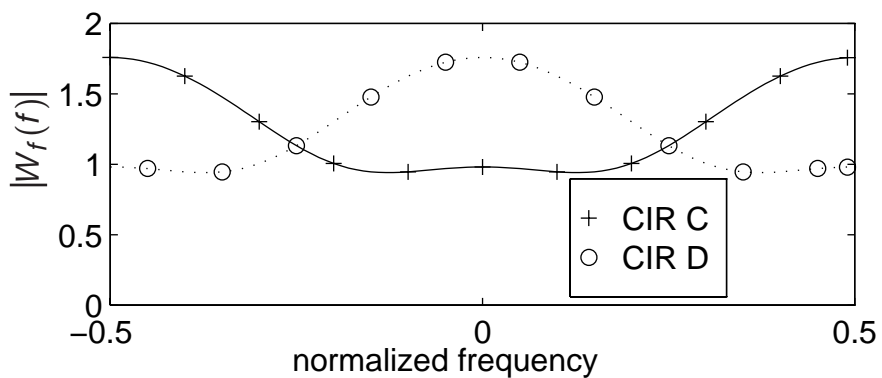


Figure 6.8: Frequency Spectra of ADFE FF (characterized at 20 dB SNR)

Third Pair of Channels (E, F)

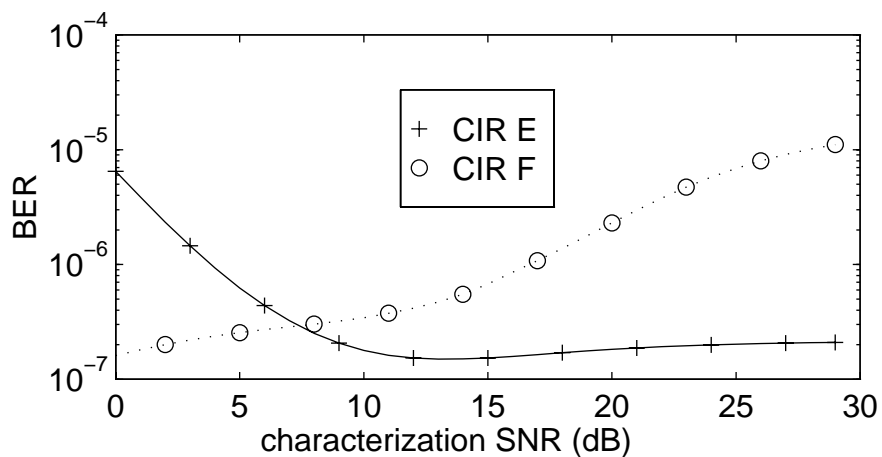


Figure 6.9: BER of ADFE with SNR Mismatch (execution SNR: 13 dB for CIR E, 19 dB for CIR F)

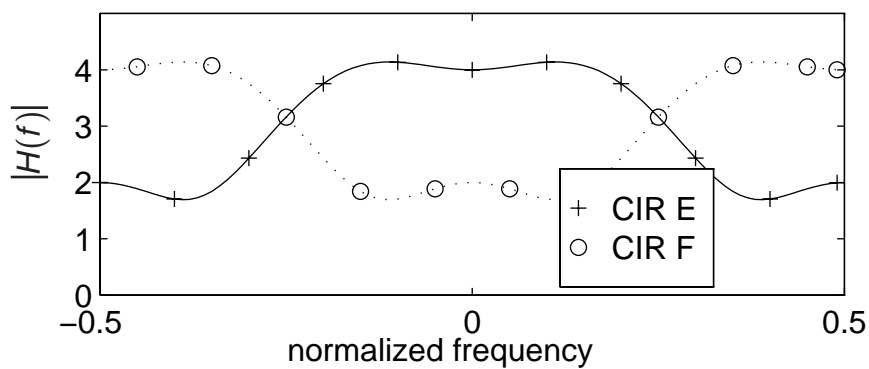


Figure 6.10: Frequency Spectra of CIR's

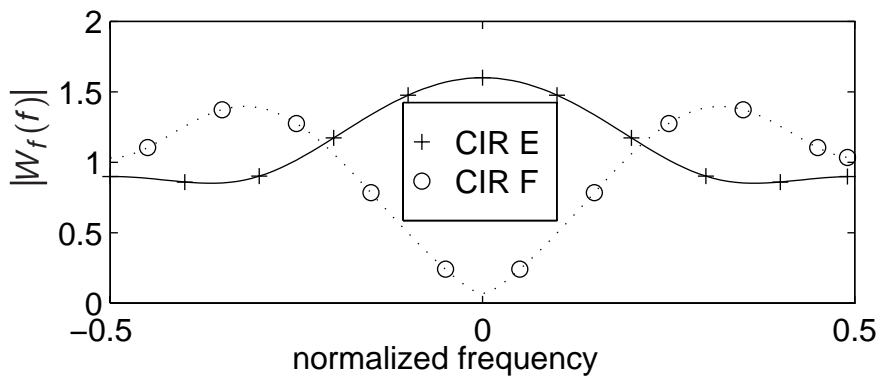


Figure 6.11: Frequency Spectra of ADFE FF (characterized at 20 dB SNR)

Fourth Pair of Channels (G, H)

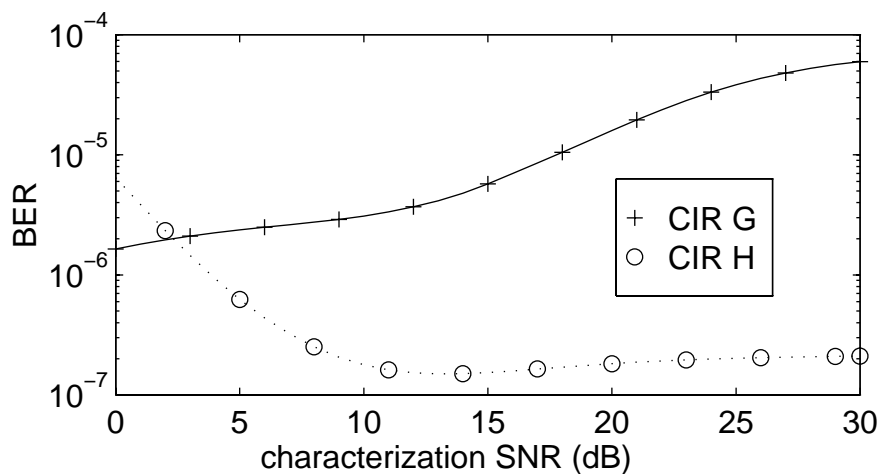


Figure 6.9: BER of ADFE with SNR Mismatch (execution SNR: 18 dB for CIR G, 13 dB for CIR H)

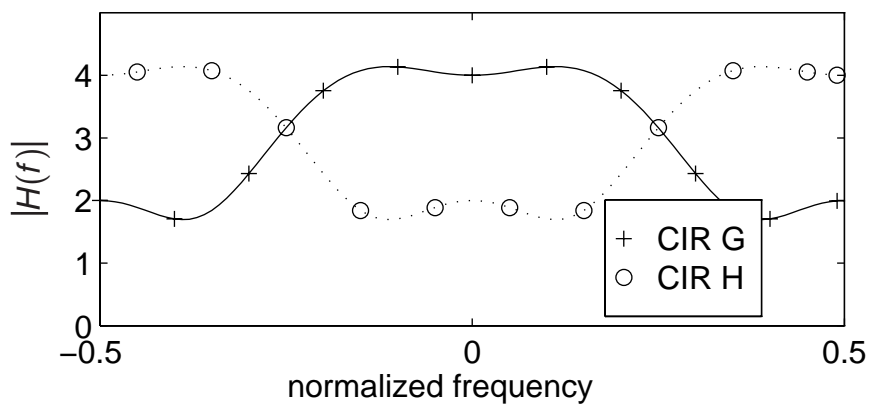


Figure 6.10: Frequency Spectra of CIR's

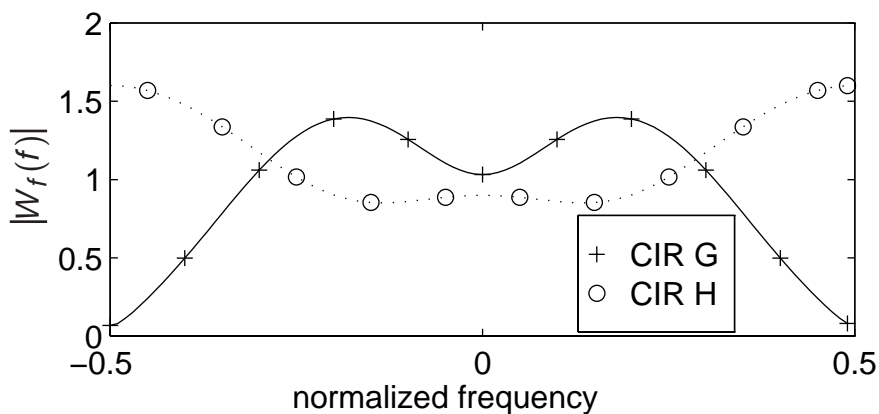


Figure 6.11: Frequency Spectra of ADFE FF (characterized at 20 dB SNR)

Although the magnitudes of precursors and postcursors are identical for all of these six channels, the BER performance varies considerably. Channels A and B exhibit an especially curious BER sensitivity to SNR mismatch. Channels C, D, F, and H have good BER performance at any training SNR above about 10 dB.

Channel A, Revisited

Figure 6.12 shows the BER versus characterization SNR for CIR A, for the ADFE and DFE. The number of FF taps is increased from 4 to 5. This does not appear to alter the general shape of the BER curve.

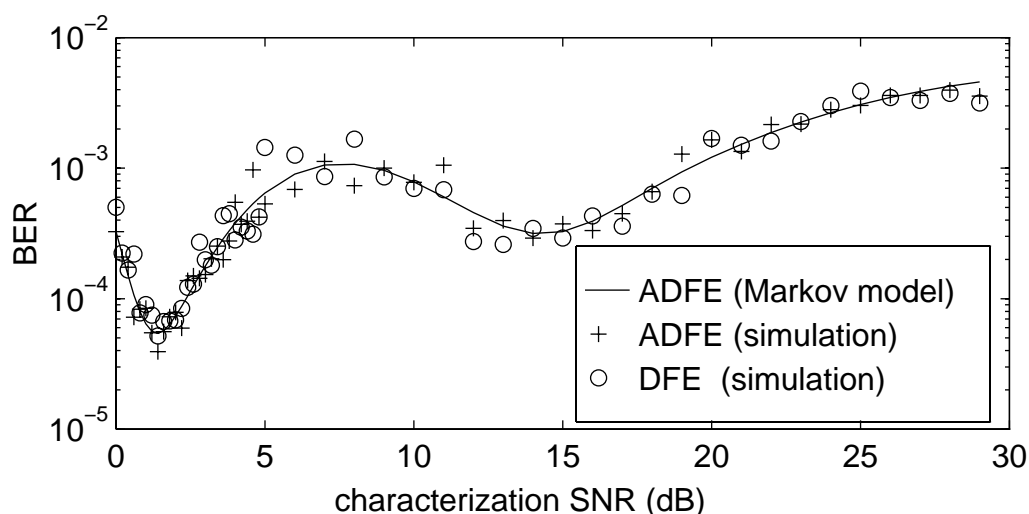


Figure 6.12: BER of ADFE and DFE with SNR Mismatch

It appears that the Markov model results are supported by simulation of the ADFE, and also that the DFE exhibits a similar sensitivity to SNR mismatch. Figure 6.13 examines a number of signal components (residual precursors, MSE, FF norm, FBF) within the DFE/ADFE which are related to BER performance. Variations in any of these parameters which coincide with the BER minima may indicate the cause of these minima.

Table 6.3: Parameters for Figures 6.12, 6.13

equalizer	ADFE, DFE
CIR	[1 2 2 1]
SNR	21 dB
delay	1
N_f	5
N_b	2
data format	BPSK
BER	Markov model and simulation
equalizer characterization	MMSE

For both the DFE and ADFE, residual precursor ISI is defined as the precursor ISI present in the convolution of the FF and CIR. The residual precursor metric is the squared sum of the magnitudes of the residual precursor ISI. This metric is normalized by the magnitude of the main ray of the convolution of the FF and CIR. As the SNR is high, it is suspected that this peak distortion (to borrow the term from zero forcing equalization) may play a dominant role in decision errors. Hence, this metric, rather than the L_2 norm, is used to indicate the degree of residual precursor ISI. A metric greater than unity would indicate that a decision error may be caused by residual precursor ISI alone.

The MSE is the mean square error in the estimated (unquantized) equalizer output.

The FF norm is the L_2 norm of the FF coefficients. This serves as an indication of the (effective) noise amplification, based on the DFE/ADFE model of Figure 4.6.

The FBF metric is the squared sum of the absolute values of the FBF coefficients. As with the residual precursor ISI, this metric is selected instead of the L_2 norm as it is expected to be more indicative of decision errors, and error propagation as well.

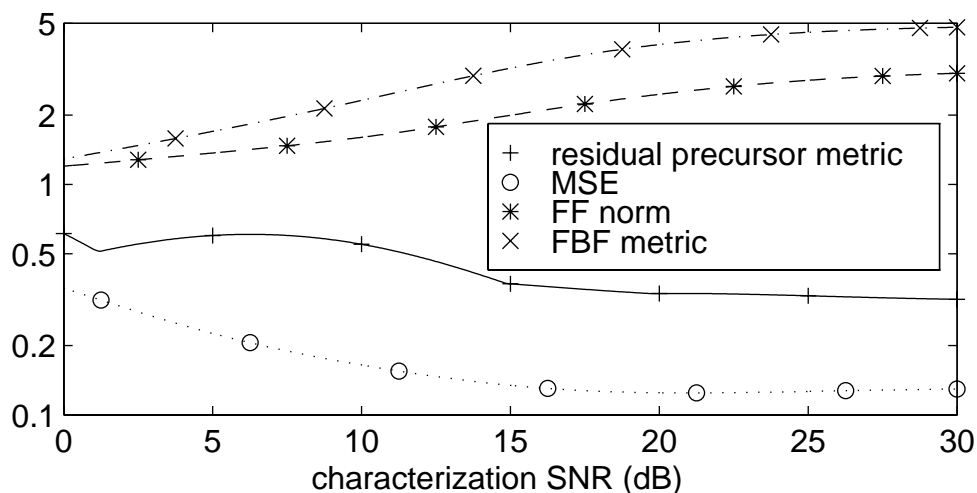


Figure 6.13: Signal Components within DFE/ADFE

The only parameter whose behavior appears to correlate with BER behavior is the residual precursor metric. There appears to be an abrupt change in slope of this curve at 1.4 dB and 15 dB, the locations of the BER minima. The results shown in Figure 6.13 do not seem to provide sufficient information to draw conclusions regarding relationship of BER to characterization SNR. Such knowledge, if obtained, might provide insight into the general problems of SNR mismatch and nonlinear feedback equalizer performance.

6.2 Sensitivity to Timing Error

Timing or synchronization involves both the timing phase and the choice of the main ray (of the sampled CIR). This section investigates the effect of timing error on the reverse and forward links of the ADFE system, for equalizers with a T_{sym} spaced and fractionally ($T_{sym}/2$) spaced FF. Variable timing is obtained from the CIR by interpolation with an RC (TSE) or SQRC (FSE) pulse shape followed by resampling. The received signal energy before (down) sampling is maintained constant, to simulate the effect of a constant SNR at the receiver input. Thus, the SNR after sampling will vary with the timing phase of the receiver. All equalizer coefficients are permitted to adapt to the timing error imposed as it is presumed that the timing phase will be maintained constant during training and reception.

Reverse Link (DFE)

In the ADFE system, the base receiver must establish an appropriate synchronization (timing phase and choice of main ray) to the reverse link signal, prior to or as part of the DFE training. This choice of timing will affect the reverse link performance. Figure 6.14 illustrates the effect of varied synchronization on the BER of the reverse link, for a DFE with a TS FF and a FS FF.

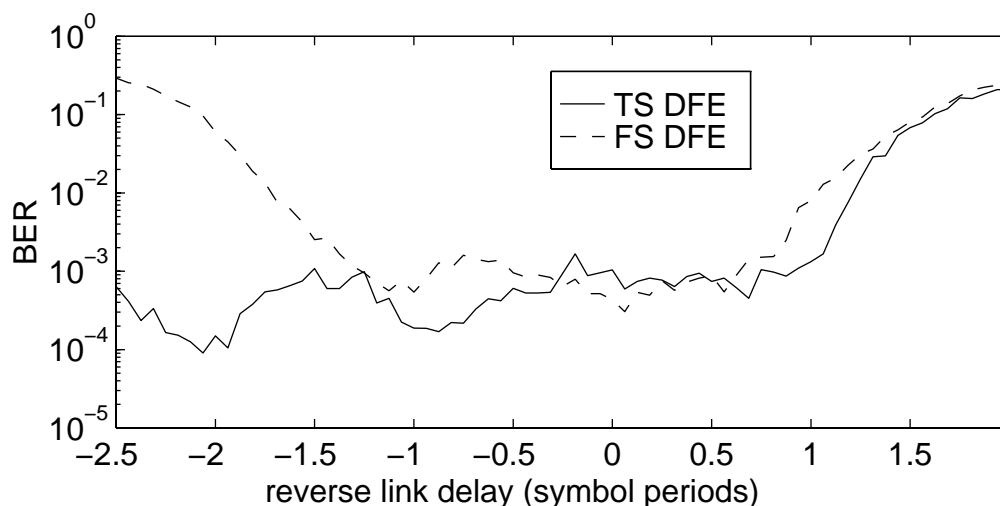


Figure 6.14: BER Timing Sensitivity of Reverse Link (DFE)

Table 6.4: Parameters for Figures 6.14 - 6.17

CIR	[1 2 1]
SNR	15
delay	1
N_f	5
N_b	1
data format	BPSK
FF, FBF characterization	MMSE
DFE BER	simulation
ADFE BER	Markov model, except as noted

For the selected channel, the DFE FF is able to synthesize the appropriate timing over a fairly wide range of delays. Despite the prediction of Qureshi [Qureshi,

page 1373], there is no apparent advantage in timing sensitivity from using a FS FF. However, it would be rash to draw a general conclusion without investigation of different channels, SNR's, and filter lengths.

Forward Link (ADFE)

On the forward link of the ADFE system, the task of synchronization is shared to some degree by transmitter and receiver, as the choice of main ray is predetermined by the FF at the transmitter (at the base). This may simplify synchronization at the portable. However, as the receiver (at the portable) must synchronize to the predetermined main ray, the receiver has practically no freedom in selecting the main ray. As the receiver has no FF, there is no opportunity to synthesize a delay characteristic, and very little timing error can be tolerated.

Figure 6.15 shows the effect of forward link timing error on the forward link performance. The reverse link timing, used to characterize the FF, is fixed at the near-optimal values (by inspection) of $-2T_{sym}$ for the TSE and 0 for the FSE.

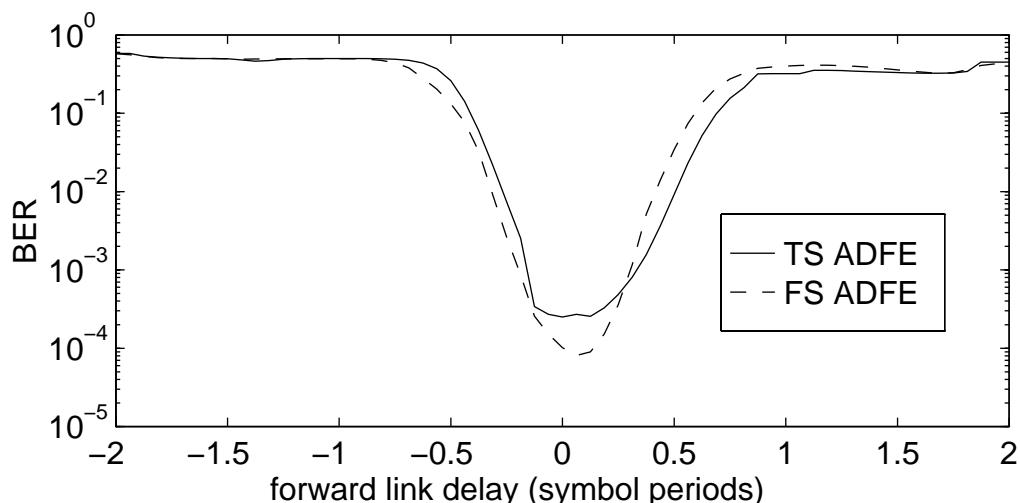


Figure 6.15: BER Timing Sensitivity of Forward Link (ADFE)

The timing sensitivity of the ADFE receiver might be reduced by employing a fractionally spaced channel estimator. A simple heuristic could select a main ray with minimal relative residual precursor ISI, possibly taking into account the

amount of postcursor ISI. The increased complexity of training, due to the increased number of taps, might be compensated for by an improvement in performance and simplification of synchronization.

Joint Timing Error

Joint timing error refers to the effect of timing error in the characterization of the FF on the ADFE (the forward link of the ADFE system) performance. This timing error in the FF arises from timing error during reverse link training of the DFE FF and FBF, as the FF is re-used for the forward link.

The previous experiment, involving forward link timing error, assumed suitable values for the reverse link timing, which is applied to the FF characterization. This filter is characterized according to the CIR, timing phase, and delay established in reverse link training, and is subsequently made part of the effective forward link channel for the purposes of timing recovery, training, and data transmission. A poor choice of reverse link timing will be reflected in the forward link performance.

Figure 6.16 illustrates the effect of reverse link timing (used to characterize the FF) on the forward link ADFE performance.

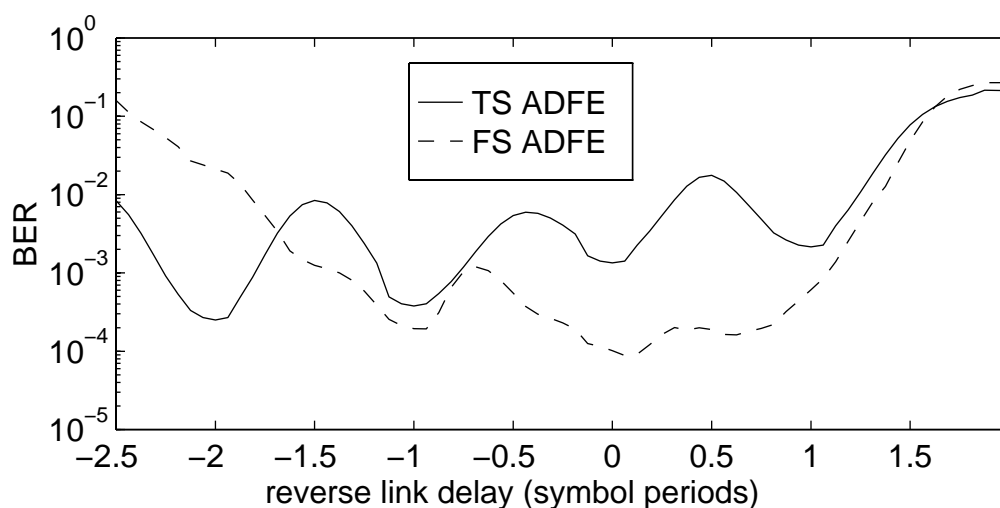


Figure 6.16: BER Joint Timing Sensitivity of Forward Link (ADFE)

The FSE seems to impart the benefit of reduced sensitivity of the forward link to reverse link (training) timing error. There is no apparent explanation for why the TS DFE (Figure 6.14) exhibits less timing sensitivity than the TS ADFE (Figure 6.16). One might ask if this is an erroneous conclusion, due to the ‘noisy’ nature of the DFE simulation results. The ADFE curves are much smoother as they are determined by Markov model. Because of this question, the ADFE BER timing sensitivity was also determined by simulation, and the result is shown in Figure 6.17.

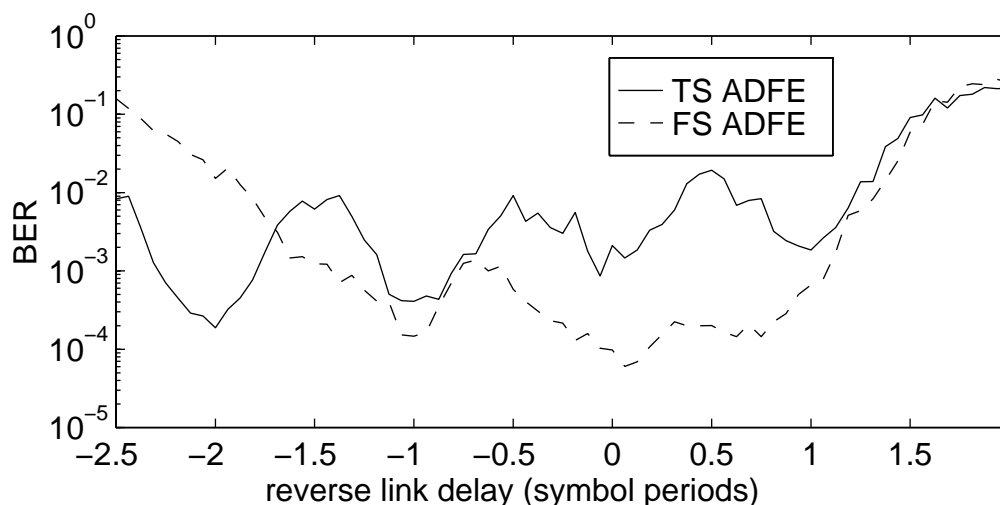


Figure 6.17: Joint BER Timing Sensitivity of Forward Link, by Simulation

Although ADFE results by simulation are not as smooth as those by Markov model, the T_{sym} spaced ADFE sensitivity to reverse link (training) timing is still evident in Figure 6.17. This supports the hypothesis that the TS ADFE is more sensitive to timing error (in the FF) than is the TS DFE.

This foregoing investigation of joint timing sensitivity has assumed near-optimal reverse link timing, which affects the characterization of the ADFE FF. An investigation of the effect of combined forward and reverse link timing error on the forward link performance was performed, using the parameters of Table 6.4. The results, best presented in three dimensions with BER as a function of the two timing errors, are not shown here. Figure 6.16 illustrates a slice of this surface with at zero forward link delay. When the reverse link delay is varied in either

direction, the BER at any reverse link delay increases rapidly, after the manner shown in Figure 6.15.

6.3 Adaptive Training

The ADFE system uses RLS training (or a “fast” RLS variant) to characterize the DFE, and the ADFE FF. LSCE is used to characterize the ADFE FBF. These forms of training approximate the MMSE solution. The MMSE solution itself is used in most parts of this thesis for simplicity and in order to isolate the examination of other factors from training. It is valuable to compare the performance of adaptive training with MMSE characterizations to validate this substitution and to examine the required training length for a selected channel.

Figures 6.18 and 6.19 compare equalizer BER performance with MMSE characterization and adaptive training. While MSE is often used to evaluate equalizer convergence, the BER is more indicative of actual performance. It was shown in Section 6.1 that subtle differences in MSE characterization and performance may have a significant impact on BER performance.

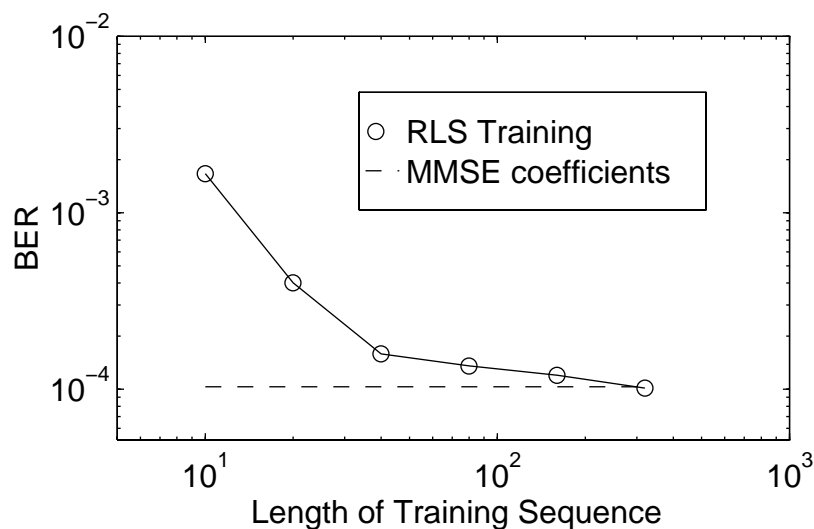
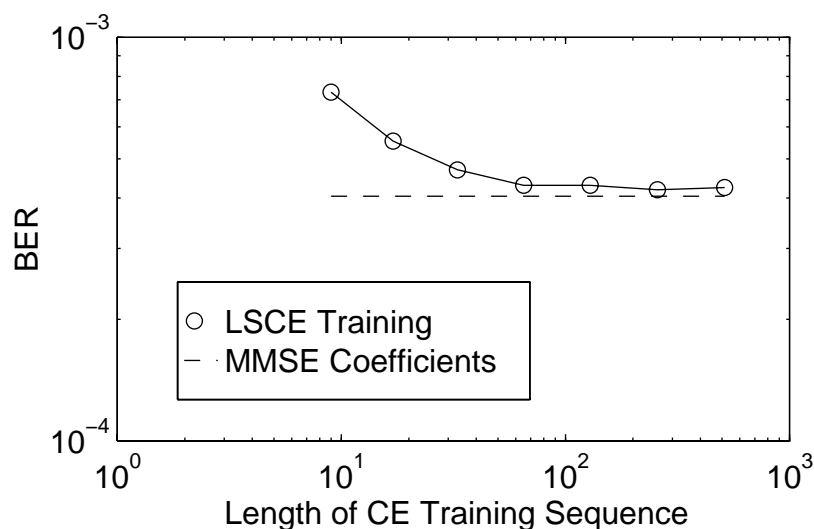


Figure 6.18: DFE Adaptive RLS Training

Table 6.5: Parameters for Figure 6.18

equalizer	DFE
CIR	[1 2 1]
SNR	17 dB
delay	1
N_f	4
N_b	1
data format	BPSK
BER	simulation
FF, FBF characterization	RLS

**Figure 6.19: ADFE FBF Adaptive LS Training**

It appears that equalization with adaptive training is able to approximate the BER performance of MMSE coefficients, provided that a training sequence of sufficient length is used. An equalizer with more taps would generally require longer training to converge, but the required training length is expected to be linear with the number of taps. A rule of thumb for LS training is that the training sequence be about twice the number of equalizer taps.

Table 6.6: Parameters for Figure 6.19

equalizer	ADFE
CIR	[1 2 1]
SNR	17 dB
delay	1
N_f	4
N_b	1
data format	BPSK
BER	Markov model
FF characterization	RLS (320 training symbols)
FBF characterization	LSCE

6.4 Finite Precision

The accuracy of the output of equalizer structures in the ADFE system is affected by the precision of the input data and that of the internal arithmetic operations. The relationship between numerical precision and performance is difficult to analyze, especially if the metric of performance is the BER.

The effect of finite precision arithmetic was modeled by including into the FIR structures (FF, FBF) a nonlinear and memoryless quantization operation. The effect of finite precision on training is not analyzed.

The quantization operation is defined as follows:

Let B be the effective number of bits (precision) of the quantizer.

Let C be the low saturation level of the quantizer.

Let D be the high saturation level of the quantizer.

Define 2^B equidistant points between C and D (inclusive) as the set of quantizer levels.

The quantizer output $Q[x]$ is the quantizer level which is closest to its input x .

The quantization operation was incorporated into the FIR structure by quantizing the operands and products of all multiplications, and the filter output itself. One possible effect not modeled is that of quantizer saturation, due to an intermediate sum lying outside of the saturation levels. A fixed-point implementation of an equalizer could easily (with little added complexity) avoid this undesirable effect by using extended precision to represent intermediate sums.

If an FIR filter has coefficients $w(k)$ and an input signal $x(n)$, the effect of finite precision is modeled as follows:

$$\begin{aligned} w_Q(k) &= Q[w(k)] \\ x_Q(n) &= Q[x(n)] \\ y_Q(n) &= Q\left[\sum_{k=0}^{N_w-1} w_Q(k)x_Q(n-k)\right]. \end{aligned} \tag{6.1}$$

$y_Q(n)$ is the output of the finite-precision arithmetic FIR filter.

Figure 6.20 illustrates the quantizer input/output characteristic for $B = 4$ bit precision, with saturation levels $C = -10$ and $D = 10$.

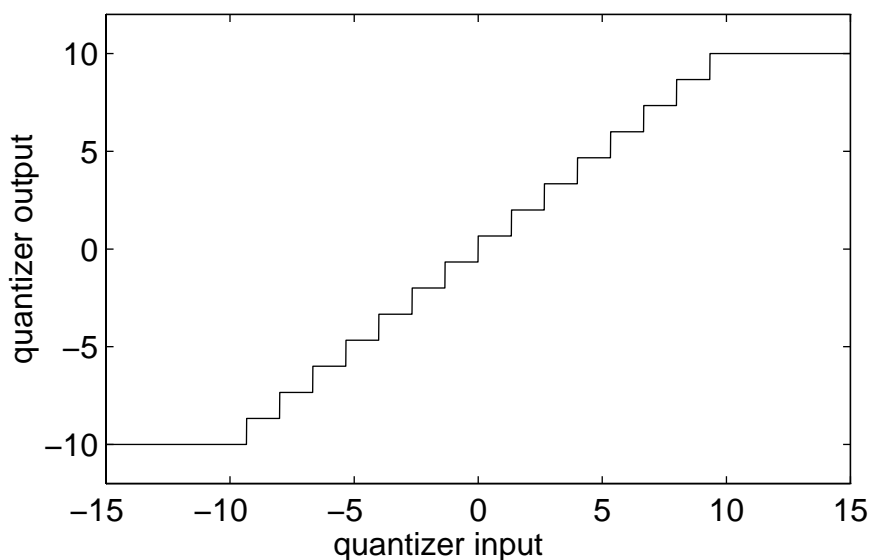


Figure 6.20: Quantizer Input/Output Characteristic

For the results of this section, the saturation levels of the quantizer were fixed at $C = -10$ and $D = 10$. In all cases, the quantizer inputs were never outside of these bounds, so that quantizer saturation was not an issue.

Figures 6.21, 6.22, and 6.23 illustrate the performance of the ADFE and Gibbard precoder with finite precision arithmetic. Results for the Gibbard precoder are included as its performance with finite precision arithmetic is of interest, for comparison with the ADFE. The highest precision of 128 bits is beyond the internal precision of the computer used to implement the simulation (about 52), so this region of the figures reflects performance with high-precision floating-point arithmetic.

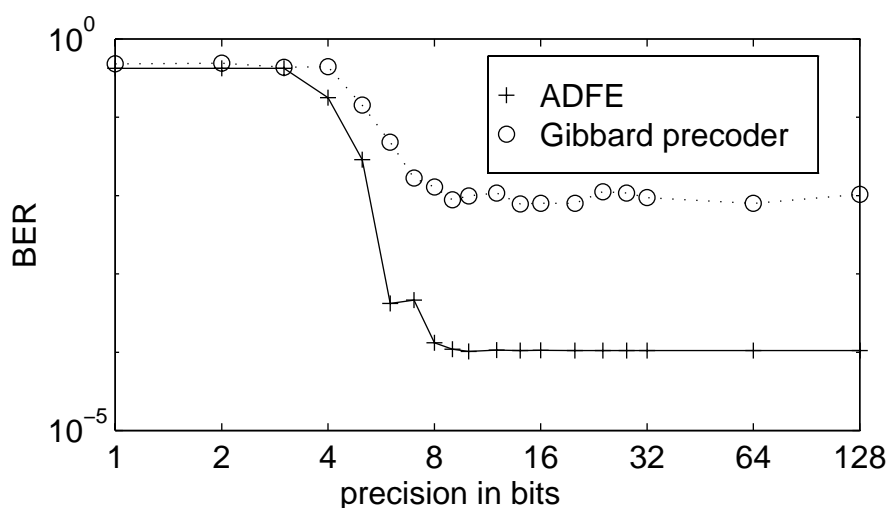


Figure 6.21: Equalizer Performance with Finite Precision Arithmetic

Table 6.7: Parameters for Figure 6.21

equalizer	ADFE, Gibbard Precoder
CIR	[1 2 2 1]
SNR	24 dB
delay	1
N_f	3
N_b	2
data format	BPSK
BER	Markov model (ADFE) simulation (Gibbard)
equalizer characterization	MMSE

The Gibbard precoder is expected to have performance similar to that of the ADFE, in the absence of AGC error. The impaired performance of the Gibbard precoder does not seem to stem from finite precision, as performance does not approach that of the ADFE, even at the highest precision. In fact, in an additional trial at full precision (not shown), the BER of the Gibbard precoder was still about 10^{-2} .

Figure 6.22 illustrates the results of a subsequent experiment to determine if the performance of the Gibbard precoder will improve with more FF taps and increased SNR.

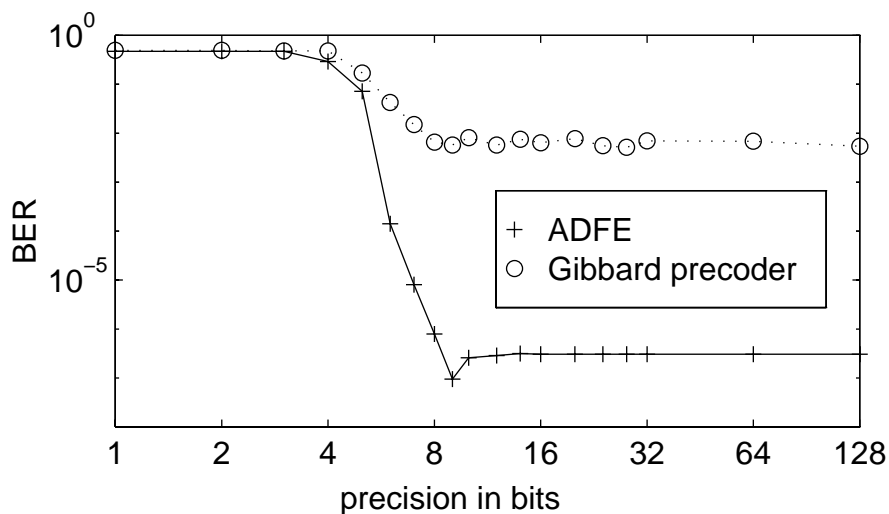


Figure 6.22: Equalizer Performance with Finite Precision Arithmetic

Table 6.8: Parameters for Figure 6.22

equalizer	ADFE, Gibbard Precoder
CIR	[1 2 2 1]
SNR	27 dB
delay	1
N_f	5
N_b	2
data format	BPSK
BER	Markov model (ADFE) simulation (Gibbard)
equalizer characterization	MMSE

Figure 6.23 illustrates another experiment comparing the ADFE and Gibbard precoder, with a different (less severe) channel. In this case, both equalizers performed satisfactorily at higher precisions. This difference from the two previous situations (Figures 6.21, 6.22) indicates that the poor performance of the Gibbard precoder may be due to the choice of CIR.

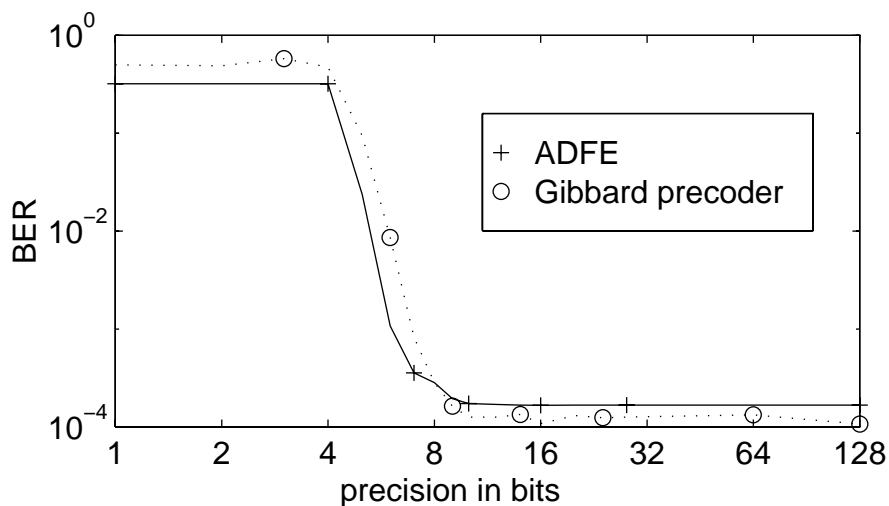


Figure 6.23: Equalizer Performance with Finite Precision Arithmetic

Table 6.9: Parameters for Figures 6.23, 6.24

equalizer	ADFE, Gibbard Precoder
CIR	[-1 2 2 -1]
SNR	11 dB
delay	1
N_f	3
N_b	2
data format	BPSK
BER	Markov model (ADFE) simulation (Gibbard)
equalizer characterization	MMSE

The [1 2 2 1] channel is particularly difficult to equalize, and the MMSE FF leaves behind a significant amount of residual precursor ISI, which may degrade the performance of the Gibbard precoder. The residual precursor ISI may be seen in Figure 6.24, which shows the convolution of the FF and CIR. $q(0)$ is the main ray, and the preceding rays are the residual precursor ISI.

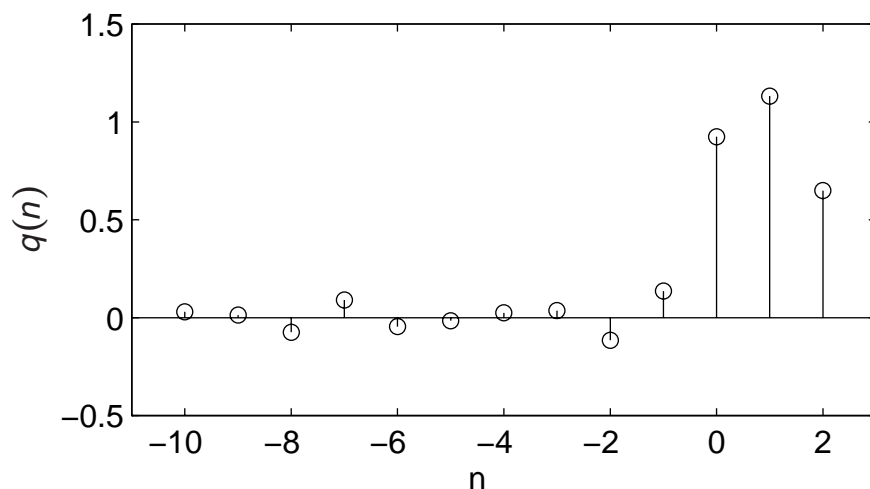


Figure 6.24: Residual Precursor ISI (convolution of FF and CIR)

Based on the suspicion that the Gibbard precoder may be especially sensitive to residual precursor ISI, a further experiment was carried out in which a CIR with precursor ISI (one ray) is equalized by a Gibbard precoder and ADFE with a single-tap FF. As both equalizers will be incapable of mitigating the precursor, it is hoped that this situation will simulate the effect of residual precursor ISI. The CIR is $[p \ 2 \ 2 \ 1]$, where p is varied to control the amount of unresolved precursor ISI.

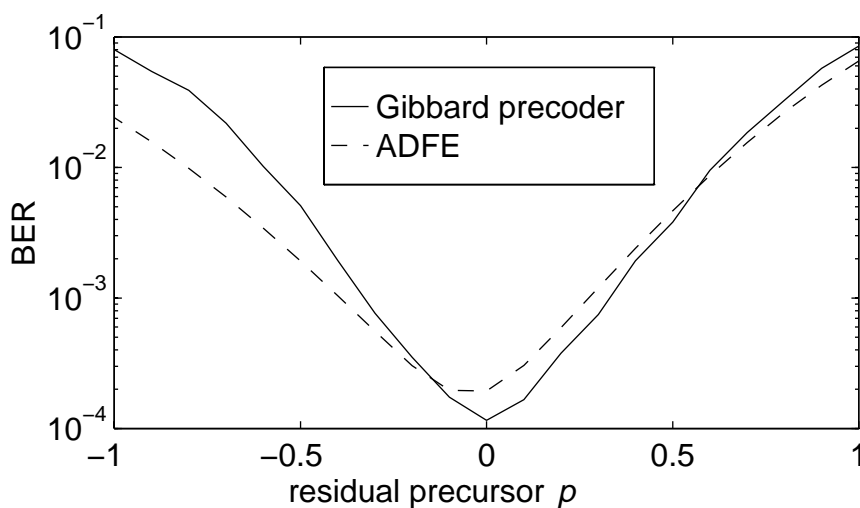


Figure 6.25: Equalizer Performance with Residual Precursor ISI

Table 6.10: Parameters for Figure 6.25

equalizer	ADFE, Gibbard Precoder
CIR	[p 2 2 1] p is the abscissa
SNR	12 dB
delay	1
N_f	1
N_b	2
data format	BPSK
BER	Markov model (ADFE) simulation (Gibbard)
equalizer characterization	MMSE

The results of Figure 6.25 do not support the hypothesis that the Gibbard precoder is more sensitive to unresolved precursor ISI than the ADFE.

6.5 Conclusions

This chapter has presented results on the effect of some expected non-idealities on the performance of the ADFE system: training SNR mismatch, timing error, adaptive training, and finite precision. In general, reasonable levels of any non-ideality were shown to have little or no deleterious effect on BER performance. The Gibbard precoder was found to suffer from an error floor over a particular channel, for which the ADFE does not. This difference in performance is unexpected, and its cause is not understood.

The results of this chapter are not exhaustive, as each non-ideality is considered separately, and a few cases, such as the effect of finite precision on the DFE, are not covered. As well, a real system may suffer from other non-idealities not conceived of in this thesis.

SNR mismatch

It is difficult to generalize about the impact of SNR mismatch on performance. The degree of effect appears to vary significantly over different channels, even those with similar magnitudes of precursor and postcursor ISI.

Results indicate that MSE-based characterization of the DFE or ADFE may be improved by manipulating the effective characterization SNR. It is straightforward to do so if adaptation consists of explicitly estimating the CIR and SNR. If implicit methods are used, then the training SNR may be lowered by injecting noise into the received signal during training. A similar effect might be achieved via the tap-leakage algorithm [Gitlin] or manipulation of the RLS forgetting factor.

In much of the literature, it seems that an underlying, tacit assumption is applied to the design and analysis of equalizers: MSE performance approximates MPE performance, and hence MMSE characterization is a reasonable approximation of MPE characterization. Although the Saltzberg bound [Saltzberg] may be used to relate MSE to BER performance, the bound is apparently not tight in all cases. The results of this section on SNR mismatch raise two caveats regarding this assumption:

1. BER performance may be significantly improved, in some situations, through a modified MSE criterion. This means that MMSE is not a close approximation for MPE characterization. This point is supported by the results shown in Figure 6.3, in which the BER may be reduced from 9.8×10^{-4} (characterization SNR equal to the execution SNR of 21 dB) to 1.6×10^{-5} (characterization SNR of 2.8 dB). As the BER results vary considerably across the small number of contrived channels used, further investigation is recommended prior to generalization.
2. Factors which have a very subtle effect on MSE performance may have a significant effect on BER performance. An example of this situation may

be seen by comparing Figures 6.12 and 6.13. The MSE curve gives no hint to the significant fluctuations in BER.

Modified characterization by manipulation of training SNR may also be beneficial for equalizers such as the DFE, ADFE, TH precoder, Gibbard precoder, and linear equalizer.

Timing Error

The effect of timing error on the ADFE system was examined. On the reverse link, as expected, the FS DFE was fairly insensitive to timing error. However, the TS DFE did not demonstrate much sensitivity to timing phase either. This result was not expected, as the principal reason for the popularity of the FS equalizer is reduced sensitivity to timing phase. This particular result might be due the unique nature of the selected CIR, or to the use of BER (rather than MSE) as a metric of performance.

On the forward link, the ADFE receiver requires accurate timing to within a fraction of T_{sym} . This sensitivity might be alleviated by combining fractionally spaced channel estimation with a simple heuristic for choosing the main ray. The forward link is subject to reverse link timing error in training the FF. This joint timing error has an effect on the ADFE similar to that of timing error on the DFE. One difference is that the TS ADFE is quite sensitive to the timing phase, while the TS DFE is not.

The relative merits of TS and FS equalization for the ADFE system will depend on the nature of the channel and the difficulty associated with establishing good timing. In general, use of a FSE will relax the timing requirements (at least on the forward link), while possibly requiring a greater number of FF taps.

Adaptive Training

As expected, RLS training of the DFE and ADFE was demonstrated to converge to a solution with performance virtually equivalent to the MMSE characterization.

It remains to formulate and investigate an algorithm which incorporates the advantages of the SNR mismatch (see Section 6.1) into adaptive training.

Finite Precision

Based on a model of a finite precision arithmetic implementation, the ADFE and Gibbard precoder do not appear to suffer from extreme sensitivity to finite precision arithmetic. A more complete examination of this topic might include a greater variety of channel conditions, including measured CIR's.

For one CIR, the Gibbard precoder suffered from an error floor unrelated to finite precision. As this scenario involved a significant amount of residual precursor ISI, a further experiment was carried out to compare the performance of the ADFE and Gibbard precoder with a controlled amount of residual precursor ISI. As this experiment revealed no significant difference in performance, it is still not clear why the Gibbard precoder exhibited the error floor over one channel. The difference between the two equalizers may be dependent on the choice of CIR.

7. ADFE System Performance over Measured Channels

7.1 The Indoor Channel Database

In order to gain a better indication of the ADFE system performance in an actual implementation, simulations were performed over measured channels. These channels were selected from a database of channel measurements prepared by Morrison and Tholl [Morrison]. The database contains indoor channel measurements from two different office buildings at varied locations and transmitter/receiver separations. For this work, channels from one building having a transmitter/receiver separation of 30 metres were selected.

There are 1500 different channel measurements from one building (the Alberta Government Telephones, or Telus, offices) having a transmitter/receiver separation of 30 metres (the largest separation available in the database). For the simulations in this chapter, 200 or 300 CIR's were uniformly sampled from this set of 1500. As channel ordering in the database corresponds to physical location of transmitter/receiver, this sampling should give a subset of channels with maximum independence.

The channel information in the database is stored as complex samples of the channel frequency response from 900 MHz to 1300 MHz. Each channel underwent the following processing to yield a (time domain) baseband equivalent CIR with a suitable sampling rate.

1. The channel spectrum is delay-pass filtered [Morris, page 20] with a Kaiser window. The stopband is defined as a segment of the time domain

CIR which contains noise and a spurious signal component which is likely due to crosstalk between the test equipment connections.

2. The channel spectrum is downsampled in the frequency domain to effectively truncate the CIR in the time domain.
3. The channel energy is normalized across the full bandwidth of 400 MHz. This step is performed to remove the effect of flat fading, while preserving narrowband fading characteristics [Gibbard2]. Because of this normalization, the SNR must be considered an average SNR across the ensemble of channels, each channel will may introduce a gain or penalty in SNR, according to its frequency characteristics.
4. A SQRC matched filter characteristic (with rolloff $\beta = 0.35$) is applied to the channel, still in the frequency domain.
5. A portion of the signal, in the frequency domain, is truncated, effectively reducing the sampling rate in the time domain. The truncated portion of the spectrum has a value of zero, due to the matched filter applied in the previous step.
6. The channel spectrum information is transformed into the time domain (via the inverse fast Fourier transform) to yield the CIR with a sampling rate of $T_{sym}/2$ with a symbol rate of $1/T_{sym} = 50$ MHz.

7.2 Method of Simulation

Error Collection

During simulation, measures were taken to ensure that sufficient errors were accumulated for each point on the BER curve, while reducing unnecessary computations. A BER for each of the 200 channels was determined at a reduced SNR, in order to estimate the relative performance over each channel at the desired SNR. The 'worst' channel (highest BER at reduced SNR) was simulated

at the desired SNR until at least 100 bit errors were collected. The number of transmitted bits for this simulation was recorded. Each of the remaining channels was then simulated (at the desired SNR) until either 100 errors were collected or the number of transmitted bits reached the number transmitted for the ‘worst’ channel. The average BER for the ensemble of channels was then computed. This method ensured that errors from all channels are weighted equally, and that at least 100 errors are collected per average BER. It took about a week for a DEC Alpha workstation to generate the simulation results for this chapter, using a combination of Matlab and C programs.

Adaptive Training

The DFE was characterized with RLS training, using a training sequence of 100 QPSK symbols. The ADFE FF was also characterized in the same way. The ADFE FBF was characterized according the method described in Section 4.3, except that RLS channel estimation was used instead of computationally efficient LS channel estimation. The reason for this change of method is that a training sequence with ideal autocorrelation properties would be excessively long (on the order of 2^{16}), given the number of FBF taps (16). A realistic approach to implementation, given a large number of FBF taps, might utilize a training sequence of reasonable length with near-ideal autocorrelation properties. M-sequences satisfy these requirements, with the possibility of low-complexity training [Crozier2]. In these simulations, all training sequences consisted of 100 (randomly determined) QPSK symbols. This length was deemed sufficient to allow the equalizers to converge during training.

Data Transmission and Retraining

Data was transmitted in frames of 2000 QPSK symbols. In the data transmission subsequent to a training, the filters (and CIR) were kept constant. The number of data frames between equalizer retraining began at one, and was increased by one frame after each retraining. If T represents a (re)training and D represents a data frame, then they are arranged as follows:

T D T DD T DDD T DDDD T DDDDD T DDDDDD T DDDDDDD ...

The number of data frames between retraining was increased thusly so that a moderate number of retrainings would take place for each channel, whether small or large number of data frames were transmitted. This helped to reduce the computational burden of simulating transmission of many frames (at low error rates), while ensuring that performance is effectively averaged over a number of retrainings.

Number of FF/FBF Equalizer Taps

An excessive number of FF and FBF taps were used, to ensure that performance was not limited by the lengths of equalizer filters. A reasonable implementation of the ADFE system would likely use the minimum number of taps required to effectively equalize the channel. This minimum could be determined for any filter by conducting additional BER simulations in which the number of filter taps is varied. Table 7.1 compares the numbers of (TS) FF and FBF taps selected in other trials involving channels from the same indoor channel database.

Table 7.1: Summary of DFE Filter Lengths

method of	FF/FBF taps	symbol rate	data modulation
Gibbard [Gibbard3]	9/13	50 MHz	QPSK
Morris [Morris]	5/11	37.5 MHz	QPSK
Ebel [Ebel]	12/12	20 MHz	16-QAM

Synchronization

Receiver synchronization was based on a perfect knowledge of the channel, by choosing the main ray to be the first ray with magnitude greater than 0.7 times the magnitude of the largest ray [Ebel, pp. 114-117]. A fractionally spaced FF was used to allow the DFE to synthesize optimal or near-optimal timing. The ADFE receiver had its synchronization automatically set in agreement with the timing established by the FF. In practice, synchronization of the ADFE receiver

should be simple due to the minimum-phase nature of the effective FF-CIR combination.

7.3 Simulation Results

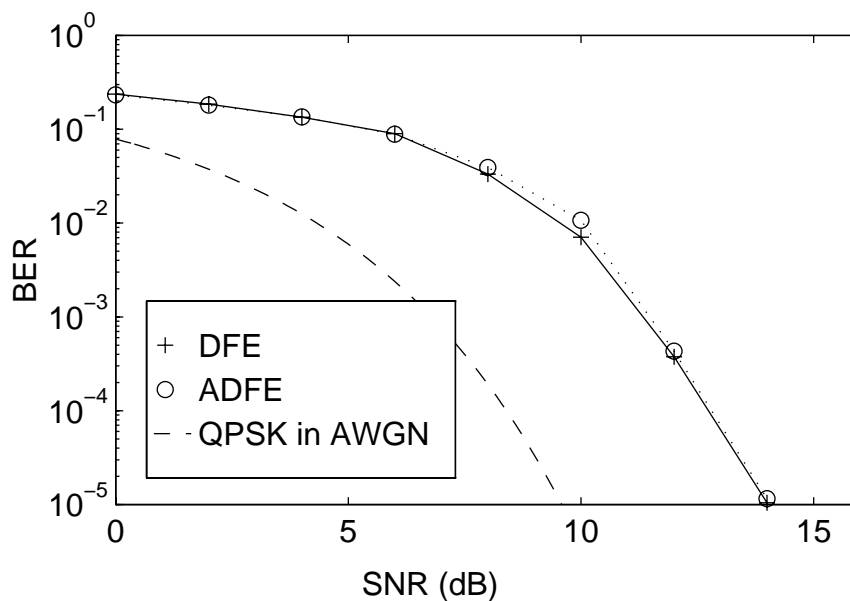


Figure 7.1: Average BER for Measured Channels

Table 7.2: Parameters for Figure 7.1

equalizer	ADFE and DFE, both with fractionally spaced ($T_{sym}/2$) FF
CIR	200 channel measurements
delay	set according to CIR
N_f	20
N_b	16
data format	QPSK, $T_{sym} = 20\text{ns}$
BER	simulation
equalizer characterization	RLS training

Figure 7.1 shows the average BER as a function of (average) SNR for the ADFE system. The dashed line indicates the BER for QPSK transmission in an AWGN

channel with no ISI. As Figure 7.1 only shows the average BER over the ensemble of channels, one might wonder what sort of distribution of BER's this average is composed of. Figure 7.2 illustrates this distribution, at a fixed (average) SNR of 11 dB. The histogram is normalized so it approximates the BER probability distribution over the ensemble of channels.

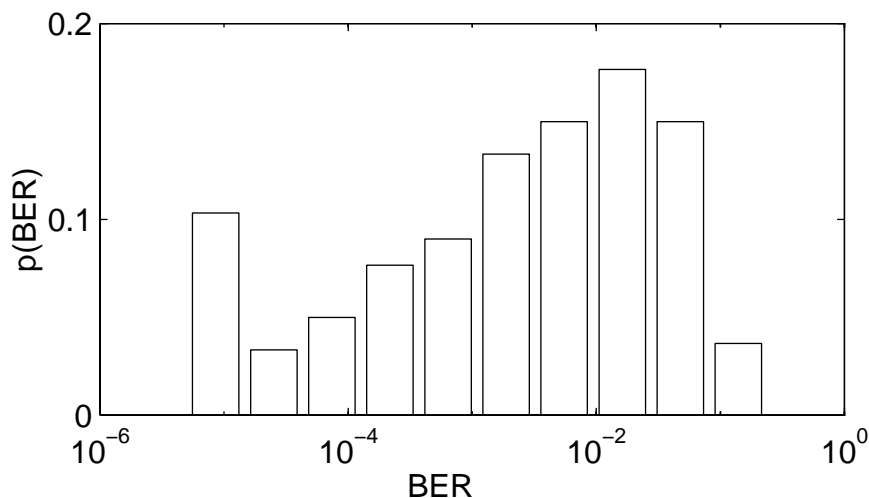


Figure 7.2: BER Distribution

Table 7.3: Parameters for Figures 7.2, 7.3

equalizer	ADFE with fractionally spaced ($T_{sym}/2$) FF
CIR	300 channel measurements
SNR	11 dB
delay	set according to CIR
N_f	20
N_b	16
data format	QPSK, $T_{sym} = 20\text{ns}$
BER	simulation
equalizer characterization	MMSE

The simulation program used to obtain the above data was required to collect at least 100 bit errors per channel to estimate a BER. The number of transmitted bits per channel was restricted to 2×10^7 bits, after which simulation is halted

(see Section 5.2). Hence, it is not possible to estimate a BER below 5×10^{-6} , as the maximum number of bits are transmitted before 100 errors are collected. Since it is then possible to conclude that the BER is no more than 5×10^{-6} , this BER is assigned as an upper bound. Figure 7.3 is based on the same raw results as Figure 7.2, but without the restriction that 100 bit errors must be collected to estimate a BER. The lowest bin shown is composed entirely of channels which had no errors after transmission of 2×10^7 bits.

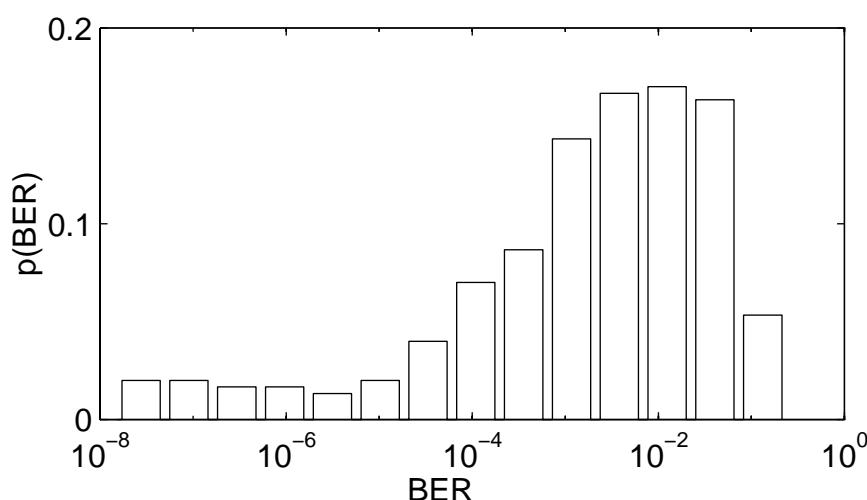


Figure 7.3: BER Distribution (relaxed error requirements)

The above figure shows a tail of BER's extending down below 10^{-6} , indicating that there are a few channels which are very favorable to data transmission. This tail must be viewed with some suspicion as it is based on the collection of very few errors. The leftmost bin represents the channels for which zero errors were collected. Except for Figure 7.3, no other results or figures in this work are based on this questionable interpretation of BER results.

Although the average BER is 1.66×10^{-2} , the BER over any given channel can easily vary from 10^{-5} to 10^{-1} . This may have a significant effect on the system performance and design requirements, since most communication systems require that a level of BER performance be met with high probability.

As an aside, it is curious to note that the average BER of 1.66×10^{-2} at 11 dB SNR for the Figure 7.3 is slightly inferior to the adaptive ADFE of Figure 7.1, which has a BER of 1.07×10^{-2} at 10 dB SNR. This discrepancy may be due to the uncertainty in BER estimation by simulation.

Figures 7.4 through 7.7 show four baseband equivalent channels from the set used in Figure 7.2. Each figure illustrates the discrete-time CIR (sampled at $T_{sym}/2$) used for simulation. These channels represent the 0, 33, 66, and 100th percentiles of BER performance. The channel at the 0th percentile is the lowest BER, which is the best BER performance. Table 7.4 specifies the BER for each of the four channels, for the conditions specified in Table 7.3.

Table 7.4: BER of Selected Channels

BER	Percentile of BER	Figure
$\leq 5 \times 10^{-6}$	0	7.4
9.0×10^{-4}	33	7.5
1.1×10^{-2}	66	7.6
2.4×10^{-1}	100	7.7

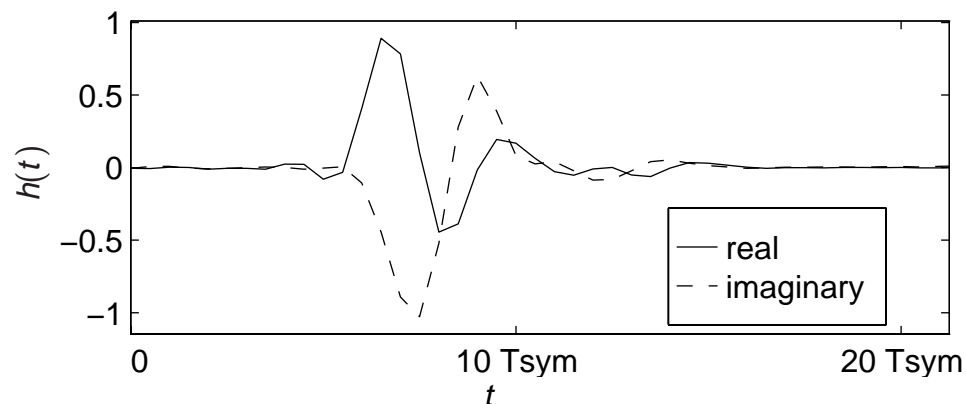


Figure 7.4: Indoor Channel Impulse Response

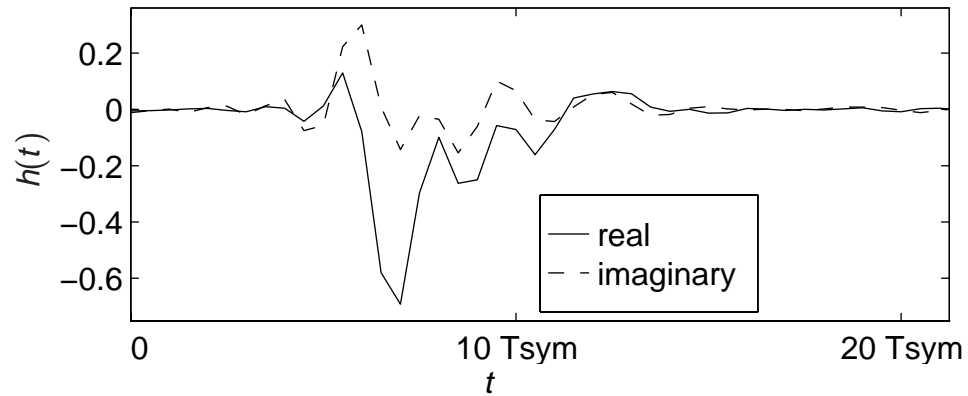


Figure 7.5: Indoor Channel Impulse Response

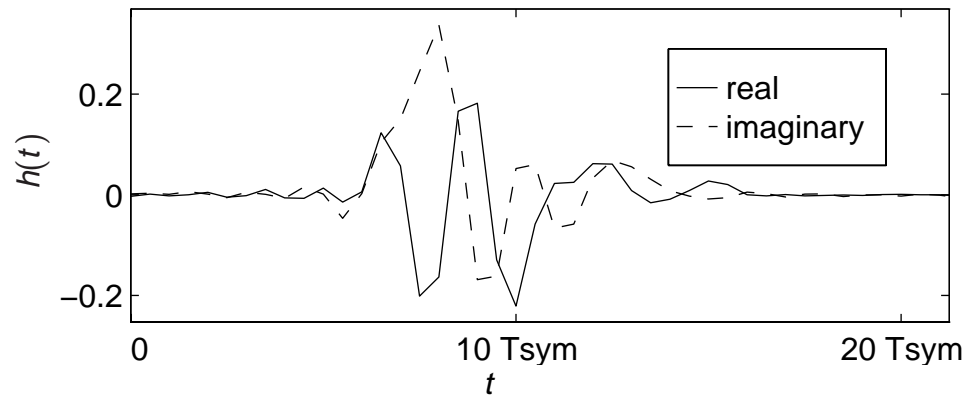


Figure 7.6: Indoor Channel Impulse Response

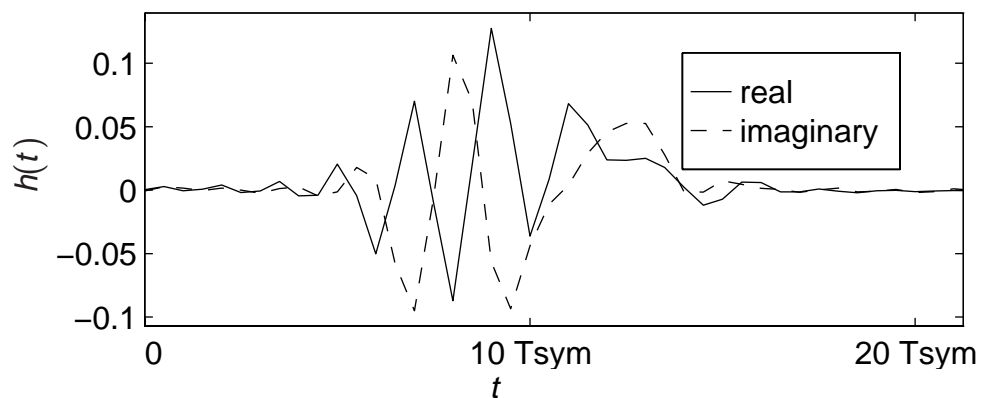


Figure 7.7: Indoor Channel Impulse Response

A casual examination of the four preceding channels hints at a relationship between BER and the energy of the CIR (fading). The variation in CIR energy is entirely due to the normalization of the CIR energy within the 400 MHz

bandwidth, prior to bandlimiting to 67.5 MHz. Although this normalization may contribute to the variation in BER over the different channels, it may not be the only cause. In the plots of the four selected channels, the amount of ISI appears to be inversely correlated with the CIR energy and BER performance.

Figure 7.8 plots the relationship between CIR energy (the squared magnitude of the sampled CIR) and BER for the set of 300 channels.

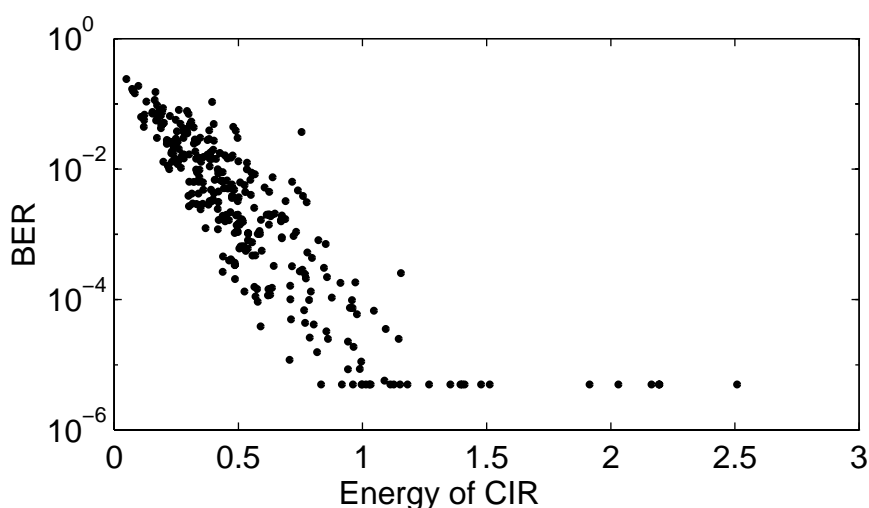


Figure 7.8: BER Performance versus Energy of CIR

7.4 Conclusions

BER curves indicate that the ADFE system is able to satisfactorily equalize data transmission over a number of measured indoor channels. The average BER begins to drop sharply at higher SNR's. This result should be taken with caution, as the BER distribution at one SNR indicates that one will often encounter performance better or worse than the average. Other factors such as diversity and error correcting codes may play a major role in determining the ultimate system performance.

Although efforts were taken to ensure that this use of the measured channels should effectively model the channels and fading that a full implementation would encounter, there are a number of additional factors to consider. Some of these

factors may be SNR mismatch, joint timing sensitivity, finite precision in training and equalization, realistic synchronization, jitter, and Doppler fading.

Despite these shortcomings, this chapter offers a partial glimpse of the expected performance of the ADFE system in an indoor office environment. The performance is so highly dependent on the CIR and fading that most of these results tell as much or more about the nature of the channel than about equalizer performance.

8. Conclusion

8.1 Summary of Thesis

This thesis has presented a new equalization structure, the Asymmetric Decision Feedback Equalizer (ADFE), and a system for asymmetric equalization, the ADFE system. Following background material on digital communications and equalization, the ADFE was subjected to the usual analyses of MSE and BER performance. The BER analysis was facilitated by application of a finite discrete Markov process to model the effects of noise, residual precursor ISI, and error propagation. The effects of SNR mismatch, timing error, adaptive training, and finite precision arithmetic on BER were determined by modeling and simulation. These investigations turned up some results which were unexpected, especially in the area of SNR mismatch. The BER performance of certain equalizers over some channels can be improved markedly by changing the SNR of training, or MMSE characterization.

As ADFE system is intended for application in an indoor wireless LAN, the performance of the ADFE system was determined by simulation using an ensemble of measured indoor wireless channels. Although the average performance over the ensemble is satisfactory and predictable, its variation from one channel to another is considerable. Judicious exploitation of this variation might enhance the performance of a system, while its neglect may hamper performance.

8.2 Topics for Further Research

There are many areas which could or should have been addressed within this thesis, but were not. Some of these are absent due to constraints of time or of computing resources, while others extend into subject areas that are beyond the scope of this thesis to handily encompass.

Most of the tests and simulations in this thesis could be expanded upon by varying the CIR, SNR, and equalizer type and size. The effect of finite precision arithmetic on the adaptive training and execution of the DFE could be investigated. As suggested in Chapter 6, it may be beneficial to combine fractionally spaced channel estimation with a simple synchronization heuristic in the ADFE receiver. The appropriate or optimal number FF/FBF taps required to achieve a desired level of BER performance could also be investigated.

A prototype implementation of the ADFE system would be useful to verify its performance. Such a project would involve many design considerations such as data rate, number of FF/FBF taps, performance level, and expected severity of multipath ISI. A specific algorithm for reverse link training would need to be chosen or designed, and a non-optimal forward link training sequence chosen, as the optimal sequences are too long if the number of FBF taps is not small. More extensive and specific analysis and simulations would be needed along the way to facilitate these and other design decisions.

Some interesting results in this thesis were presented as an initial indication of new and interesting phenomena in the hope that they may be properly investigated in other works. One of the most significant of these is the SNR mismatch, which may find use as a compromise between MMSE and MPE characterizations. An understanding of the strange BER behavior of Figure 6.12 may lead to greater insight into fundamental principles of equalization and data errors. In any case, it may be desirable to seek alternatives to MMSE characterization and analysis of equalizers, as the simplicity of MSE analysis may not always justify the penalty in BER performance.

Finally, the range of performance of the ADFE system over measured indoor channels could certainly bear more rigorous and complete investigation. This is a factor which may affect performance of a system more than the equalizer itself, but which is much harder to analyze due to its statistical nature.

To summarize, this thesis presents some promising results for the ADFE and SNR mismatch, which require further research and experimentation to verify their ultimate usefulness.

References

- [Altekar] S. A. Altekar, N. C. Beaulieu, "Upper bounds to the error probability of decision feedback equalization," *IEEE Transactions on Information Theory*, vol. 39, no. 1, pp. 145-156, January 1993.
- [Austin] M. E. Austin, "Decision-feedback equalization for digital communication over dispersive channels," *M.I.T. Research Lab. Elect., Cambridge, Mass.*, Tech. Rept. 461, August 1967.
- [Belfiore] C. A. Belfiore, J. H. Park Jr., "Decision feedback equalization," *Proceedings of the IEEE*, vol. 67, no. 8, pp 1143-1156, August 1979.
- [Chennakeshu] S. Chennakeshu, G.J. Saulnier, "Differential detection of $\pi/4$ -shifted-DQPSK for digital cellular radio," *Proceedings of the 41st IEEE Vehicular Technology Conference*, pp. 186-191, May 1991.
- [Cioffi] J. M. Cioffi, T. Kailath, "An Efficient exact-least-squares fractionally spaced equalizer using intersymbol interpolation," *IEEE Journal on Selected Areas in Communications*, vol. SAC-2, no. 5, pp.743-756, September 1984.
- [Crozier1] S. N. Crozier, "Short-Block Data Detection Techniques Employing Channel Estimation for Fading Time-Dispersive Channels," Ph.D. Thesis, Carleton University, Ottawa, Canada, 1990.
- [Crozier2] S. N. Crozier, D. D. Falconer, S. A. Mahmoud, "Least sum of squared errors (LSSE) channel estimation," *IEE Proceedings part F*, vol. 138, no. 4, pp 371-378, August 1991.
- [Despins] C. L. B. Despins, D. D. Falconer, S. A. Mahmoud, "Compound strategies of coding, equalization, and space diversity for wideband TDMA indoor wireless channels," *IEEE Transactions on Vehicular Technology*, vol. 41, no. 4, pp. 369-379, November 1992.
- [Duttweiler] D. L. Duttweiler, J. E. Mazo, D. G. Messerschmitt, "An upper bound to the error probability in decision-feedback equalization,"

IEEE Transactions on Information Theory, vol. IT-20, pp. 490-497, July 1974.

- [Ebel] B. A. Ebel, "Searching for Marduk: Tomlinson-Harashima precoding and the indoor radio channel," M.Sc. Thesis, Department of Electrical and Computer Engineering, University of Calgary, 1994.
- [Falconer] D. D. Falconer, L. Ljung, "Application of fast Kalman estimation to adaptive equalization," *IEEE Transactions on Communications*, vol. COM-26, no. 10, pp. 1439-1446, October 1978.
- [Forney] G. D. Forney, Jr., "The Viterbi algorithm," *Proceedings of the IEEE*, vol. 61, pp. 268-278, March 1973.
- [Freeburg] T. A. Freeburg, "Enabling technologies for wireless in-building network communications — four technical challenges, four solutions," *IEEE Communications Magazine*, vol. 29, no. 4, pp. 58-64, April 1991.
- [Freeny] S. L. Freeny, B. G. King, T. J. Pedersen, "Digital transmission system employing bandlimited analog medium with adaptive equalizer at transmitter," U.S. Patent No. 3593142, issued July 13, 1971.
- [Gibbard1] M. R. Gibbard, "Asymmetric equalization of the indoor radio channel," M.Sc. Thesis, Department of Electrical and Computer Engineering, University of Calgary, 1994.
- [Gibbard2] M. R. Gibbard, G. Morrison, A. Sesay, M. Fattouche, "Broadband TDMA over the indoor radio channel," *Electronics Letters*, vol. 30, no. 4, pp. 285-287, February 1994.
- [Gibbard3] M. R. Gibbard, A. B. Sesay, L. Strawczynski, "Asymmetric equalization structure for broadband indoor wireless data communications," in *Proceedings of the Sixth International Conference on Wireless Communications (Wireless '94)*, vol. 2, (Calgary, Alberta), pp. 521-535, July 11-13, 1994.
- [Gitlin1] R. D. Gitlin, S. B. Weinstein, "Fractionally-spaced equalization: an improved digital transversal equalizer," *Bell System Technical Journal*, vol. 60, no. 2, pp. 275-296, February 1981.
- [Gitlin2] R. D. Gitlin, H. C. Meadors, Jr., S. B. Weinstein, "The Tap-leakage algorithm: an algorithm for the stable operation of a digitally implemented, fractionally spaced adaptive equalizer,"

- Bell System Technical Journal*, vol. 61, no. 8, pp. 1817-1839, October 1982.
- [Hagmanns] F.J. Hagmanns, V. Hespelt, "On the detection of bandlimited direct-sequence spread-spectrum signals transmitted via fading multipath channels," *IEEE Journal on Selected Areas in Communications*, vol. 12, no. 5, pp. 891-899, June 1994.
- [Harashima] H. Harashima, H. Miyakawa, "Matched-transmission technique for channels with intersymbol interference," *IEEE Transactions on Communications*, vol. COM-20, no. 4, pp. 774-780, August 1972.
- [Haykin] S. Haykin, *Adaptive filter theory*. Englewood Cliffs, NJ 07632: Prentice Hall, 1991.
- [Kabal] P. Kabal, S. Pasupathy, "Partial-response signaling," *IEEE Transactions on Communications*, vol. COM-23, no. 9, pp. 921-934, September 1975.
- [Karr] L. J. Karr, "Polled data network auto-equalizer system and method," U. S. Patent No. 4969162, issued Nov. 6, 1990.
- [Korevaar] G. J. Korevaar, "Terminal arrangement for a duplex transmission system," U. S. Patent No. 4535433, issued Aug. 13, 1985.
- [Ling] F. Ling, J. G. Proakis, "Adaptive lattice decision-feedback equalizers - their performance and application to time-variant multipath channels," *IEEE Transactions on Communications*, vol. COM-33, no. 4, pp. 348-356, April 1985.
- [Lucky] R. W. Lucky, J. Salz, E. J. Weldon, *Principles of data communications*, McGraw-Hill, 1968.
- [Monsen1] P. Monsen, "Feedback equalization for fading dispersive channels," *IEEE Transactions on Information Theory*, vol. IT-17, pp. 56-64, January 1971.
- [Monsen2] P. Monsen, "Adaptive equalization of the slow fading channel," *IEEE Transactions on Communications*, vol. COM-22, no. 8, pp. 1064-1075, August 1974.
- [Morrison] G. D. Morrison, "A Frequency domain measurement system for indoor ultrahigh frequency radio propagation studies," M.Sc. Thesis, Department of Electrical and Computer Engineering, University of Calgary, 1991.

- [Morris] B. J. Morris, "Optimization of a broadband modulation scheme for the indoor radio channel," M.Sc. Thesis, Department of Electrical and Computer Engineering, University of Calgary, 1993.
- [Mueller] M. S. Mueller, J. Salz, "A unified theory of data-aided equalization," *Bell System Technical Journal*, vol. 60, no. 9, pp. 2023-2038, November 1981.
- [Pottie] G. L. Pottie, M. V. Eyuboglu, "Combined coding and precoding for PAM and QAM HDSL systems", *IEEE Journal on Selected Areas in Communications*, vol. 9, no. 6, pp. 861-870, August 1991.
- [Proakis] J. G. Proakis, *Digital Communications, 2nd edition*, McGraw-Hill, 1989.
- [Qureshi] S. H. Qureshi, "Adaptive equalization," *Proceedings of the IEEE*, vol. 73, no. 9, pp 1349-1387, September 1985.
- [Salazar] A. C. Salazar, "Design of transmitter and receiver filters for decision feedback equalization," *Bell System Technical Journal*, vol. 53, no. 3, pp 503-523, March 1974.
- [Saltzberg] B. R. Saltzberg, "Intersymbol interference error bounds with application to ideal bandlimited signalling," *IEEE Transactions on Information Theory*, vol. IT-14, no. 4, pp. 563-568, July 1968.
- [Salz] J. Salz, "Optimum mean-square decision feedback equalization," *Bell System Technical Journal*, vol. 52, no. 8, pp. 1341-1373, October 1973.
- [Sari] H. Sari, G. Karam, "Asymmetric baseband equalization," *IEEE Transactions on Communications*, vol. 36, no. 9, pp. 1073-1078, September 1988.
- [Shamash] E. Shamash, K. Yao, "On the structure and performance of a linear decision feedback equalizer based on the minimum error probability criterion," *Rec. Int. Conf. Commun.*, ICC-74 (Minneapolis, MN), June 17-19, 1974.
- [Shuckla] P. K. Shukla, L. F. Turner, "Channel-estimation-based adaptive DFE for fading multipath radio channels," *IEE Proceedings-I*, vol. 138, no. 6, pp. 525-543, December 1991.

- [Stephens] W. E. Stephens, H. Samueli, G. Cherubini, "Guest editorial copper wire access technologies for high performance networks," *IEEE Journal on Selected Areas in Communications*, vol. 13, no. 9, pp.1537-1539, December 1995.
- [TIA] Telecommunications Industry Association, *EIA/TIA interim standard: cellular system dual-mode mobile station-base station compatibility standard: IS-54-B*. Washington DC, USA, Apr. 1992.
- [Tomlinson] M. Tomlinson, "New automatic equalizer employing modulo arithmetic," *Electronics Letters*, vol. 7, pp 138-139, March 1971.
- [Ungerboeck] G. Ungerboeck, "Fractional tap-spacing equalizer and consequences for clock recovery in data modems," *IEEE Transactions on Communications*, vol. COM-24, no. 8, pp 856-864, August 1976.
- [Yang] J. Yang, S. Roy, "Joint transmitter-receiver optimization for multi-input multi-output systems with decision feedback," *IEEE Transactions on Information Theory*, vol. 40, no. 5, pp. 1334-1347, September 1994.
- [Zhuang1] W. Zhuang, W. A. Krzymein, P. A. Goud, "Adaptive channel precoding for personal communications," *Electronics Letters*, vol. 30, pp 1570-1571, September 1994.
- [Zhuang2] W. Zhuang, V. Huang, "Nonlinear phase precoding for personal communications," *Electronics Letters*, vol. 30, pp 2010-2011, November 1994.

Appendix

This appendix contains a listing of a Matlab function entitled “markov” which computes the BER and error pattern probabilities for an ADFE. Two other functions are included (“base2num” and “num2base”) which are used by “markov” and are listed in this Appendix.

The comment sections at the beginning of each function specify the input and output parameters and other information for the function.

Listing of markov.m

```
function [ Pe, p2, p1 ] = markov( h, wf, wb, snr, delay, verbose )
% [ PE, P2, P1 ] = MARKOV( H, WF, WB, SNR, DELAY, VERBOSE )
%
% This function models precursor ISI, noise, and error propagation in the ADFE
% as a 1st order Markov process. The state is defined by previously
% transmitted and detected symbols. All input arguments must be real, and BPSK
% data is assumed.
%
% PE is the average probability of bit error.
%
% P2 (optional) is the vector of error state probabilities. P2 is printed out along
% with the accompanying error patterns if MARKOV4 is called with no output
% arguments. Each element of P2 is the probability of the error state given
% by one less than the binary representation of the element index, as follows:
%
%    0000 means no errors
%    1000 means one error was just made
%    1110 means 3 errors were just made
%    etc.
```

```

%
% P1 (optional) is the probability of error assuming correct past decisions
% (i.e. neglecting error propagation).
%
% H is the sampled channel impulse response (sampled at the symbol rate).
%
% WF is a vector of the FF coefficients.
%
% WB is a vector of the FBF coefficients.
%
% SNR is the signal to noise ratio, in dB, assuming that the norm of H is 1.
% The variance of the noise is given by  $10^{(-SNR / 20)} / \text{SQRT}(2)$  .
%
% DELAY specifies which is the main ray of H. H(DELAY+1) is taken to be
% the main ray. If DELAY == [] then an appropriate delay value will be computed
% by this function.
%
% VERBOSE is a flag which if present and nonzero causes additional information
% to be output during execution of the function.
%

if exist( 'verbose' ) ~= 1
    verbose = 0;
end;

if ( delay == [] )
    delay = find( abs( h ) > 0.7 * max( abs( h ) ) );
    delay = delay( 1 ) - 1;
end;

delay2 = delay + length( wf ) - 1;

%%%%%%%%%% The pre-equalizing filter and the linear channel will be combined
%%%%%%%%%% into a single equivalent linear system called q.

```

```

r2 = sqrt( 2 );
sigma = 10 ^ ( -snr / 20 ) * norm( wf ) * norm( h ) / r2;
nb = length( wb );
wb = wb(:);
q = conv( h, wf );
nq = length( q );
q = reshape( q, nq, 1 );
if nb + delay2 > nq
    q = [ q; zeros( nb + delay2 - nq, 1 ) ];
    nq = length( q );
end;

ns = 2 ^ ( nq + nb );           % number of states
P = sparse( [], [], [], ns, ns, 4*ns );

for row = 1 : ns
    if verbose & ( rem( row, 100 ) == 0 )
        fprintf( 1, 'processing row %d/%d.\n', row, ns );
    end;

    present_state = num2base( row-1, 2, nq + nb );
    a = present_state( 1 : nq )' * 2 - 1;
    d = present_state( nq + 1 : nq + nb )' * 2 - 1;
    for next_tx = [ -1 1 ]
        for next_rx = [ -1 1 ]
            next_a = [ next_tx; a( 1 : nq - 1 ) ];
            next_d = [ next_rx; d( 1 : nb - 1 ) ];
            next_state = ( [ next_a; next_d ] + 1 ) / 2;
            num = - next_rx * ( q' * next_a + wb' * d );
            den = r2 * sigma;
            if num == 0 & den == 0
                den = eps;
            end;
            prob = 0.25 * erfc( num / den );
        end;
    end;
end;

```

```

        col = base2num( next_state, 2 ) + 1;
        P( row, col ) = prob;
        end;
    end;
end;

%%%%%%%%%%%% now P is the probability transition matrix

I = sparse( 1 : ns, 1 : ns, 1 );
P = P' - I;
row = 1;
P( row, : ) = ones( 1, ns );
x = zeros( ns, 1 );
x( row ) = 1;
p = P \ x;

    % p2 is a vector of state probabilities,
    % where    0000 means no errors
    %          1000 means one error was just made
    %          1110 means 3 errors were just made
    %          etc.

ns2 = 2 ^ nb;                % reduced number of states
p2 = zeros( ns2, 1 );
state2 = zeros( 1, nb );

for k = 1 : ns
    state1 = num2base( k-1, 2, nq + nb );
    a = state1( 1 : nq );
    d = state1( nq + 1 : nq + nb );
    state2 = xor( a( delay2 + 1 : nb + delay2 ), d );
    j = base2num( state2, 2 ) + 1;
    p2( j ) = p2( j ) + p( k );
end;

```

```

Pe = sum( p2( ns2/2 + 1 : ns2 ) );

state1 = [ 1; zeros( nb-1, 1 ) ];
state2 = zeros( nb, 1 );

p1 = 1 / ( 1 + p2( base2num( state2, 2 ) + 1 ) / p2( base2num( state1, 2 ) + 1 ) );

if nargout > 2 & wb(nb) ~= 0
    error( 'The last feedback tap must be zero to determine P1' );
end;

if nargout == 0
    fprintf( 1, 'error pattern          probability\n' );
    for k = 1 : ns2
        state = num2base( k - 1, 2, nb );
        fprintf( 1, '%1d', state );
        fprintf( 1, '          %g\n', p2( k ) );
    end;
    fprintf( 1, '\nProbability of bit error: %g\n', Pe );
    if wb(nb) == 0
        fprintf( 1, 'Probability of bit error without error propagation: %g\n', p1 );
    end;
end;

```

Listing of base2num.m

```

function x = base2num( v, base )
% X = BASE2NUM( V, BASE )
%
% Converts a vector containing the base BASE representation to
% a number, X.
%

```

```

x = 0;
power = 1;
for i = length( v ) : -1 : 1
    x = x + v( i ) * power;
    power = power * base;
end;

```

Listing of num2base.m

```

function v = num2base( x, base, digits )
% V = NUM2BASE( X, BASE, DIGITS )
%
% Converts number X into a vector containing the base BASE representation
% of X. DIGITS specifies the length of V, or the number of digits to use.
% The number is right-justified in V, with zero padding as necessary.
% For example, NUM2BASE( 5, 2, 4 ) returns the binary representation
%
%           [ 0 1 0 1 ]
%
v = zeros( 1, digits );
for i = 1 : digits
    v( 1, digits - i + 1 ) = rem( x, base );
    x = fix( x / base );
end;

```